

**Sedimentology and Organic Biogeochemistry of the  
Ordovician Redmans Formation, Bell Island, Newfoundland**

by

© Tiffany Rose Miller, B.Sc., Geol. I.T.

A thesis submitted to the

School of Graduate Studies

in partial fulfillment of the requirements for the degree of

**Master of Science**

**Department of Earth Sciences**

Memorial University of Newfoundland

**September 2014**

St. John's

Newfoundland

## ABSTRACT

Understanding the processes that control the sequestration of organic matter are critical to the reconstruction of atmospheric CO<sub>2</sub> levels on geological time scales. Muddy, high-energy coastlines are subject to frequent wave reworking, tide-controlled grain-size sorting, and bioturbation. These processes control the remineralization efficiency of organic particles and impact the total organic carbon content (TOC, wt %) and quality ( $\delta^{13}\text{C}_{\text{org}}$ , ‰) of sedimentary organic matter. The combination of detailed facies descriptions, in conjunction with geochemical analysis of mudstones and siltstones can be integrated into a paleoenvironmental framework that allows for detailed interpretation of facies control on organic matter geochemical signatures. This Masters thesis aims to develop a better understanding of the effects physical and biological seafloor processes have on geochemical variability within and between facies in the Early Ordovician, Redmans Formation from Bell Island, Newfoundland. Isotopic trends are used herein to determine if bulk organic carbon isotopic values can be applied to the correlation of global organic carbon signatures.

## **ACKNOWLEDGEMENTS**

I would like to take this opportunity to extend my thanks to those who have helped guide and support me these past two years. First, I would like to thank Dr. Duncan McIlroy for accepting me as his student and providing mentorship throughout the completion of this project. I have had the opportunity to develop as both a researcher and individual under his guidance. Thanks to Dr. Richard Callow, my supervisory committee member, for asking the right questions and providing the support to answer them. Dr. Dario Harazim, without your expertise and patience I would be lost in vast quantities of data, thank you. The Department of Earth Sciences, School of Graduate Studies, and teaching assistantships financed this project and without their support this project would not have been possible. I gratefully acknowledge the financial support provided by Chevron Canada Limited Rising Star Award.

I would like to extend my appreciation and gratitude to the MUN Ichnology group for making this an incredible experience; Mary, Eli, Katie, Robyn, Jill, Edgars, Elisabeth, Chris, and Colin. The support and friendship offered from the kind and hilarious members of the geophysics, hard rock, and environmental geology community of the fourth and fifth floor cannot be appreciated enough. Huge thanks to Helen Gillespie, Alison Pye, Wanda Aylward, and Kris Poduska who always found the time to help with lab support and data processing. Thanks to my incredible office mates Matt Johnston, Megan McDonald, and Samantha Green.

To my family who have always supported my every decision, even if it meant moving to the most easterly point in North America. Thanks to my mother, who inspires me with her compassion, my father, with his voice of reason, my sister, with her perseverance, and my grandma, with her wit. Thanks to my cousin Cody for inspiring me to pursue geology. Thanks to Neil whose support and belief in me has been essential in the completion of this degree. I sincerely could not have done this without him or the wonderful people who are a part of my life. Thank you!

## Table of Contents

<b>ABSTRACT</b> .....	<b>ii</b>
<b>ACKNOWLEDGEMENTS</b> .....	<b>iii</b>
<b>Table of Contents</b> .....	<b>iv</b>
<b>List of Tables</b> .....	<b>vii</b>
<b>List of Figures</b> .....	<b>viii</b>
<b>List of Symbols, Nomenclature or Abbreviations</b> .....	<b>x</b>
<b>List of Appendices</b> .....	<b>xi</b>
<b>Co-Authorship Statement</b> .....	<b>xii</b>
<b>Chapter 1-Introduction and Overview</b> .....	<b>1-1</b>
1.1 Project overview and the problem stated .....	1-1
1.1.1 Processes controlling mud-rich marginal marine organic matter geochemistry: Physical and biological reworking .....	1-2
1.2 Objectives and analytical approach.....	1-6
1.3 Geological Context .....	1-6
1.4 Figures.....	1-8
1.5 References.....	1-11
<b>Chapter 2-Sedimentology and Stratigraphy of a Wave-dominated Delta from the Early Ordovician Redmans Formation, Bell Island, Newfoundland</b> .....	<b>2-1</b>
2.1 Abstract .....	2-1
2.2 Introduction.....	2-2
2.3 Geological Setting.....	2-3
2.4 Sedimentology .....	2-5
2.4.1 Sandstone Facies .....	2-5
2.4.2 Siltstone Facies .....	2-11
2.4.3 Heterolithic Facies.....	2-13



2.4.4 Mudstone Facies .....	2-14
2.5 Depositional Setting .....	2-16
2.6 Sequence Stratigraphy .....	2-20
2.7 Conclusion .....	2-21
2.8 Acknowledgements .....	2-22
2.9 Figures and Tables .....	2-23
2.10 References .....	2-35
<b>Chapter 3-Implications for Organic Carbon Cycling in an Early Ordovician Wave-</b>	
<b>dominated Delta: Redmans Formation, Bell Island, Newfoundland .....</b>	<b>3-1</b>
3.1 Abstract .....	3-1
3.2 Introduction .....	3-2
3.3 Methods and materials .....	3-6
3.3.1 Sampling strategy and rock description .....	3-6
3.3.2 Geochemical measurements .....	3-6
3.3.3 Fourier-Transform-Infrared Spectroscopy (FTIR) .....	3-6
3.4 Results .....	3-7
3.4.1 Geochemical characteristics .....	3-7
3.5 Discussion .....	3-10
3.5.1 The effect of sediment transport on TOC and $\delta^{13}\text{C}_{\text{org}}$ .....	3-12
3.5.2 Organism-sediment interaction .....	3-13
3.5.3 Implications for global organic carbon cycling .....	3-15
3.6 Conclusion .....	3-17
3.7 Acknowledgements .....	3-18
3.8 Figures and Tables .....	3-19
3.9 References .....	3-36

<b>Chapter 4-Summary .....</b>	<b>4-1</b>
4.1 Review of objectives .....	4-1
4.2 Summary of conclusions .....	4-2
4.2.1 Paleoenvironmental interpretation of the Redmans Formation .....	4-2
4.2.2 Facies-scale depositional mechanisms and biological-sediment interactions with respect to organic carbon cycling .....	4-3
4.2.3 Implications for global organic carbon cycling using bulk organic matter isotopic trends correlations .....	4-5
4.3 References .....	4-6

## **List of Tables**

### **Chapter 2**

Table 2.1 Facies descriptions for the mudstones, siltstones, and sandstones of the Redmans Formation .....	2-34
--	------

### **Chapter 3**

Table 3.1 Combined sedimentological and geochemical evaluation of the Redmans Formation's facies .....	3-36
--	------

## List of Figures

### Chapter 1

- Figure 1.1 Location map of Bell Island, Newfoundland with study interval ..... 1-8
- Figure 1.2 Chemostratigraphic comparison of the Redmans Formation with the Honghuayuan section in the Guizhou Province of southern China ..... 1-10

### Chapter 2

- Figure 2.1 Location map of Bell Island, Newfoundland with study interval ..... 2-23
- Figure 2.2 Summary log of the Redmans Formation ..... 2-24
- Figure 2.3 Sandstone facies – S1 to S6 ..... 2-25
- Figure 2.4 Siltstone facies - SS1 to SS3 ..... 2-26
- Figure 2.5 Mudstone and heterolithic facies – M1, M2, and H1 ..... 2-27
- Figure 2.6 Bioturbation diversity and intensity ..... 2-29
- Figure 2.7 Idealized distributary mouth bar in core ..... 2-30
- Figure 2.8 Idealized distributary mouth bar parasequence ..... 2-31
- Figure 2.9 Wave-dominated deltaic paleoenvironment ..... 2-32

### Chapter 3

- Figure 3.1 Location map of Bell Island, Newfoundland with study interval ..... 3-20
- Figure 3.2 Wave-dominated deltaic paleoenvironment ..... 3-22
- Figure 3.3 Summary log of sedimentological and geochemical properties ..... 3-24

Figure 3.4 Organic rich mudstones .....	3-25
Figure 3.5 Erosive mudstone facies – M1 and M2 .....	3-26
Figure 3.6 Deposit feeding bioturbated facies – H1 and SS1 .....	3-27
Figure 3.7 Siltstone and silty sandstone facies – SS2, SS3, S5, and S6 .....	3-28
Figure 3.8 Graphical representations of individual facies $\delta^{13}\text{C}_{\text{org}}$ (‰) versus TOC (%) cross-plots .....	3-30
Figure 3.9 Box and whisker plots for $\delta^{13}\text{C}_{\text{org}}$ (‰) versus TOC (%) of individual facies.....	3-31
Figure 3.10 Paleoenvironmental and geochemical model .....	3-32
Figure 3.11 Chemostratigraphic comparison of the Redmans Formation with the Honghuayuan section in the Guizhou Province of southern China .....	3-33

## **List of Symbols, Nomenclature or Abbreviations**

ATR – Attenuated total reflection

DIC – dissolved inorganic carbon

FT-IR – fourier transform infrared spectroscopy

OM– organic matter

TOC – total organic carbon

XRD – X-ray diffractometry

## List of Appendices

<b>Appendix A</b> .....	Appendix - 1
Sedimentology and stratigraphy	
<b>Appendix B</b> .....	Appendix - 8
Whole rock stable organic carbon isotopic and total organic carbon (TOC) data, Bell Island	
<b>Appendix C</b> .....	Appendix – 11
X-ray Diffractometry (XRD)	
<b>Appendix D</b> .....	Appendix – 15
Fourier Transform Infrared (FT-IR) Spectroscopy	

## **Co-Authorship Statement**

This Master's thesis is subdivided into four chapters. Chapter 1 describes the thesis project overview and an assessment of the problems that will be addressed in the following chapters. The aims and objectives of this study are outlined and the study area is introduced. Chapters 2 and 3 are written in manuscript format that present the completed research. Chapter 4 reviews the objectives, materials and methods, and a summary of the finalized conclusions for the thesis manuscripts.

Chapters 2 and 3 are collaborative manuscripts between others and myself. Chapter 2 investigates the detailed sedimentology of the Redmans Formation from Bell Island, Newfoundland. This chapter is a collaborative effort between Prof. D. McIlroy, Dr. R. Callow, and myself. Chapter 3 is concerned with the organic carbon geochemical properties of the core from the Redmans Formation. I performed the laboratory work and have interpreted the data with the assistance of both Dr. D. Harazim, and Prof. Duncan McIlroy. Dr. K. Poduska was an important contributor to the methods and materials of Chapter 3. As lead author, I have written the manuscripts (Chapters 2 and 3) with editorial support from the contributing co-authors.



## Chapter 1

### **Introduction and Overview**

---

#### **1.1 PROJECT OVERVIEW AND THE PROBLEM STATED**

Ancient fine-grained marginal marine depositional systems dominated by mudstone: sandstone heterolithic facies are generally poorly understood. This project is focussed on the Lower Ordovician (Floian) Redmans Formation of Bell Island, Newfoundland, Canada. Paleoenvironmental conditions during deposition of the Redmans Formation were substantially different from their modern marginal marine counterparts with respect to organic matter composition and paleoenvironmental distribution since terrestrial ecosystems did not yet include land plants (Kenrick and Crane, 1997; Wellman et al., 2003; Gensel, 2008; Kenrick et al., 2012). Without terrestrial organic matter input, a more simplified marine carbon cycle is likely to have existed in terms of organic matter provenance with the absence of mixed-sourcing that is common to most post-Ordovician sediments (Kenrick et al., 2012; Harazim, 2013). The biogeochemistry of organic matter preserved in the Redmans Formation is likely to reflect the carbon composition of seawater as modified by physical and biological degradation.

Understanding the processes that control the textural and geochemical attributes of mudstones is important for several aspects of sedimentary geology (e.g. petroleum geology; stratigraphy; sedimentology; geochemistry; biogeochemistry; and

geochronology). Increased understanding of the processes that control the texture and geochemical properties of mudstone facies in marginal marine environments is significant to petroleum geology since mudstones are important components of hydrocarbon plays, acting as source rocks, seals, and reservoirs (Potter et al., 2005; Passey et al., 2010; Aplin and Macquaker, 2011). The integrated approach used herein that uses both sedimentological and geochemical analyses aims to improve paleoenvironmental and geochemical understanding of Ordovician mud-rich depositional systems (see also Harazim, 2013).

### **1.1.1 Processes controlling mud-rich marginal marine organic matter biogeochemistry: Physical and biological reworking**

Biological activity and physical reworking in the marine environment impact organic matter quality and quantity represented by organic carbon isotopic signatures ( $\delta^{13}\text{C}_{\text{org}}$ , ‰) and total organic carbon (TOC, wt%) (Checkley and Entzeroth, 1985; Harazim, 2013). Incorporating both sedimentological and geochemical rock properties will provide high-resolution data pertinent to the understanding of organic matter cycling in marginal marine environments at the facies/sediment fabric level.

In this MSc thesis, the Redmans Formation of Bell Island, Newfoundland is studied to provide insight into: a) the processes that control depositional heterogeneities in the interbedded mudstone, siltstone, and sandstone facies; b) paleoenvironment of deposition; c) the effect of physical and biological reworking on organic matter quality and quantity; and d) bulk organic matter isotopic characteristics in relation to global organic carbon signatures.

Relatively little work has been undertaken on the Redmans Formation of Bell Island, Newfoundland, perhaps due to the inaccessibility of the outcrops. The Redmans Formation is composed of inter-bedded quartz-arenites, siltstones, and mudstones. Sandstones in the Redmans Formation form laterally extensive beds, or lenses, separated by thin (<10cm) mudstone inter-beds (Brenchley et al., 1993). Three main parasequences, forming a broadly aggradational parasequence set, have been previously described as part of an early highstand systems tract (Brenchley et al., 1993). Both tide and storm influences have been recorded in previous paleoenvironmental studies of the Redmans Formation (Ranger et al., 1984; Brenchley et al., 1993). The Redmans Formation was originally interpreted as an offshore bar complex, forming part of a thick storm-dominated deltaic succession (Fillion and Pickerill, 1990), though subsequently has been reinterpreted as being deposited on a wave-dominated shelf (Brenchley et al., 1993).

Previous studies of the Redmans Formation do not provide a detailed facies assessment of the mudstone and siltstone inter-beds. This is probably due to poor exposure of the formation in steep, highly weathered cliffs. The core that forms the basis of this study provides an exceptional opportunity to study the sedimentology and biogeochemistry of the, otherwise obscure, fine-grained facies of the Redmans Formation. The integrated approach used herein combines detailed facies descriptions with sedimentology, geochemistry, ichnology, and sequence stratigraphic interpretation in the Redmans Formation. Chapter 2 describes the sedimentological and paleoenvironmental framework upon which the geochemical studies of Chapter 3 are built.

The purpose of Chapter 3, and the primary focus of this thesis project, is to address the stated null hypothesis: *“Near-shore marine environments have organic carbon isotopic trends that represent the oceanic values of  $\delta^{13}C_{org}$ , and are independent of seafloor processes and the effects of detritivory”*.

Stable carbon isotopes (carbonate and organic) have been widely used for chemostratigraphy (e.g. Gunter 1986), as well as identification of hydrocarbon sources, organic matter typing, paleo-oceanography, and paleoenvironmental analysis (Tyson, 1995). Chemostratigraphic studies involving carbonate and organic stable carbon isotope ratios ( $\delta^{13}C$ , ‰) have been used to interpret environmental and sedimentological changes and correlate strata on a global scale (Magaritz et al., 1992). Through geological time the ratio of  $^{13}C/^{12}C$  in the oceans has changed in response to changes in the global carbon cycle. The resultant isotopic curve allows the correlation and dating of rocks through the recognition of isotopic excursions that are inferred to be isochronous (Saltzman and Thomas, 2012).

Chemostratigraphic studies typically focus on carbonate carbon ( $\delta^{13}C_{carb}$ , ‰), rather than organic carbon ( $\delta^{13}C_{org}$ , ‰) with some exceptions (Buggisch et al., 2003; Zhang et al., 2010; Jahren et al., 2013). Carbon isotopes in carbonates are used to measure changes in dissolved inorganic carbon (DIC) during carbonate precipitation in marine environments (Saltzman and Thomas, 2012). Carbon isotopes in biominerals and precipitated carbonates, in the absence of diagenetic alteration, are inferred to directly correspond to represent the oceanic DIC content of the ocean (Saltzman and Thomas, 2012). Factors that can impact carbonate carbon isotopic values include diagenesis and

meteoric mixing (Allan and Matthews, 1982; Saltzman and Thomas, 2012). The carbon in organic matter has an isotopic composition that reflects the original carbon fractionation process (Bickert, 2006; Álvaro et al., 2008). Secondary processes such as biological sediment interactions, and physical sediment reworking, are suggested to have a substantial impact on organic matter quality and quantity (Pratt et al., 1986; Tyson, 1995; Rullkötter, 2006). These processes are predicted to have the potential to generate significant shifts in total organic carbon (TOC) and isotopic values ( $\delta^{13}\text{C}_{\text{org}}$ ) relative to the original source (Harazim, 2013).

Chemostratigraphic studies using  $\delta^{13}\text{C}_{\text{org}}$  have been completed from few Floian successions in Argentina, China, and Ireland (Buggisch et al., 2003; Zhang et al., 2010; Jahren et al., 2013). The aforementioned studies use variability in  $\delta^{13}\text{C}_{\text{org}}$  for correlation with global isotopic excursions derived from carbonates. The Hunghuayuan and Meitan Formations in Guizhou Province of southern China span the entire Floian stage (Zhang et al., 2010). Trends in  $\delta^{13}\text{C}_{\text{org}}$  seen in the succession show a spread of approx. 8 ‰, and have been considered to reflect global perturbations in the carbon cycle (Fig. 1.2; Zhang et al., 2010). Comparison of the  $\delta^{13}\text{C}_{\text{org}}$  curve from the Redmans Formation and that of other Floian successions is an aim of Chapter 3. In order to understand the controls on organic matter preservation and composition in the Redmans Formation, organic matter is characterized with respect to sedimentary facies and fabrics, enabling the possible influence of bioturbation and physical reworking to be assessed. This project is to the best of our knowledge the first attempt to understand the interrelationship between depositional processes, TOC and  $\delta^{13}\text{C}_{\text{org}}$  in an Ordovician succession. Understanding

variations in TOC and  $\delta^{13}\text{C}_{\text{org}}$  on a local scale has significant potential impact on the validity of studies that use  $\delta^{13}\text{C}_{\text{org}}$  curves in global chemostratigraphic studies.

## **1.2 OBJECTIVES AND ANALYTICAL APPROACH**

In order to test the above hypotheses for this MSc project, three main objectives were formulated to: 1) describe and interpret the paleoenvironment of deposition for the Redmans Formation, based on detailed facies and facies associations; 2) understand the effect of physical and biological seafloor reworking on organic carbon geochemical variability, with particular focus on organic matter composition and abundance; and 3) determine whether bulk organic matter isotopic trends can be correlated with global carbon isotope curves.

## **1.3 GEOLOGICAL CONTEXT**

Bell Island is located approximately 5 km off the coast of the Avalon Peninsula in Conception Bay, Newfoundland. Over 1500 m of shallow marine Cambrian-Ordovician inter-bedded micaceous sandstones, siltstones, mudstones, and ironstones have been subdivided into two groups and eleven formations (Fig. 1.1; Ranger et al., 1984). The Bell Island successions have a north-northwest dip of  $8^\circ$  to  $10^\circ$  and lie within an inferred graben structure defined by the northeasterly trending Topsail Fault Zone (Rose, 1952; Ranger et al., 1984).

The 79 m thick Redmans Formation of the Bell Island Group, was deposited during the Early Ordovician Floian stage, approximately 477.7 Ma, in a warm temperate environment (Ranger et al., 1984; Cocks et al., 1997). The Redmans Formation outcrops only on Bell Island, with exposures at Redmans Head and Freshwater Cove, with minor exposures at Big Head and Bell Cove (Fig. 1.1; Ranger et al., 1984). The newly acquired core that forms the basis of this thesis is the only example of the Redmans Formation in sub-crop.

## 1.4 FIGURES

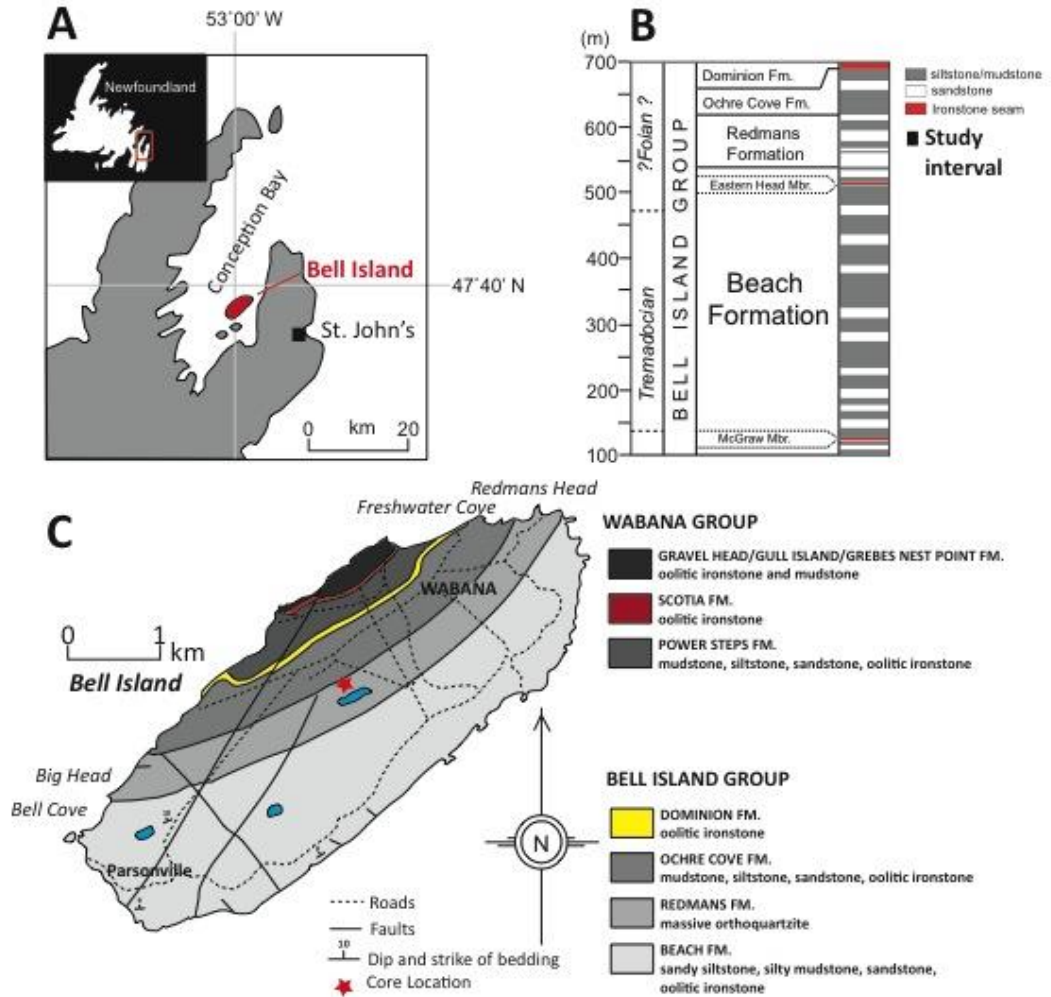
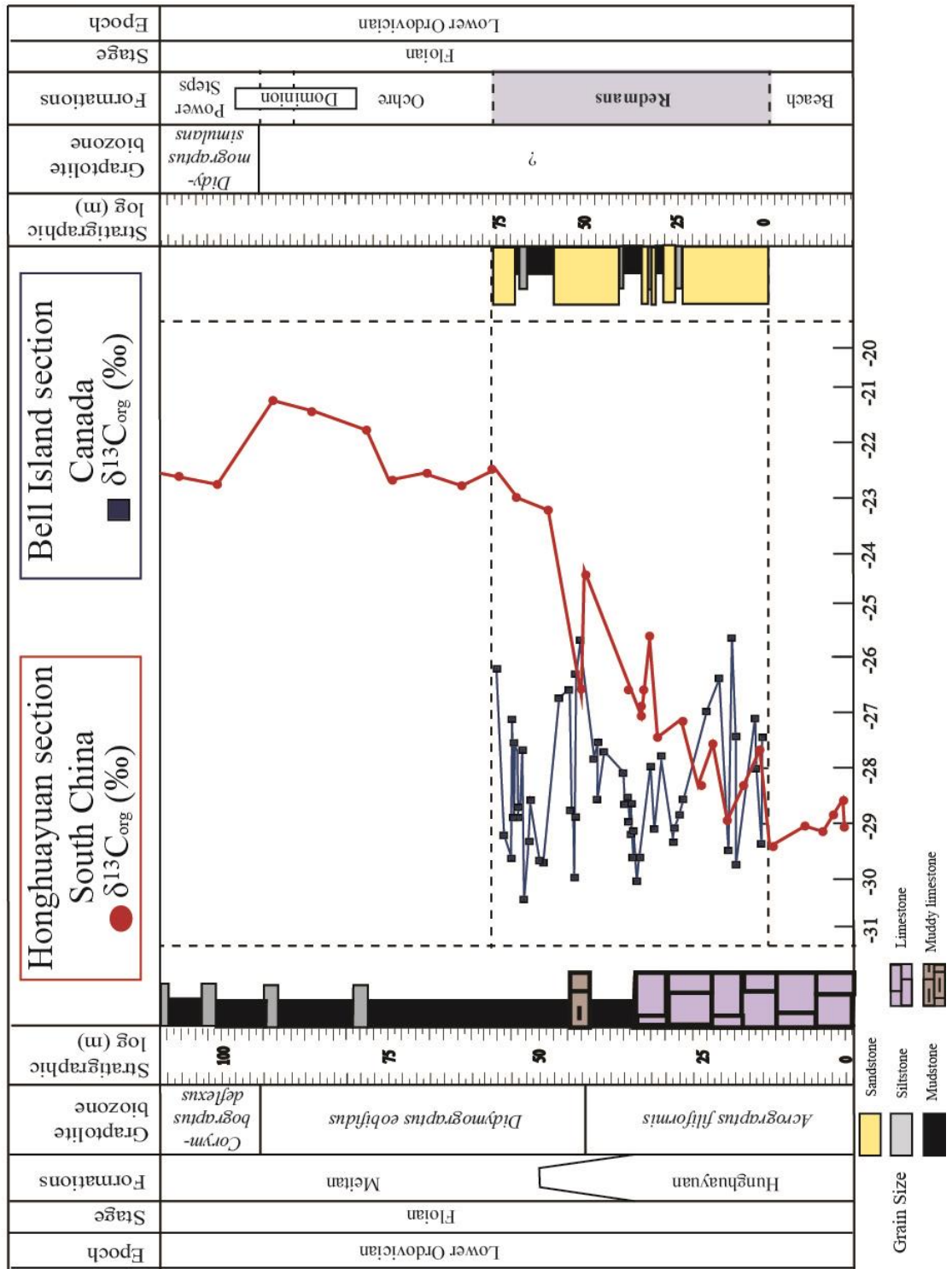


Fig. 1.1: (a) Bell Island, Newfoundland location map. (b) Stratigraphic section of the Bell Island Group, Redmans Formation. Redmans Formation is Floian in age (~477.7 Ma). (c) Bell Island geological map with the studied core location indicated (modified after Ranger et al., 1984; Harazim et al., 2013).



**Fig. 1.2: A small portion of the Honghuayuan section in the Guizhou Province of southern China have  $\delta^{13}\text{C}_{\text{org}}$  spreads of approximately 8 ‰ (Zhang et al., 2010). The isotopic spread has been interpreted as a global perturbation in the carbon cycle; in contrast the Redmans Formation has an unparalleled isotopic expression derived from physical and biological reworking.**



## 1.5 REFERENCES

- Allan, J., and Matthews, R., 1982, Isotope signatures associated with early meteoric diagenesis: *Sedimentology*, v. 29, no. 6, p. 797-817.
- Álvaro, J. J., Bauluz, B., Subías, I., Pierre, C., and Vizcaino, D., 2008, Carbon chemostratigraphy of the Cambrian-Ordovician transition in a midlatitude mixed platform, Montagne Noire, France: *Geological Society of America Bulletin*, v. 120, no. 7-8, p. 962-975.
- Aplin, A. C., and Macquaker, J. H. S., 2011, Mudstone diversity: Origin and implications for source, seal, and reservoir properties in petroleum systems: *AAPG Bulletin*, v. 95, no. 12, p. 2031-2059.
- Bickert, T. (2006). Influence of geochemical processes on stable isotope distribution in marine sediments. In *Marine Geochemistry*, p. 339-369, Springer Berlin Heidelberg.
- Brenchley, P. J., Pickerill, R. K., and Stromberg, S. G., 1993, The role of wave reworking on the architecture of storm sandstone facies, Bell Island Group (Lower Ordovician), eastern Newfoundland: *Sedimentology*, v. 40, no. 3, p. 359-382.
- Buggisch, W., Keller, M., and Lehnert, O., 2003, Carbon isotope record of Late Cambrian to Early Ordovician carbonates of the Argentine Precordillera: *Palaeogeography, Palaeoclimatology, Palaeoecology*, v. 195, no. 3, p. 357-373.
- Checkley, D. M., and Entzeroth, L. C., 1985, Elemental and isotopic fractionation of carbon and nitrogen by marine, planktonic copepods and implications to the marine nitrogen cycle: *Journal of Plankton Research*, v. 7, no. 4, p. 553-568.

- Cocks, L. R. M., McKerrow, W. S., and vanStaal, C. R., 1997, The margins of Avalonia: Geological Magazine, v. 134, no. 5, p. 627-636.
- Fillion, D., and Pickerill, R. K., 1990, Ichnology of the Upper Cambrian? to Lower Ordovician Bell Island and Wabana groups of eastern Newfoundland, Canada: Palaeontographica Canadiana.
- Gensel, P. G., 2008, The earliest land plants: Annual Review of Ecology, Evolution, and Systematics, v. 39, p. 459-477.
- Gunter, F., 1986, Principles of Isotope Geology, John Wiley and Sons.
- Harazim, D., 2013, High-energy seafloor processes and biological reworking as first-order controls on mudstone composition and geochemistry [PhD: Memorial University of Newfoundland.
- Jahren, A. H., Schubert, B. A., Marynowski, L., and Wilson, J. P., 2013, The Carbon Isotope Organic Geochemistry of Early Ordovician Rocks from the Annascaul Formation, County Kerry: Irish Journal of Earth Sciences, p. 1-12.
- Kenrick, P., and Crane, P. R., 1997, The origin and early evolution of plants on land: Nature, v. 389, no. 6646, p. 33-39.
- Kenrick, P., Wellman, C. H., Schneider, H., and Edgecombe, G. D., 2012, A timeline for terrestrialization: consequences for the carbon cycle in the Palaeozoic: Philosophical Transactions of the Royal Society B: Biological Sciences, v. 367, no. 1588, p. 519-536.
- Magaritz, M., Krishnamurthy, R., and Holser, W. T., 1992, Parallel trends in organic and

- inorganic carbon isotopes across the Permian/Triassic boundary: *American Journal of Science*; (United States), v. 292, no. 10.
- Passey, Q. R., Bohacs, K., Esch, W. L., Klimentidis, R., and Sinha, S., 2010, From oil-prone source rock to gas-producing shale reservoir: Geologic and petrophysical characterization of unconventional shale-gas reservoirs: International Oil and Gas Conference and Exhibition, Beijing, China, June 8-10, 2010, SPE Paper 131350, p.29
- Potter, P. E., Maynard, J. B., and Depetris, P. J., 2005, *Mud and mudstones: Introduction and overview*, Springer.
- Pratt, L. M., Claypool, G. E., and King, J. D., 1986, Geochemical imprint of depositional conditions on organic matter in laminated—bioturbated interbeds from fine-grained marine sequences: *Marine Geology*, v. 70, no. 1–2, p. 67-84.
- Ranger, M. J., Pickerill, R. K., and Fillion, D., 1984, Lithostratigraphy of the Cambrian? – Lower Ordovician Bell Island and Wabana groups of Bell, Little Bell, and Kellys islands, Conception Bay, eastern Newfoundland: *Canadian Journal of Earth Sciences*, v. 21, no. 11, p. 1245-1261.
- Rose, E. R., 1952, Torbay map-area, Newfoundland: Geological Survey of Canada, v. Memoir 265.
- Rullkötter, J., 2006, Organic Matter: The Driving Force for Early Diagenesis. In *Marine Geochemistry*, p. 125-168, Springer Berlin Heidelberg.
- Saltzman, M., and Thomas, E., 2012, Carbon isotope stratigraphy: The Geologic Time Scale, v. 2012, p. 207-232.
- Tyson, R. V., 1995, *Sedimentary organic matter*, London, UK, Chapman & Hall.

Wellman, C. H., Osterloff, P. L., and Mohiuddin, U., 2003, Fragments of the earliest land plants: *Nature*, v. 425, no. 6955, p. 282-285.

Zhang, T., Shen, Y., and Algeo, T. J., 2010, High-resolution carbon isotopic records from the Ordovician of South China: Links to climatic cooling and the Great Ordovician Biodiversification Event (GOBE): *Palaeogeography, Palaeoclimatology, Palaeoecology*, v. 289, no. 1, p. 102-112.

## Chapter 2

# **Sedimentology and Stratigraphy of a Wave-Dominated Delta from the Early Ordovician Redmans Formation, Bell Island, Newfoundland**

---

Tiffany Miller, Duncan McIlroy

### **2.1 ABSTRACT**

Marginal marine mudstone-dominated systems are poorly known from the early Palaeozoic. This paper presents the results of a combined sedimentological-ichnological analysis of 76.5 m of core from a mud-rich, wave-dominated, tide-influenced deltaic succession. The Redmans Formation is characterized by meter-thick packages of medium- to coarse-grained quartz-arenites, inter-bedded with meter-thick intervals of silt- and clay-rich mudstones. Sandstone facies are typically sparsely bioturbated (0-10%) and contain low diversity trace fossil assemblages dominated by *Diplocraterion* and *Planolites*. Unbioturbated mudstones in the succession were deposited under high-energy conditions and contain recalcitrant organic matter unsuitable for the support of a deposit feeding biota. In contrast the silt- and clay-rich mudstone facies with abundant high quality organic matter are intensely bioturbated (30-90%) containing diverse ichnological assemblages including *Cruziana*, *Planolites*, *Trichophycus*, and *Diplocraterion*. Twelve sedimentological facies have been identified, and are inferred to have been deposited in proximal, central, and distal distributary mouth bar environments, that experienced significant reworking by waves and tides.

## **2.2 INTRODUCTION**

Delineating the sedimentological and stratigraphic character of the Redmans Formation is significant to the understanding of Early Ordovician mud-rich depositional systems. Mudstone source-rocks and seals are significant for the development of hydrocarbon plays in the energy sector. The development of mudstones as important reservoir rocks for the shale hydrocarbon industry, have focused attention on mudstone-rich successions (Schieber and Zimmerle, 1998; Potter et al., 2005; Passey et al., 2010). Understanding the processes that control the deposition and distribution of mudstone facies is key to realistic paleoenvironmental and facies analysis. This in turn provides the basis for improved reservoir geology in mud-rich depositional systems (Schieber and Zimmerle, 1998; Potter et al., 2005).

Marine mudstones are relatively poorly understood with respect to the physical and biological processes active during deposition of mud-rich deposits (Harazim, 2013). The inter-relationships between thick tabular sandstone facies and the bioturbated and unbioturbated mudstones inter-bedded with them in shallow marine depositional environments are not well documented. Paleoenvironmental interpretations of inter-bedded sandstones and associated mudstones in marine shelf depositional systems play a critical role in both hydrocarbon storage and migration (Schieber and Zimmerle, 1998). In this study, 76.5 m of core from the Redmans Formation have been evaluated using high-resolution sedimentology, ichnology, and petrography. The research aims to determine the hydrodynamic conditions under which the several mudstone and sandstone



facies were deposited and integrate those data/understandings into a unified paleoenvironmental model. Through study of the core, and integration with previously studied outcrop datasets, a facies scheme composed of twelve sedimentary facies has been created and forms the basis of a new paleoenvironmental and sequence stratigraphic interpretation of the Redmans Formation.

### **2.3 GEOLOGICAL SETTING**

Bell Island is located approximately 5 km off the coast of the Avalon Peninsula in Conception Bay, Newfoundland (Fig. 2.1). The Avalon Peninsula of Newfoundland is considered to have been part of the Avalonian Terrane, on the western margin of Gondwana (Cocks et al., 1997; Cocks and Torsvik, 2002). Avalonia is considered to have separated from Gondwana during the Floian (478 Ma), with the opening of the Rheic Ocean, followed by rapid movement of Avalonia northward (Cocks et al., 1997; Cocks and Torsvik, 2002). The Redmans Formation was deposited in the Floian during early rifting of Avalonia away from Gondwana (Cocks et al., 1997; Prigmore et al., 1997; Cocks and Torsvik, 2002).

Over 1500 m of Cambro-Ordovician strata are exposed in Conception Bay, Newfoundland. The succession is subdivided into the Bell Island and Wabana groups and their eleven constituent formations, all of which are composed of shallow marine siliciclastic strata (Ranger, 1979; Ranger et al., 1984; Fig. 2.1, 2.2). The Bell Island and Wabana groups have a north-northwest dip of 8° to 10° and lie within an inferred graben in Conception Bay (Rose, 1952; Miller, 1983). To the southeast and northwest of Bell

Island lie Precambrian and Cambrian strata and thus any detailed assessment of regional facies distribution beyond Bell Island is not possible (Brenchley et al., 1993).

The paleoclimatic regime during deposition of the Redmans Formation was one of warm temperate conditions (Ranger et al., 1984; Cocks et al., 1997). The Redmans Formation succession consists of approx. 79 m of white-grey quartz arenites inter-bedded with siltstones and mudstones (Ranger et al., 1984). The best outcrops of the formation are at Redmans Head and Freshwater Cove, with smaller exposures at Big Head and Bell Cove (Fig. 2.1; Ranger et al., 1984).

The contacts separating the Redmans Formation from the underlying Beach Formation and the overlying Ochre Cove Formation are both conformable and gradational. The Redmans Formation is defined as the interval in the Bell Island group in which the proportion of sandstone is greater than that of siltstone/mudstone (Ranger et al., 1984). The great thickness of sediment in the Bell Island and Wabana Groups suggests the presence of a delta (Ranger et al., 1984). The presence of such large thicknesses of mudstone is, however, anomalous but may have resulted from the weathering of penecontemporaneous volcanic deposits possibly associated with the Shelvian Orogeny during the closing of the Tornquist Sea (Torsvik, 1998).

The Redmans Formation has previously been interpreted as both part of an offshore bar complex (Ranger et al., 1984), and alternatively as an open, wave-dominated, shelf environment (Brenchley et al., 1993). In both models a combination of tidal and storm influence have been inferred (Ranger et al., 1984; Brenchley et al., 1993). The sandstones of the Redmans Formation include both laterally extensive beds and laterally discontinuous lenses separated by mudstone inter-beds less than 10cm thick

(Brenchley et al., 1993). This study builds on the pre-existing work on the Redmans Formation through consideration of a newly available core with essentially 100% recovery. The lack of weathering of the core allows detailed examination of sediment fabrics both in sandstones and also the mudstones not easily studied in the field.

## **2.4 SEDIMENTOLOGY**

The facies of the Redmans Formation core include thin mudstone beds that have been considered in detail, owing to their exceptional preservation in the core. Sedimentological core descriptions and petrographic data from all facies are incorporated into common facies successions in order to aid consideration of their spatial distribution (Table 2.1, Fig. 2.2). The diverse assemblage of trace fossils known from bedding plane expressions of facies in the field (Fillion and Pickerill, 1990), are not matched by similar ichnodiversity in core, partly because many of the taxa are not well known in cross section. In addition, many of the taxa are comparatively rare and are thus unlikely to be intersected by the cut surfaces of the core. This work follows the ichnological approach advocated by McIlroy (2004a, 2008), which treats trace fossil assemblages as components of sedimentary facies rather than employing prescriptive Seilacherian ichnofacies (Seilacher, 1967; Pemberton et al., 1992; Goldring, 1995).

### **2.4.1 Sandstone Facies**

#### ***2.4.1.1 Facies S1: Medium grained, trough cross-stratified sandstone***

Facies S1 consist of poorly sorted medium grained sandstones with sharp erosional bases commonly with a lag of sub-angular to sub-rounded pebble-sized mudstone rip-up clasts. The sandstones are trough cross-bedded and unbioturbated, occurring in bedsets up to 15cm thick (Fig. 2.3a). This facies is mineralogically immature, containing accessory detrital calcite, plagioclase, and chert along with muscovite, biotite, quartz, and opaque minerals. This facies occurs rarely throughout the core. This facies has abundant chlorite and calcite cements. Facies S1 is commonly inter-bedded with the fine-grained silty mudstones of Facies SS2 and is associated with sandstone Facies S3 as it is typically deposited directly above Facies S3, described below.

#### *Interpretation of Facies S1*

The trough cross-bedded sandstones have sharp changes in grain size, from medium to fine grained, suggesting a strong, possibly tidally-modulated, current. This interpretation is similar to that inferred for herring-bone cross stratified sandstones from the inter-bar facies of Ranger et al. (1984), though it is noted that no herring-bone cross stratification has been documented in this study. Apparently opposing trough cross sets are common in trough cross-bedded successions and it may have been to these that Ranger et al. (1984) erroneously refer. The combination of the anomalously coarse medium grained sandstones, and low mineralogical maturity, suggests rapid deposition and/or short sediment transport paths.

#### ***2.4.1.2 Facies S2: Structure-less sandstone***

The massive, well-sorted silty sandstones of Facies S2 are rich in platy grains of phosphatic material that increase in abundance towards the top of beds (Fig. 2.3b). The mineralogical composition of S2 is dominated by quartz, with lower proportions of muscovite, plagioclase, chlorite, and opaque minerals such as pyrite. The only trace fossils present are rare *Diplocraterion* and *Palaeophycus*. Both ichnotaxa are commonly rich in framboidal pyrite and are present in low abundance in ichnofabrics in beds showing approx. 10% bioturbation. The beds of facies S2 range in thickness up to a maximum of 150 cm.

#### *Interpretation of Facies S2*

Massive beds are notoriously difficult to interpret in core. The most common reasons for a lack of sedimentary structures are: dewatering, bioturbation, and rapid deposition of extremely well sorted sediment (Davies et al., 1971; Bhattacharya and Walker, 1991). The presence of some trace fossils in this unit suggests intense bioturbation is the most likely reason for an absence of lamination, which in turn implies that the rate of bioturbation greatly exceeded the rate of sedimentation. Such conditions are commonly met in association with a hiatuses on a clean, sand-dominated seafloor.

#### ***2.4.1.3 Facies S3: Planar cross-stratified, mud draped sandstone***

Low angle, very well sorted, fine-grained planar cross-stratified sandstones are common in the Redmans Formation. Facies S3 is mineralogically composed of quartz, muscovite, chlorite, and rare plagioclase, and opaque minerals. The sandstone is dominantly fine-grained with abundant, but diffuse, fine-grained laminae (Fig. 2.3c).

Mud-drapes, some of which are present in couplets are common in the slightly upward coarsening beds. In addition small phosphatic grains are present, particularly towards the tops of beds. Trace fossils are sparse, with the most common taxa being *Diplocraterion* aff. *habichi* and *Teichichnus* cf. *rectus* (Fig. 2.6b,c). Where bioturbation is intense, pressure solution seams are commonly developed around the traces rendering their morphology diffuse.

#### *Interpretation of Facies S3*

Field studies have identified similar thick, laminated sandstones with convex-upward geometries that have previously been interpreted as hummocks (Brenchley et al., 1993). The upward coarsening beds with abundant clay couplets of this facies imply that the bedforms were probably produced over a period of many days by tidally-modulated currents (Brettle et al., 2002; Quin, 2011). As such these cross-stratified sandstones are more likely to be mouth-bars than storm-generated hummocks (cf. Quin, 2011).

#### ***2.4.1.4 Facies S4: Flaser bedded very fine-grained sandstone***

Facies S4 consists of flaser bedding with wave ripples in very fine-grained sandstones, and is most common in the uppermost portion of the core (Fig. 2.3d). The dominant mineralogy is quartz with lower proportions of chlorite, biotite, muscovite, plagioclase, and opaque minerals. Phosphatic nodules less than 1cm in diameter are rare. Low diversity and intensity of bioturbation is present in the form of sparse unidentifiable vertical burrows below 5% abundance. The maximum bed thickness for Facies S4 is approximately 75cm, and subtly fines upwards.

#### *Interpretation of Facies S4*

The presence of flaser bedding indicates high, but fluctuating, hydrodynamic energy and high sediment concentrations. The low intensity and diversity of the ichnofaunal assemblage is consistent with high hydrodynamic energy. The depositional environment was interpreted as a reworked portion of a proximal distributary mouth bar during a period of basin shallowing.

#### ***2.4.1.5 Facies S5: Parallel to ripple cross-laminated sandstone***

The cross-laminated sandstones of this facies may show trends from parallel to ripple cross-laminae within individual beds approx. 30cm in thickness. The thin laminae are prominent, owing to their dark color (Figs 2.3e). The sandstones are typically fine grained with abundant silt- and clay-sized clasts that are particularly abundant on the foresets of oscillation ripples at the top of bedsets. The prominent drapes to the ripples are clay and organic-matter rich, and are commonly found as couplets. This facies may be bioturbated with a diffuse *Planolites*-like ichnofabric that consists of bedding-parallel tubular trace fossils with no lining and uncommon *Rosselia* (Fig. 2.5a). Trace fossils are generally rare in this facies, but are most common in some of the centimeter thick clay drapes.

#### *Interpretation of Facies S5*

The presence of clay couplets indicates a tidal influence on this facies, this is most likely to be due to the presence of tidally modulated outflow onto a wave and storm dominated shelf (Nio and Yang, 1991). The representation of drapes formed during both high-water and low-water slacks demonstrates the sub-tidal position of this depositional

environment. The common association with Facies S3, and finer grain-size suggest that this facies was deposited in association with the same facies architectural element, but in a slightly more distal depositional setting. The presence of ripple cross laminae similarly suggests a more quiescent depositional setting with low flow regime conditions prevailing in the later stage of development of the bedsets. The depositional setting is inferred to be that of a more distal expression of the distributary mouth bar with episodic deposition, possibly due to autocyclic lobe switching.

#### ***2.4.1.6 Facies S6: Parallel laminated very fine-grained sandstone and silty sandstone***

Facies S6 consists of inter-laminated very fine-grained sandstone and silty sandstone with parallel lamination. Laminae are distinctively crinkly/wavy and variable in thickness from 0.5 mm to 1.0 mm, and may be present in couplets (Fig. 2.3f). Beds are up to 5cm in thickness and show a decrease in clay grade material upwards. Facies S6 occurs consistently on top of Facies S3, cross-stratified, mud draped sandstone. There is little bioturbation in this facies although escape traces are locally present (Figs 2.3g, 2.6e).

#### ***Interpretation of Facies S6***

The occurrence of clay-rich couplets likely represents tidal influences in a low energy flow regime associated with distributary mouth bars (Nio and Yang, 1991; Prigmore et al., 1997; McIlroy, 2004b). As indicated by the stacking of Facies S6 on top of Facies S3 deposition occurs proximal to shore in sub-tidal environment. Since bioturbation occurs primarily as escape traces—and since deposition was sub-tidal and



thus unlikely to be of significantly lowered salinity—sedimentation was likely too rapid for colonization and therefore inhospitable for bioturbating organisms. Facies S6 is interpreted to be associated with the proximal distributary mouth bar in a comparatively low hydrodynamic regime with significant tidal influence.

## **2.4.2 Siltstone Facies**

### ***2.4.2.1 Facies SS1: Intensely bioturbated sandy siltstone***

Intensely bioturbated sandy siltstones with abundant sand-filled bedding-parallel burrows, destroy approx. 80% of the original sedimentary fabric (Fig. 2.4a,b). The *Planolites* burrows are 0.5-1.5 mm in diameter, ellipsoidal in cross section and have greater concentrations of clay minerals around the burrow. The rock shows some evidence for parallel lamination as a relict fabric where not bioturbated. The dominant lithology is well sorted with silt and very fine sand grains consisting of quartz, clay, and muscovite, with accessory biotite, chlorite, and opaque minerals and rare plagioclase. Facies SS1 can range in thickness from approximately 10 cm up to a rare maximum thickness of 1.5m averaging approximately 20 cm.

#### *Interpretation of Facies SS1*

It is likely that this facies results from a local reduction in sediment supply, perhaps due to local changes in hydrodynamics resulting from autocyclic distributary mouth bar abandonment and reworking by waves and tides.

### ***2.4.2.2 Facies SS2: Thinly laminated micaceous clay-rich siltstone***

The clay-rich siltstones of Facies SS2 are parallel laminated and highly micaceous (Fig. 2.4c,d). Beds are up to 7 cm in thickness, and alternate between being quartz and mica-rich. The intensity of bioturbation is very low, with only rare *Planolites* burrows recognized. Facies SS2 is inter-bedded with S1 and S4 in the uppermost extent of the core.

#### *Interpretation of Facies SS2*

Rhythmic grain-size changes under which this facies was deposited, suggest a fluctuating hydrodynamic conditions. There is no evidence of clay couplets or strong tidal influence on this facies. The depositional setting is thus unclear but is most likely a fluid mud deposit. Inter-bedding with Facies S1 and S4 suggest Facies SS2 was deposited in a proximal distributary mouth bar.

#### **2.4.2.3 Facies SS3: Siltstone with erosive-base**

This pyritic siltstone facies contains only rare mudstone laminae, has a high clay mineral and mica content, intense bioturbation, and few discrete unidentifiable trace fossils distinguishing it from Facies SS1 (Fig. 2.4e,d). The base of this facies is commonly erosive, and the beds may subtly upward-fine. Facies SS3 is commonly inter-bedded with Facies S3.

#### *Interpretation of Facies SS3*

The lack of primary depositional fabric is attributed to a hyperpycnal fluid mud deposit although it is difficult to determine with certainty. An erosive base supports this interpretation. The high pyrite content suggests an originally organic-rich depositional

environment (Potter et al., 2005). Facies SS3 may have been part of the proximal distributary mouth bar.

### **2.4.3 Heterolithic Facies**

#### ***2.4.3.1 Facies H1: Heterolithic bioturbated silty mudstone and fine-grained sandstone***

Distinctive thin heterolithic inter-beds of silty mudstone and fine-grained sandstone (approx. 10cm thick) are moderately bioturbated and common in basal portions of individual parasequences of the Redmans Formation (Fig. 2.5a,b). The very fine-grained sandstone inter-beds are ripple cross-laminated with abundant bioturbation, predominantly *Cruziana*, *Trichophycus*, and *Teichichnus*. *Trichophycus* occurs at the base of sandstone beds in association with the organic-rich tops of the underlying mudstone (Fig. 2.6d). Silt-rich mudstone inter-beds are more intensely bioturbated with trace fossils that show deposit-feeding activity (Fig. 2.5b). The majority of burrows are ellipsoidal due to compaction that postdates bioturbation. Thick beds of Facies S5 (approx. 25cm) separate intervals of thinly inter-bedded H1, M1, and S5 facies.

#### *Interpretation of facies H1*

The conditions under which the sandstones and siltstones were deposited were likely waning flows, though with more limited clay content than in Facies M1. Silt- and clay-rich inter-beds are formed under lower energy conditions than the associated Facies M1 and S5. The silt and clay rich portions of the heterolithic facies are heavily bioturbated probably due to high organic matter content and low rates of sedimentation.

Facies H1 is inferred to have been deposited in prodelta and/or the distal portion of the distributary mouth bars.

#### **2.4.4 Mudstone Facies**

##### ***2.4.4.1 Facies M1: Upward-fining, mudstones with erosive bases and sand-filled burrows***

The upward fining mudstone beds with erosive bases are approximately 2cm in thickness and are commonly inter-bedded with heterolithic mudstones (Facies H1) and sharp-based sandstones (Facies S5) (Fig. 2.5a, 2.7). The mudstones have erosive bases, low bioturbation intensity, and commonly have sand-filled intra-stratal shrinkage cracks (see Harazim et al. 2013). The only burrows are sharp-margined sand-filled burrows that are lithologically identical to the overlying sandstone that crosscut microbial mats (Fig. 2.5c, 2.6f, g, h; cf. Harazim et al., 2013).

##### *Interpretation of Facies M1*

Facies M1 is inferred to have been deposited from a waning mud-rich hyperpycnal flows or “fluid muds” (cf. Harazim et al., 2013). The intra-stratal sand-filled shrinkage cracks demonstrate that the mudstone underwent early burial compaction and dewatering. Since the intra-stratal sand-filled shrinkage cracks (formerly synaeresis cracks, Harazim et al. 2013) are cut by later uncompacted sand-filled (originally open) burrows these burrows post-date sediment compaction but, since they are shallow tier, also demonstrate that the sediment compaction occurred close to the sediment-water interface (Lobza and Schieber, 1999; Harazim, 2013). The frequency of inter-bedding between facies M1, H1,

and S5 suggests deposition in closely associated paleoenvironments. The mudstone for facies M1 is considered to have a riverine source in a wave-dominated setting. This is consistent with the presence of tidal flow modulation observed in Facies S3, S5, and S6 influenced by mixed fluvio-tidal regimes. A riverine source is required to cause deposition of muds in otherwise sand-dominated open marine depositional settings. Sedimentation is however likely to be common in distributary mouth bar settings (cf. McIlroy 2004b).

#### ***2.4.4.2 Facies M2: Thin black mudstone with erosive base***

The homogeneous mudstone beds have low silt content, are up to 5 cm in thickness, and overlie erosive surfaces with up to 6cm of relief (Fig. 2.5d,e). The associated sandstone facies are Facies S1, S3, and S5 with Facies M2 typically occurring at the top of the sandstone beds.

##### *Interpretation of Facies M2*

Facies M2 always immediately postdates erosive events that cut into sandstone beds. The erosional to depositional events are likely to have been powerful mud-laden sediment gravity flows (cf. Harazim et al., 2013). Since the mudstones show no gradational fining it was interpreted that deposition could have occurred instantaneously as a rapidly decelerating event bed (MacKay and Dalrymple, 2011) or may simply reflect the lack of availability of other grain sizes. This facies typically caps inter-bedded genetically related successions of Facies S1, S3 and S5 that are inferred to have been deposited in proximal to distal distributary mouth bar paleoenvironments. Facies M2 was

likely deposited during periods of high fluvial outflow (hyperpycnal flow) and storm-dominated coastal conditions.

## **2.5 DEPOSITIONAL SETTING**

The Redmans Formation is dominated by successions of inter-bedded sandstones, siltstones, and mudstones organized into vertically repeating progradational packages (Fig. 2.7). A combination of thin coarsening upward, cross-stratified, sand-dominated packages inter-bedded with siltstones and erosive mudstones indicates the presence of stacked, prograding distributary mouth bars controlled by autocyclic processes (Tankard and Barwis, 1982; Olariu and Bhattacharya, 2006). The proximal distributary mouth bar deposits are characterized by high-energy hydrodynamic conditions demonstrated by low angle cross-bedding and low levels of bioturbation. The mineralogically immature composition of Facies S1 to S3 is taken to infer a more proximal sediment source and rapid deposition. The presence of the rhythmic mud couplets in these proximal setting indicates a tidally influenced system with rapid deposition (Nio and Yang, 1991). Sandstones inter-bedded with hyperpycnal fluid mudstone are typical of distributary mouth bars with the mudstone partings decreasing in frequency through mouth bar bedsets (Tankard and Barwis, 1982; McIlroy, 2004b). The lack of ichnological evidence for deposit feeding organisms in the mouth bar-associated mudstones is probably due to rapid sediment deposition of the mud-laden sediment gravity flows and burial by subsequent sand-rich deposits.

The more distal distributary mouth bar facies are composed of finely inter-bedded sandstone and siltstone with bioturbation, ripples, and tidal couplets of Facies H1, M1, M2, and S5. Sandstones have sharp contacts and occur as thin beds (approx. 5 cm) with parallel to ripple cross-laminae deposited under varying flow conditions. The presence of tidal couplets in Facies S5 demonstrates tidal influence and a sub-tidal depositional regime (Nio and Yang, 1991). The intense bioturbation but low ichnodiversity in the mudstones of facies H1 suggest high nutrient availability in the sediment but “stressed” environmental conditions. Bed thickness variability within and between facies was related to the hydrodynamics of the depositing event and sediment supply.

The erosive nature of Facies M1, M2, SS2, and SS3 in both the distal and proximal expressions of the distributary mouth bar deposits were likely created under conditions of high-energy, hyperpycnal river discharge producing near-bed mud suspensions with a concentration of >10 g/L suspended sediment (Ichaso and Dalrymple, 2009; Harazim and McIlroy, in press). The generation of these fluid muds indicates proximity to a mud-rich turbidity maximum zone, either in association with the distributary mouth or in a back-barrier setting (cf. McIlroy 2004b). Factors such as the angle of slope, depositional energy, and mud density influence the distance and erosive power of these fluid muds (Ichaso and Dalrymple, 2009; Baas et al., 2011; MacKay and Dalrymple, 2011). The presence of such fluid mud deposits in association with tide-and wave-influence sandstone facies suggests a proximal environment (McIlroy, 2004b). The absence of trace fossils produced by deposit feeding organisms suggests either rapid mud deposition and burial (i.e. sedimentation removes organic matter beyond the reach of the deepest tier burrowers), or that the organic matter deposited is of low quality due to

organic matter remineralization prior to deposition (cf. Harazim and McIlroy, in press). Seafloor turbulence generated by wave- and tide-influence has the potential to remobilize sediment as fluid mud flows (Parsons et al., 2001; Bhattacharya and MacEachern, 2009). As shown in the Tilje Formation from offshore Norway, fluid muds or mud-laden sediment gravity flows, occur quite frequently in distributary mouth bar deltaic settings due to river-flood high mud density discharge deposits (McIlroy, 2004b; McKee et al., 2004).

In a wave-influenced system, mouth bars form close to the channel mouth and form rapidly due to the presence of small waves (Nardin et al., 2013). Mouth bar accretion and terminal distributary channel infilling decrease flow velocity and sediment discharge, resulting in bar abandonment (Olariu and Bhattacharya, 2006). Abandoned distributary mouth bars are subject to lower rates of sedimentation and reworking as indicated by the presence of the highly bioturbated siltstones of Facies SS1. The occurrences of thick packages of heavily bioturbated siltstone likely indicate an abandoned distributary mouth bar.

The Redmans Formation has previously been interpreted as a wave-dominated shelfal paleoenvironment (Brenchley et al., 1993) and as an offshore bar complex (Ranger et al., 1984). Both of these depositional settings are characterized by heterolithic siliciclastic sedimentation with storm and tide influence. In earlier outcrop studies of the Redmans Formation, these sandstones have been demonstrated to be laterally extensive beds or lensoidal beds separated by mudstone inter-beds less than 10cm thick (Brenchley et al., 1993). The great thickness of these sandstone and mudstone deposits in the Bell Island and Wabana Groups (1500m) suggests the presence of a proximal delta with high



rates of sedimentation (Ranger et al., 1984). This study has documented the presence of stacked distributary mouth bar deposits in the Redmans Formation. These mouth bar deposits are, by definition, associated with a riverine system, providing direct evidence of a deltaic system that—given the abundance of storm dominated sedimentation (Brenchley et al. 1993)—is likely to have been wave-dominated delta with tidal processes modulating wave action in ebb tidal deltaic sub-environments (Fig. 2.9). The preservation potential of distributary mouth bars in a wave-dominated delta is dependent upon the efficacy of wave reworking—i.e. wave regime or fetch— (Weise, 1980; Tankard and Barwis, 1982; Dominguez, 1996; Bhattacharya and Giosan, 2003), but also by the rate of sediment supply and availability of accommodation. Distributary mouth bar deposits in low accommodation settings have been considered to have an increased preservation potential in distal delta front environments (Olariu and Bhattacharya, 2006). The distal expression of the Redmans Formation results in the lack of distributary channel and beach facies deposits (Weise, 1980; Bhattacharya and Willis, 2001; Bhattacharya and Giosan, 2003; Olariu and Bhattacharya, 2006).

Hummocky cross stratification indicating oscillatory waves generated by storms have been identified in the Redmans Formation and adjacent formations although it is difficult to identify these features in core (Brenchley et al., 1993). These same facies in core include sedimentological indicators such as tidal couplets and mud drapes indicating the presence of mouth bars—likely wave and storm influenced—rather than straightforward shelfal hummocky cross stratification. Shallow water wave-dominated deltas are typically lobate in shape and build out by the coalescence of distributary mouth bars (Coleman and Wright, 1975; Olariu and Bhattacharya, 2006). The occurrence of

fluid mud deposits supports the presence of a local riverine source (McIlroy, 2004b; Ichaso and Dalrymple, 2009).

## **2.6 SEQUENCE STRATIGRAPHY**

Detailed core logging has delineated three coarsening up cycles in the Redmans Formation, interpreted as parasequences (Figs 2.2, 2.8). The sandstones that comprise the majority of the parasequences coarsen and thicken upwards (Brenchley et al., 1993). The parasequences that compose the Redmans Formation vary in thickness (maximum of 30m) due to changes in time and sediment input rather than an absence of accommodation (Brenchley et al., 1993), current observations support this conclusion.

These high frequency parasequences are composed of wave-dominated delta distributary mouth bar deposits. Each parasequence is composed of a prograding distributary mouth bar complex. The development of these parasequences originates with the alternation of the basal distal distributary mouth bar deposits with more shore proximal deposits. With delta progradation, the more proximal distributary mouth bars dominate and form on top of the more distal expression of the wave-dominated delta paleoenvironment. A discernable parasequence stacking pattern was not present to help clarify the systems tract of the Redmans Formation. The mudstone dominated Beach Formation is situated below the Redmans Formation and has previously been used to infer increased progradation rates and a highstand systems tract (Brenchley et al., 1993). A recent re-evaluation of the Beach Formation mudstones has called this interpretation into question (Harazim et al., in press).

## 2.7 CONCLUSION

Marginal marine mudstone-dominated systems of Palaeozoic age remain poorly understood, and it is therefore crucial to further our knowledge of these systems to more accurately assess the interplay of marginal marine environmental processes at the facies level when assessing the paleoenvironment. Additionally, processes controlling the physical and biological reworking of mud-laden sediment are poorly constrained in the Palaeozoic rock record. The analysis of lithology, sedimentary features, bioturbation, and paleontology are used to classify individual facies and provide clarification as to pre-depositional process controls on both the mudstone and sandstone deposits. Core and thin section analysis provides insight into a detailed interpretation of the stratigraphy, sedimentological facies, and the depositional environment of the Redmans Formation's inter-bedded mudstones and sandstones. This particular core provides microscopic detail and allows for the recognition of high-resolution facies classifications that would otherwise be difficult to determine in outcrop.

The Redmans Formation is composed of thick quartz arenites inter-bedded with intervals of intensely bioturbated mudstone. Sandstone ichnofabrics primarily contain *Diplocraterion* and *Planolites* (10%), compared to mudstone traces that are more diverse and intense, which include *Cruziana*, *Planolites*, *Trichophycus*, *Diplocraterion*, as well as other unidentifiable vertical and sub-vertical traces (20-80%). Unbioturbated to post-depositional, deep tiering bioturbated fluid mudstones were frequent. Twelve sedimentological facies have been categorized into a single facies association, comprising

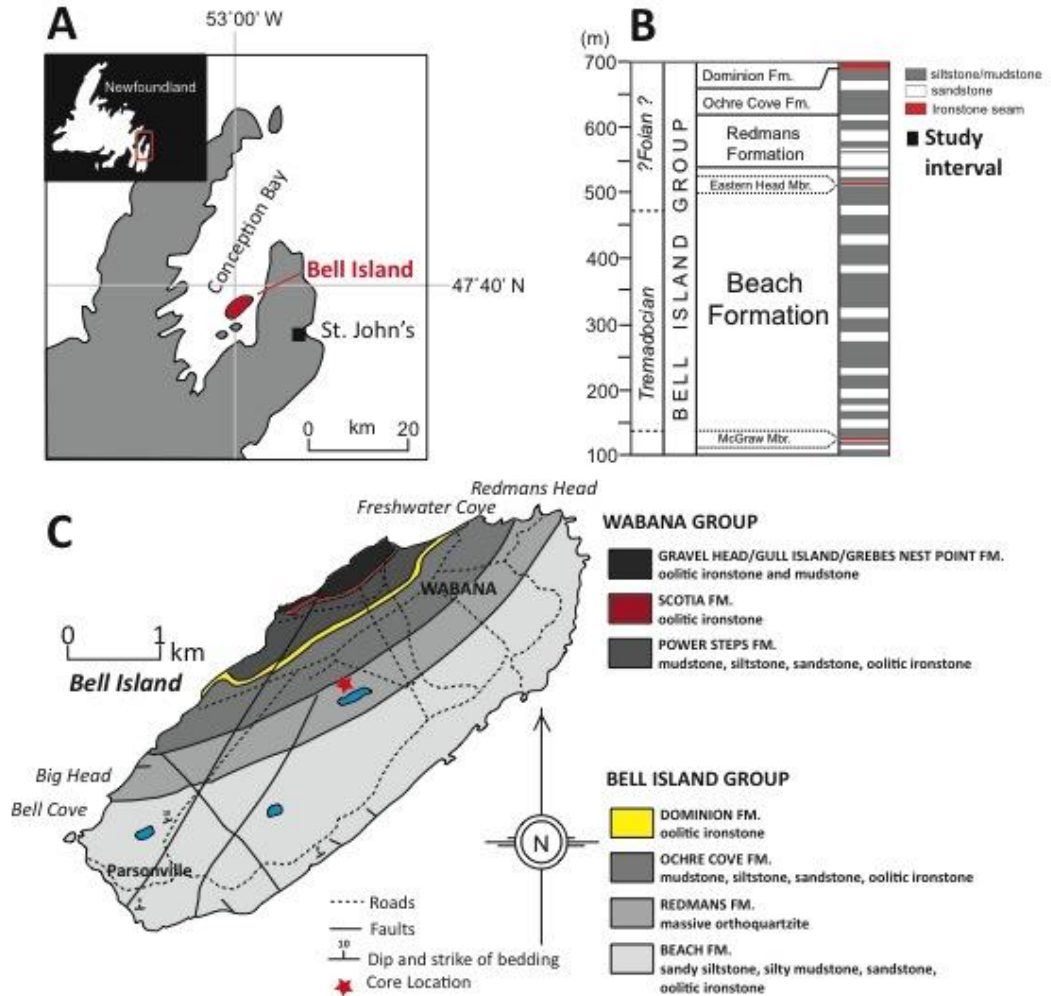
of proximal to distal distributary mouth bars that range from thick sandstones to intensely bioturbated mudstones and siltstones. This implies a unique environment with varying energy levels and probable migrating shoreline position. A wave-dominated delta is the interpreted paleoenvironment with both wave and tidal indicators. Stacked shallow marine parasequences of distributary mouth bar deposits build from a more distal expression to that of a more proximal sandstone body with storm influence. Combining facies into facies associations provides a detailed explanation for the wave-dominated deltaic conditions present during the Redmans Formation deposition during the Early Ordovician.

Further detailed geochemical study of the complicated relationships between the sandstones and mudstones of the Redmans Formation will provide a greater understanding into facies processes and their control on organic carbon isotopic signatures on the global scale. These sedimentological and future geochemical descriptions will allow for a more thorough consideration of the interplay between organic matter abundance, distribution, and biogeochemistry with respect to the paleoenvironment in the Early Ordovician Redmans Formation.

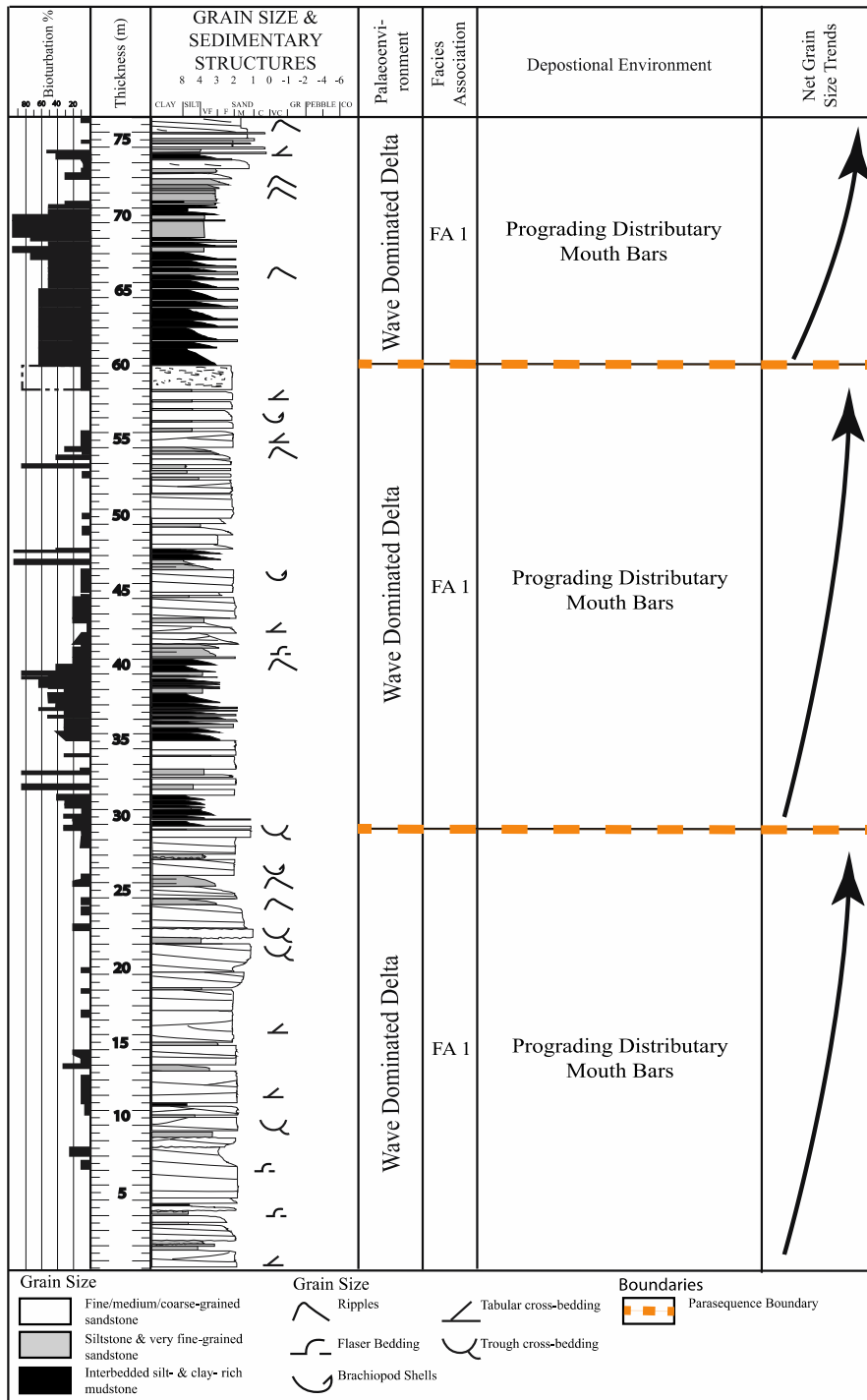
## **2.8 ACKNOWLEDGEMENTS**

We wish to acknowledge our colleagues at Memorial University of Newfoundland for their insightful contribution to the study of the Redmans Formation. Thanks to Dr. Harazim and other members of the ichnology research group at MUN for their support.

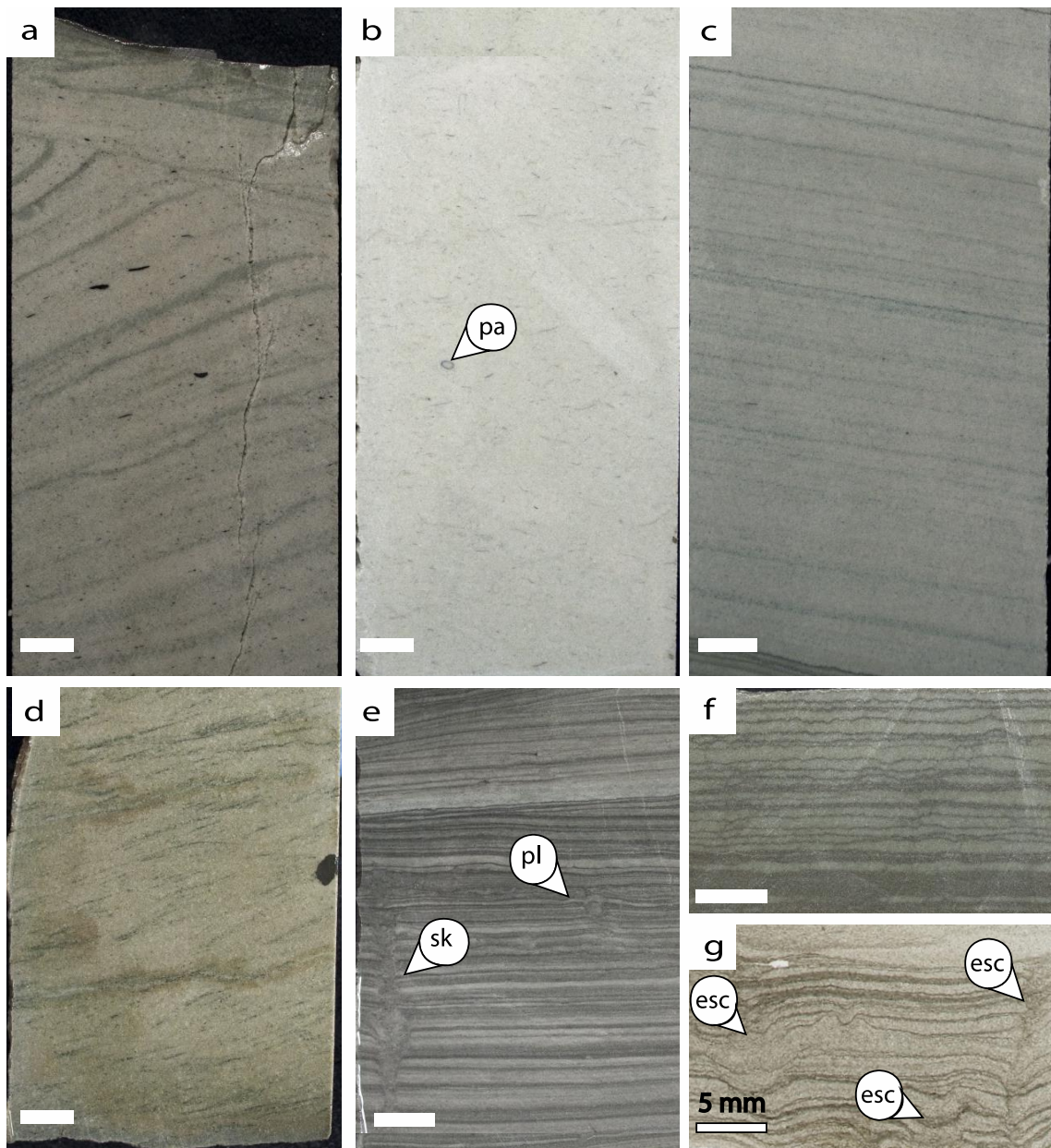
## 2.9 FIGURES AND TABLES



**Fig. 2.1. (a) Bell Island, Newfoundland location map. (b) Stratigraphic section of the Bell Island Group, Redmans Formation. Redmans Formation is Floian in age (~477.7 Ma). (c) Bell Island geological map with the studied core location indicated (modified after Ranger et al., 1984; Harazim et al., 2013).**

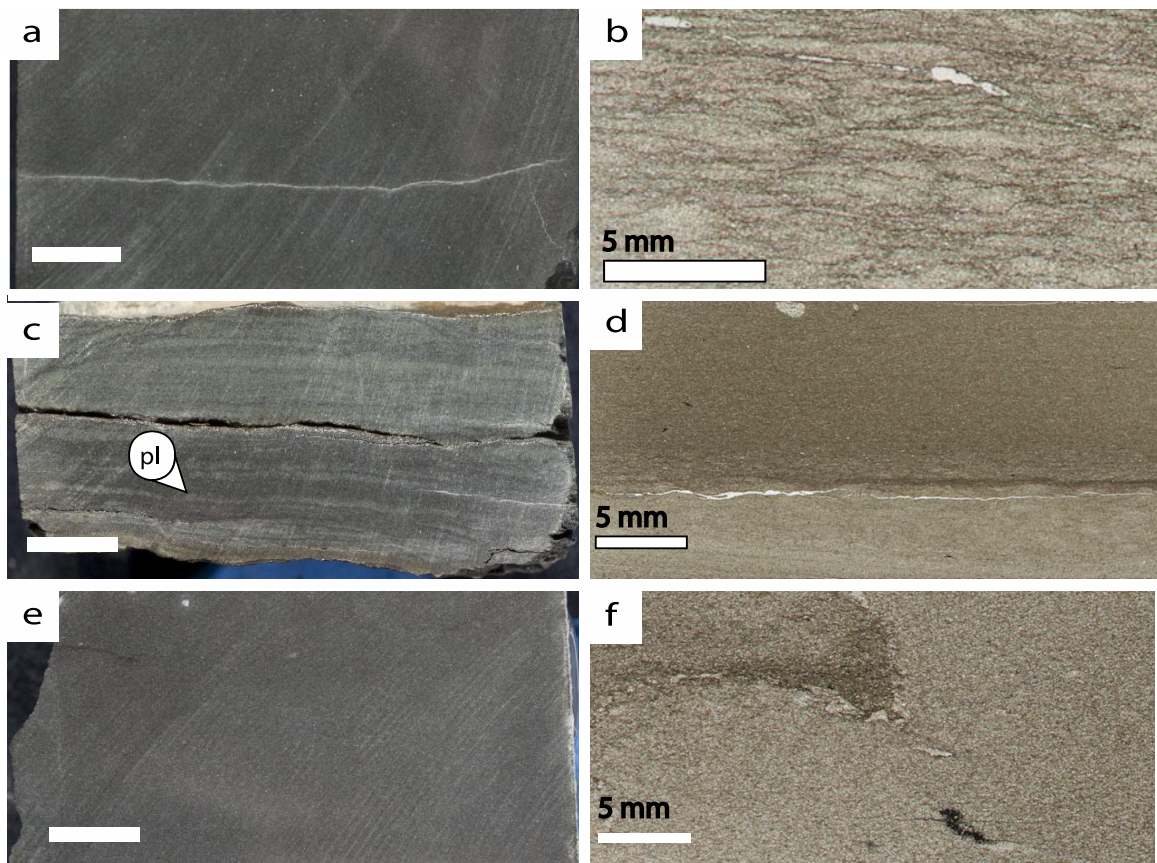


**Fig. 2.2** A summary log of the Redmans Formation's 76.5 m of core from Bell Island, Newfoundland. Showing bioturbation percentage, grain size, sedimentary structures, paleoenvironment, facies association, depositional environment, and grain size trends.



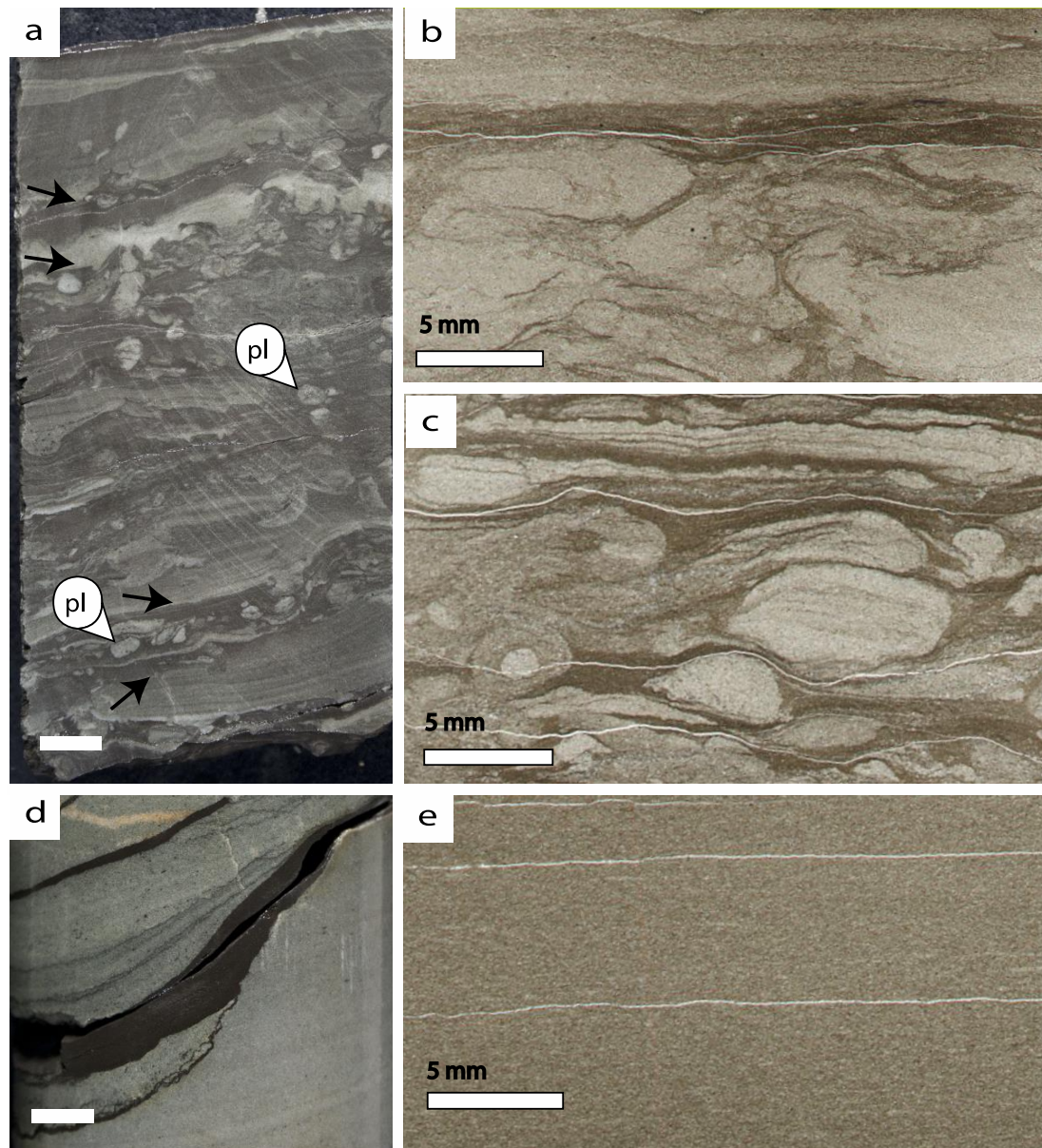
**Fig. 2.3** (a) Facies S1, showing medium-course grained trough cross-stratified sandstone. (b) Facies S2, showing structureless sandstone with possible *Palaeophycus* isp (pa). (c) Facies S3, showing tabular cross-stratified, mud draped sandstone. (d) Facies S4, showing flaser bedded very fine-grained sandstone. (e) Facies S5, showing densely parallel to ripple cross-laminated sandstone with *Planolites* isp (pl) and *Skolithos* isp (sk). (f) Facies S6, showing densely mud draped siltstone. (g) Facies S6 in a thin section scan (perpendicular to bedding) with mud couplets and escape traces (esc). Each unlabelled white box indicates a scale of 1cm.





**Fig. 2.4** (a) Facies SS1, showing silty sandstone. (b) Facies SS1, showing intensely bioturbated silty sandstone dominated by *Planolites isp* (pl) in thin section. (c) Facies SS2, showing thinly laminated clay rich siltstone with *Planolites isp* (pl). (d) Facies SS2, showing laminated clay rich siltstone and minor bioturbation. (e) Facies SS3, showing erosive based siltstone. (f) Facies SS3, showing erosive siltstone with possible unidentifiable bioturbation. Each unlabelled white box indicates a scale of 1cm.

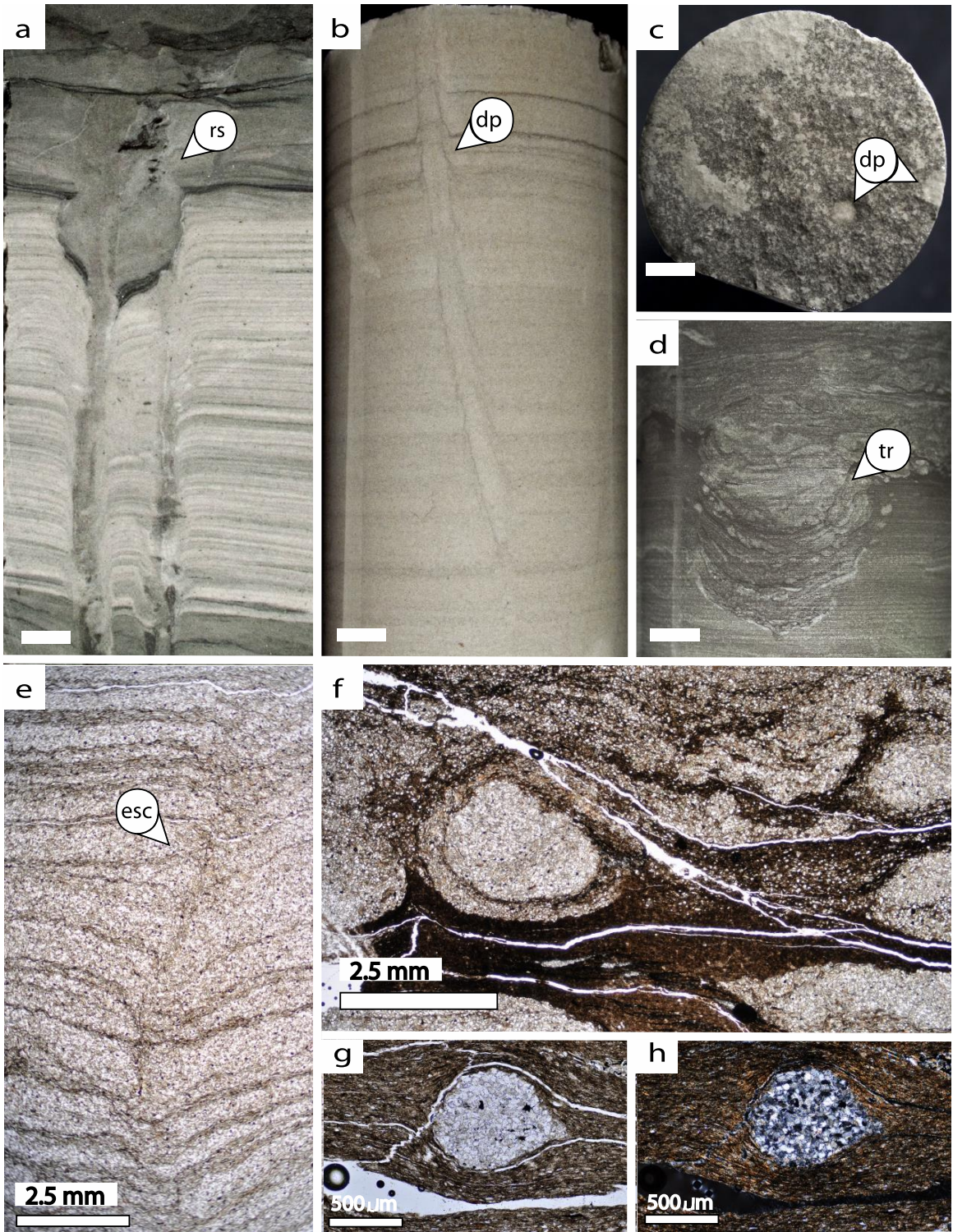




**Fig. 2.5** (a) Facies H1 and M1, showing a heterolithic bioturbated silty mudstone with interbeds of upward fining mudstones that contain sand-filled burrows including *Planolites isp* (pl) and have erosive bases marked with an arrow. (b) Facies H1, showing heterolithic silty mudstone with mantle swirl bioturbation due to deposit feeding organisms. (c) Facies M1, showing upward fining mudstone with sand-filled burrows such as *Planolites isp*, vertical dwelling burrows and erosive bases. (d) Facies M2, erosive black mudstone. (e) Facies M2, showing the erosive dark mudstones in thin section with no structures or bioturbation. Each unlabelled white box indicates a scale of 1cm.

**Fig. 2.6 (a) *Rosselia* isp (rs) from Facies S5 disturbing original laminations. (b) Facies S3 showing characteristic *Diplocraterion* isp (dp), approximately 10cm long. (c) A perpendicular cut to the core shows two openings of *Diplocraterion* isp (dp) in Facies S3. (d) Greatly disturbed section of Facies H1 and M1 by what appears to be *Trichophycus* isp (tr). (e) Escape traces (esc) of Facies S5 in a thin section scan. (f) Facies M1 sharp walled sand filled burrows with an upper wavy surface of a possible microbial mat. (g) Plan polarized and (h) cross-polarized thin section of a sharp walled burrow of Facies M1. Each white box, unless labeled otherwise, indicates a scale of 1cm.**

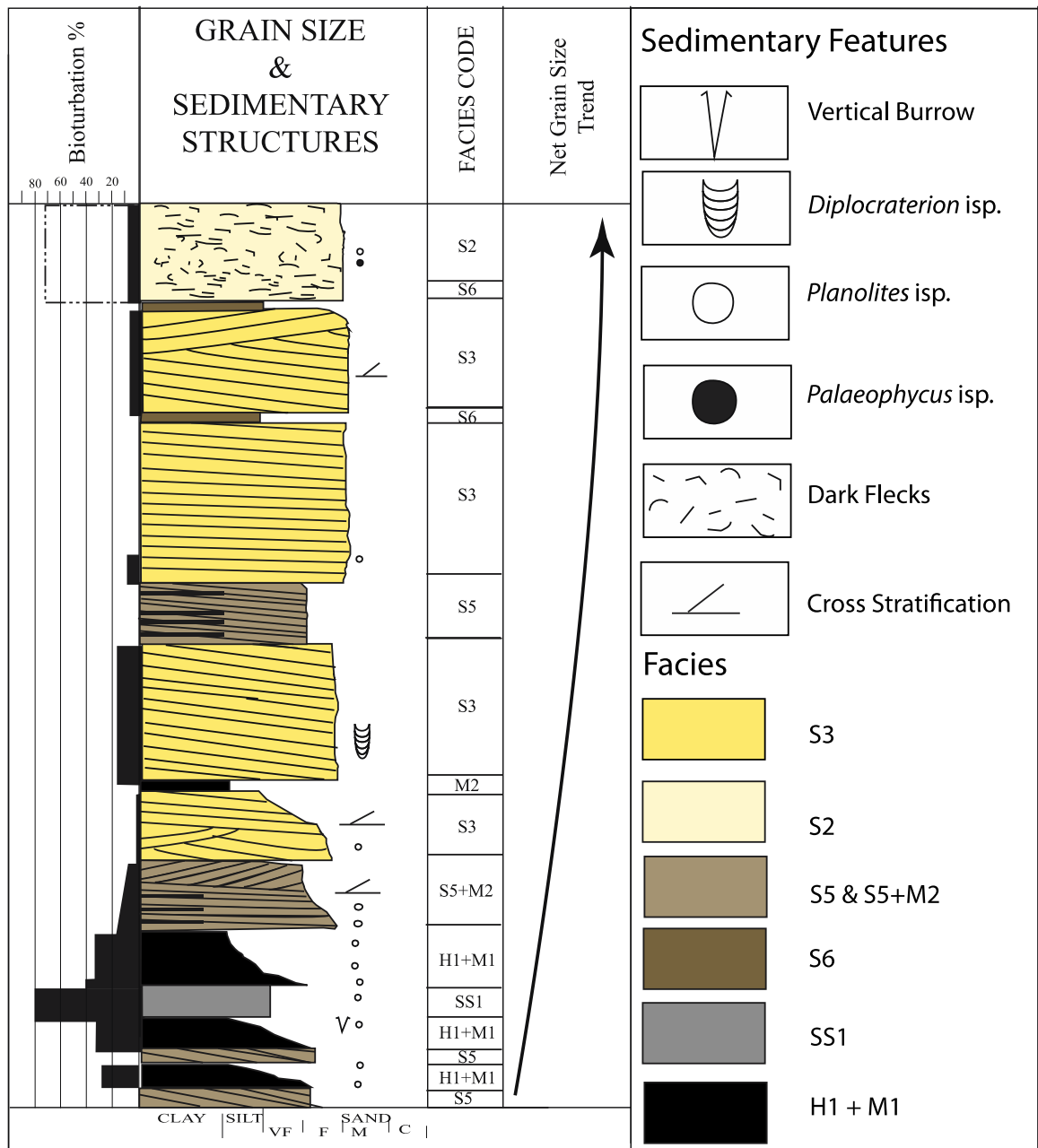




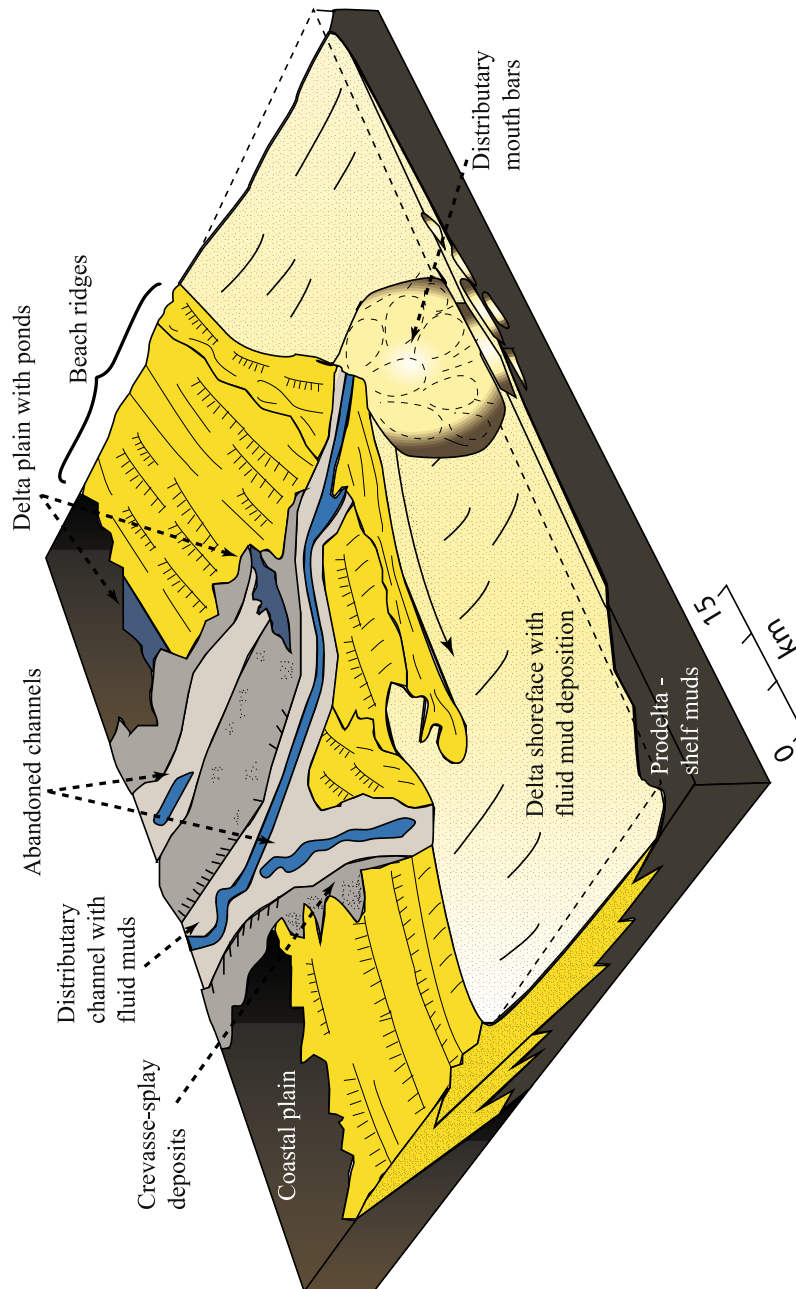


**Fig. 2.7 Idealized distributary mouth bar facies association with distal inter-bedded mudstones, siltstones, and very fine grained sandstones coarsening upwards into more proximal trough and cross-stratified sandstones with erosive muds.**





**Fig. 2.8** Idealized distributary mouth bar parasequence coarsens up from a more distal mouth bar expression to that of a more proximal mouth bar. These bars prograde and range in thickness from 7 m to 30 m.



**Fig. 2.9** Wave-dominated delta is the interpreted paleoenvironment in which the distributary mouth bars of the Redmans Formation were deposited. Erosive fluid muds were likely carried in from the distributary channel (modified from Weise, 1980).

**Table 2.1. Table summarizing the sedimentology, mineralogy, palaeontology, and ichnology of the mudstones and sandstones within the Redmans Formation.**

Facies code	Facies name	Facies Association	Lithology	Sedimentary structures and palaeontology	Composition and mineralogy	Ichtnology	Interpreted depositional environment
S1	Medium grained, rough cross-stratified sandstone	FA1	Clay, silt, and medium sand	Millimeter- to centimeter-thick steep angled cross-lamination; erosional based with mudstone rip up clasts. Phosphate: linguistid brachiopods	Bimodal: subangular quartz, chert, calcite, equant muscovite and biotite; scattered opaques, chlorite, clay minerals, and plagioclase; poliktophic calcite cement	BI 0	Proximal distributary mouth bar
S2	Structure-less sandstone	FA1	Fine to medium grained sand	Dark flecks; deswatering; no internal sedimentary features	Subangular quartz; equant muscovite; replacement of grains by chlorite; scattered plagioclase, and opaques	Possible burrow mottled or isolated remineralized burrow lining; BI 1 or BI 6	Proximal distributary mouth bar
S3	Planar cross-stratified, mud draped sandstone	FA1	Fine to medium grained sand, clay	Millimeter-sized wavy, even parallel laminae, mud drapes, mud complets, ripples and pressure solution	Subangular quartz; equant muscovite; replacement of grains by chlorite; scattered plagioclase, biotite, clay minerals, pyrite and opaques	Centimeter-sized <i>Diplocraterion</i> , <i>Tetradichinus</i> , and vertical traces; BI 2	Proximal distributary mouth bar
S4	Flaser bedded very fine-grained sandstone	FA1	Very fine sand	Millimeter thick even parallel and discontinuous even parallel laminae; flaser bedding, wave ripples	Subangular quartz; equant biotite and muscovite; replacement of grains by chlorite; scattered opaques, and plagioclase	Centimeter-sized low diversity, vertical traces; BI 1	Proximal distributary mouth bar
S5	Parallel to ripple cross-laminated sandstone	FA1	Clay-bearing, silt and very fine sand dominated	Dense millimeter even parallel to nonparallel laminations; flaser bedding, rhythmic mud laminae, wave ripples	Subangular quartz; equant muscovite and biotite; clay minerals; replacement of grains by chlorite; scattered opaques, pyrite, and plagioclase	Centimeter-sized, shallow tiered, <i>Planolites</i> , <i>Trichophyrens</i> , <i>Rossetia</i> , <i>Stalithos</i> , and escape traces; BI 0-2; rare cross-cutting	Distributary mouth bar
S6	Parallel laminated very fine-grained sandstone and silty sandstone	FA1	Silt and clay bearing	Even parallel laminae defined by quartz and clay proportions; mud complets	Subangular quartz; equant biotite and muscovite; clay minerals; replacement of grains by chlorite; clay minerals; rare plagioclase	Centimeter-size; <i>Planolites</i> , and escape burrows; BI 0-1	Subtidal distributary mouth bar
SS1	Intensely bioturbated sandy siltstone	FA1	Silt and clay	No physical sedimentary structures; rare fining up cycles	Subangular quartz; equant muscovite, and biotite; clay mineral dominant; replacement of grains by chlorite; scattered opaques, pyrite, and plagioclase	Millimeter to centimeter-sized low diversity burrow-mottled; silt infill burrows; BI 5	Abandoned distributary mouth bar
SS2	Thinly laminated micaceous clay rich siltstone	FA1	Silt and clay-rich	Millimeter even parallel laminae alter between quartzose and micaceous; ripple cross-lamination	Subangular quartz; equant biotite and muscovite; clay minerals; replacement of grains by chlorite; scattered opaques, and plagioclase	Millimeter-sized <i>Planolites</i> ; BI 0-2	Proximal distributary mouth bar
SS3	Siltstone with erosive-base	FA1	Silt and clay	Millimeter-sized even parallel quartz rich laminations at contacts; mud stringers; no internal physical sedimentary features; erosive based	Subangular quartz; equant muscovite, and biotite; clay mineral dominant; scattered opaques; pyrite	BI 0	Proximal distributary mouth bar
H1	Heterolithic bioturbated silty mudstone and fine-grained sandstone	FA1	Clay, silt, and very fine sand; very fine sand infilling burrows.	Centimeter thick heterolithic laminated sandstone and silty mudstone with ripple cross-laminae; erosional and gradational contacts	Subangular quartz grains; and rare plagioclase; equant muscovite and clay minerals dominate mudier portions; scattered opaques, plagioclase, and phosphate	Millimeter to centimeter-sized, shallow tiered <i>Planolites</i> , <i>Diplocraterion</i> , <i>Trichophyrens</i> , <i>Cruziana</i> and other unidentifiable traces, mangle and swirl structure; BI 3-4; common cross-cutting	Distal distributary mouth bar
M1	Upward-fining, mudstone with erosive bases and sand-filled burrows	FA1	Clay and silt bearing; very fine sand infilling burrows	Erosive centimeter beds; fining upwards from silty mudstone to organic rich mudstone; microbial mat upper bed boundary; shrinkage cracks, scours	Subangular quartz; equant muscovite, and biotite; clay mineral dominant; scattered opaques	Millimeter to centimeter-sized, shallow tiered <i>Planolites</i> , <i>Diplocraterion</i> , <i>Trichophyrens</i> , and <i>Cruziana</i> ; BI 1-2; common cross-cutting	Distal distributary mouth bar
M2	Thin black mudstone with erosive base	FA1	Clay and silt bearing	Erosive centimeter beds; millimeter-sized mud stringers; no internal physical sedimentary features	Subangular quartz; equant muscovite, and biotite; clay mineral dominant; replacement of grains by chlorite; scattered opaques	BI 0	Distributary mouth bar



## 2.10 REFERENCES

- Baas, J. H., Best, J. L., and Peakall, J., 2011, Depositional processes, bedform development and hybrid bed formation in rapidly decelerated cohesive (mud–sand) sediment flows: *Sedimentology*, v. 58, no. 7, p. 1953-1987.
- Bhattacharya, J., and Walker, R. G., 1991, River-and wave-dominated depositional systems of the Upper Cretaceous Dunvegan Formation, northwestern Alberta: *Bulletin of Canadian Petroleum Geology*, v. 39, no. 2, p. 165-191.
- Bhattacharya, J. P., and Giosan, L., 2003, Wave-influenced deltas: Geomorphological implications for facies reconstruction: *Sedimentology*, v. 50, no. 1, p. 187-210.
- Bhattacharya, J. P., and MacEachern, J. A., 2009, Hyperpycnal rivers and prodeltaic shelves in the Cretaceous seaway of North America: *Journal of Sedimentary Research*, v. 79, no. 4, p. 184-209.
- Bhattacharya, J. P., and Willis, B. J., 2001, Lowstand deltas in the Frontier Formation, Powder River Basin, Wyoming: implications for sequence stratigraphic models: *AAPG bulletin*, v. 85, no. 2, p. 261-294.
- Brenchley, P. J., Pickerill, R. K., and Stromberg, S. G., 1993, The role of wave reworking on the architecture of storm sandstone facies, Bell Island Group (Lower Ordovician), eastern Newfoundland: *Sedimentology*, v. 40, no. 3, p. 359.
- Brettel, M., McIlroy, D., Elliott, T., Davies, S., and Waters, C., 2002, Identifying cryptic tidal influences within deltaic successions: an example from the Marsdenian (Namurian) interval of the Pennine Basin, UK: *Journal of the Geological Society*, v. 159, no. 4, p. 379-391.

- Cocks, L., and Torsvik, T., 2002, Earth geography from 500 to 400 million years ago: a faunal and palaeomagnetic review: *Journal of the Geological Society*, v. 159, no. 6, p. 631-644.
- Cocks, L. R. M., McKerrow, W. S., and vanStaal, C. R., 1997, The margins of Avalonia: *Geological Magazine*, v. 134, no. 5, p. 627-636.
- Coleman, J. M., and Wright, L., 1975, Modern river deltas: variability of processes and sand bodies.
- Davies, D. K., Ethridge, F. G., and Berg, R. R., 1971, Recognition of barrier environments: *AAPG Bulletin*, v. 55, no. 4, p. 550-565.
- Fillion, D., and Pickerill, R. K., 1990, Ichnology of the Upper Cambrian? to Lower Ordovician Bell Island and Wabana groups of eastern Newfoundland, Canada: *Palaeontographica Canadiana*.
- Goldring, R., 1995, Organisms and the substrate: response and effect: Geological Society, London, Special Publications, v. 83, no. 1, p. 151-180.
- Harazim, D., 2013, High-energy seafloor processes and biological reworking as first-order controls on mudstone composition and geochemistry [Phd: Memorial University of Newfoundland].
- Harazim, D., Callow, R. H. T., and McIlroy, D., 2013, Microbial mats implicated in the generation of intrastratal shrinkage ('synaeresis') cracks: *Sedimentology* 60, 1621-1638.
- Harazim, D., and McIlroy, D., in press, Wave-advected dispersal of mud in the Cambro-Ordovician Bell Island Group: High-resolution stratigraphy and diagenetic framework. *Journal of Sedimentary Research*

- Ichaso, A. A., and Dalrymple, R. W., 2009, Tide- and wave-generated fluid mud deposits in the Tilje Formation (Jurassic), offshore Norway: *Geology*, v. 37, no. 6, p. 539-542.
- Lobza, V., and Schieber, J., 1999, Biogenic sedimentary structures produced by worms in soupy, soft muds: observations from the Chattanooga Shale (Upper Devonian) and experiments: *Journal of Sedimentary Research*, v. 69, no. 5.
- MacKay, D. A., and Dalrymple, R. W., 2011, Dynamic Mud Deposition In A Tidal Environment: The Record of Fluid-Mud Deposition In the Cretaceous Bluesky Formation, Alberta, Canada: *Journal of Sedimentary Research*, v. 81, no. 12, p. 901-920.
- McIlroy, D. 2004a, Some ichnological concepts, methodologies, applications and frontiers: Geological Society, London, Special Publications, v. 228, p. 3-27
- McIlroy, D., 2004b, Ichnofabrics and sedimentary facies of a tide-dominated delta: Jurassic Ile Formation of Kristin Field, Haltenbanken, Offshore Mid-Norway: Geological Society, London, Special Publications, v. 228, no. 1, p. 237-272.
- McIlroy D., 2008, Ichnological analysis: The common ground between ichnofacies workers and ichnofabric analysts: *Palaeogeography, Palaeoclimatology, Palaeoecology*, v. 270, no. 3, p. 332-338.
- McKee, B. A., Aller, R. C., Allison, M. A., Bianchi, T. S., and Kineke, G. C., 2004, Transport and transformation of dissolved and particulate materials on continental margins influenced by major rivers: benthic boundary layer and seabed processes: *Continental Shelf Research*, v. 24, no. 7-8, p. 899-926.

- Miller, H. G., 1983, A geophysical interpretation of the geology of Conception Bay, Newfoundland: *Canadian Journal of Earth Sciences*, v. 20, no. 9, p. 1421-1433.
- Nardin, W., Mariotti, G., Edmonds, D. A., Guercio, R., and Fagherazzi, S., 2013, Growth of river mouth bars in sheltered bays in the presence of frontal waves: *Journal of Geophysical Research: Earth Surface*, v. 118, no. 2, p. 872-886.
- Nio, S.-D., and Yang, C.-S., 1991, Diagnostic attributes of clastic tidal deposits: a review.
- Olariu, C., and Bhattacharya, J. P., 2006, Terminal distributary channels and delta front architecture of river-dominated delta systems: *Journal of Sedimentary Research*, v. 76, no. 2, p. 212-233.
- Parsons, J. D., Bush, J. W., and Syvitski, J. P., 2001, Hyperpycnal plume formation from riverine outflows with small sediment concentrations: *Sedimentology*, v. 48, no. 2, p. 465-478.
- Passey, Q. R., Bohacs, K., Esch, W. L., Klimentidis, R., and Sinha, S., 2010, From oil-prone source rock to gas-producing shale reservoir—geologic and petrophysical characterization of unconventional shale-gas reservoirs: Beijing, China, June, v. 8.
- Pemberton, S. G., MacEachern, J. A., and Frey, R. W., 1992, Trace fossil facies models: environmental and allostratigraphic significance: *Facies models: response to sea level change*, p. 47-72.
- Potter, P. E., Maynard, J. B., and Depetris, P. J., 2005, *Mud and mudstones: Introduction and overview*, Springer.
- Prigmore, J. K., Butler, A. J., and Woodcock, N. H., 1997, Rifting during separation of Eastern Avalonia from Gondwana: Evidence from subsidence analysis: *Geology*, v. 25, no. 3, p. 203-206.

- Quin, J. G., 2011, Is most hummocky cross-stratification formed by large-scale ripples?:  
Sedimentology, v. 58, no. 6, p. 1414-1433.
- Ranger, M. J., 1979, The stratigraphy and depositional environment of the Bell Island  
group, the Wabana group, and the Wabana iron ores, of Conception Bay,  
Newfoundland [Masters: Memorial University of Newfoundland.
- Ranger, M. J., Pickerill, R. K., and Fillion, D., 1984, Lithostratigraphy of the Cambrian?  
– Lower Ordovician Bell Island and Wabana groups of Bell, Little Bell, and  
Kellys islands, Conception Bay, eastern Newfoundland: Canadian Journal of  
Earth Sciences, v. 21, no. 11, p. 1245-1261.
- Rose, E. R., 1952, Torbay map-area, Newfoundland: Geological Survey of Canada, v.  
Memoir 265.
- Schieber, J., and Zimmerle, W., 1998, The history and promise of shale research: Shales  
and Mudstones. Basin Studies, Sedimentology and Paleontology, Stuttgart:  
Schweizerbart'sche Verlagsbuchhandlung, v. 1, p. 1-10.
- Seilacher, A., 1967, Bathymetry of trace fossils: Marine geology, v. 5, no. 5, p. 413-428.
- Tankard, A. J., and Barwis, J. H., 1982, Wave-dominated deltaic sedimentation in the  
Devonian Bokkeveld Basin of South Africa: Journal of Sedimentary Research, v.  
52, no. 3.
- Torsvik, T. H., 1998, Palaeozoic palaeogeography: a North Atlantic viewpoint: GFF, v.  
120, no. 2, p. 109-118.
- Weise, B. R., 1980, Wave-dominated delta systems of the Upper Cretaceous San Miguel  
Formation, Maverick Basin, South Texas, Bureau of Economic Geology,  
University of Texas at Austin.

## Chapter 3

# **Implications for Organic Carbon Cycling in an Early Ordovician Wave-dominated Delta: Redmans Formation, Bell Island, Newfoundland**

---

Tiffany Miller and Duncan McIlroy

### **3.1 ABSTRACT**

On the modern earth more than 50% of all organic carbon is disseminated as river-borne particulate organic matter along high-energy, muddy coastlines and is subjected to frequent wave reworking, tide-controlled grain size sorting, and bioturbation. These processes control the remineralization proficiency of organic particles and influence the total organic carbon content (TOC, wt %) and quality ( $\delta^{13}\text{C}_{\text{org}}$ , ‰) of sedimentary organic matter. The fundamental processes underlying organic carbon preservation in early Palaeozoic mud-dominated shelves are currently less well constrained. Pathways of carbon cycling and sequestration are comparatively well understood from modern muddy coastlines.

This research presents combined sedimentological and geochemical data from a mud-rich, tidally influenced, wave-dominated deltaic succession (Early Ordovician Redmans Formation, Bell Island, Newfoundland). Mudstone, siltstone, and silty sandstone exhibit TOC values with a spread of 0.8%. The compositional heterogeneity of sedimentary organic matter has an isotopic range of approx. 4.3‰, explained by varying amounts of remineralization due to both physical and biological seafloor reworking processes. A combination of detailed facies descriptions with geochemical analyses from

mudstones and siltstones can be integrated into a paleoenvironmental outline that allows for a thorough interpretation of facies control on organic carbon chemostratigraphy.

### **3.2 INTRODUCTION**

The Early Ordovician Redmans Formation of Bell Island is situated 5 km off the coast of the Avalon Peninsula, Newfoundland in Conception Bay (Fig. 3.1). This study is based on a newly acquired 76.5 m long core through the Redmans Formation. The succession is composed of thick-bedded quartz arenites inter-bedded with intervals of bioturbated and unbioturbated mudstones that are inferred to have been deposited in a tide- and wave-influenced deltaic setting (Fig. 3.2; Miller and McIlroy in press; Chapter 2). Sandstone facies are sparsely bioturbated (0-10%) and contain a low-diversity trace fossil assemblage of *Diplocraterion* and *Planolites* (Table 3.1). The mudstones can be subdivided into: 1) unbioturbated mudstone facies of the Redmans Formation, interpreted as fluid mud deposits; and 2) bioturbated (30-90%) silt- and clay-rich mudstones with an ichnological assemblage that includes *Cruziana*, *Planolites*, *Trichophycus*, and *Diplocraterion* (Table 3.1).

Within the Redmans Formation, the distributary mouth bars deposits contain both slowly deposited fair-weather mudstone beds, and rapidly deposited fluid mud deposits depending on the paleoenvironment of deposition—particularly, proximity to distributary channels—and the periodicity of hyperpycnal flows that are inferred to be related to high sediment discharge events and storm processes. Fair-weather mudstones are considered to have been deposited from suspension settling in quiescent offshore settings, and in

association with abandoned distributary mouth bars. During periods of high fluvial discharge, dense, mud-rich hyperpycnal flows fluid mudstones are inferred to have been flushed from brackish coastal paleoenvironments (turbidity maximum of channels and lagoons) and re-deposited in marginal marine environments (cf. McIlroy 2004) possibly after multiple phases of deposition and re-suspension (e.g. Harazim and McIlroy in press). The majority of the sandstones in the Redmans Formation are inferred to have been deposited in association with distributary mouth bars, since most facies show evidence for both wave and tide activity (Miller and McIlroy in press; Chapter 2). The sandstones that comprise the majority of the parasequences in the Redmans Formation show upward coarsening and thickening trends (Brenchley et al., 1993; Miller and McIlroy in press). There were no discernable parasequence stacking patterns to help elucidate the systems tract to which the Redmans Formation belongs, however, it does overlie the mudstone dominated Beach Formation, which has been used previously to infer increased progradation rates and a highstand systems tract (Brenchley et al., 1993). This however has been called into question through recent re-evaluation of the Beach Formation mudstones (Harazim and McIlroy, in press).

The Redmans Formation is constrained by graptolite and acritarch assemblages from the adjacent Power Steps, Ochre Cove, and Beach Formation. The occurrence of the *Didymograptus simulans* graptolite in the Power Steps Formation, underlying the Redmans Formation (Fig. 3.1), demonstrates that the Redmans Formation can be no younger than the upper boundary of the Floian *D. simulans* biozone. The Redmans Formation can in addition be no younger than the acritarch assemblage identified in the stratigraphically higher Floian Ochre Cove Formation: *Peteinosphaeridium palmatum*,



*Striatotheca microrugulata*, *Striatotheca principalis*, *Tunisphaeridium? eligmosum*, *Veryhachium horridum*, and *Vogtlandia flos* (Dean and Martin, 1978). The Redmans Formation can be no older than the stratigraphically lower Tremadocian/Floian Beach Formation acritarch assemblage: *Acanthodiacrodium uniforme*, *Coryphidium bohemicum*, *Cymatiogalea granulate*, *Dictyotidium? dentatum*, *Pirea aff. P. ornate*, *Striatotheca principalis parva*, *Tectitheca filigera*, *Veryhachium lairdi*, and *Vogtlandia coalita* (Dean and Martin, 1978).

Modern continental shelves are important sites for both terrigenous and autochthonous organic carbon burial (Tyson, 1995; Burdige, 2005). Despite the importance of ancient shelfal environments in petroleum systems, there is surprisingly little work relating sediment transport and bioturbation to the quality and quantity of organic matter in shelfal mudstones. This paper aims to broaden the understanding of heterolithic depositional paleoenvironments in the Paleozoic, using an integrated combination of sedimentological, ichnological, and geochemical studies.

Determining the relative importance of physical and biological controls on the remineralization efficiency of organic matter in ancient marine paleoenvironments—as reflected in TOC, and  $\delta^{13}\text{C}_{\text{org}}$ , ‰—is problematic. This is due to the effects of metabolic processes and physical seafloor reworking on the geochemical composition of sediments (Harazim, 2013). The Cambro-Ordovician is of particular importance for the development of models to explain the organic matter composition of shelfal sediments since: 1) there is no significant allochthonous organic matter from terrigenous sources (Kenrick and Crane, 1997; Wellman et al., 2003; Gensel, 2008; Kenrick et al., 2012); and 2) bioturbation is inferred to have reached effectively modern levels (McIlroy & Logan

1999). As such the carbon cycle is simpler than that of modern shelfal systems, allowing us to study the inter-relationships of autochthonous basinal productivity as it is affected by physical process and bioturbation in the absence of terrigenous plant material. This study aims to investigate the significance of biogenic and physical reworking on the relationships between total organic carbon content (TOC, wt %) and quality ( $\delta^{13}\text{C}_{\text{org}}$ , ‰) on a facies by facies basis.

Chemostratigraphy focuses on geochemical perturbations in the global carbon cycle, identified by excursions or shifts in stable isotopic signatures (Pancost et al., 1999; Blair and Aller, 2012; Davies et al., 2012). The Early Ordovician carbon cycle is however relatively uneventful with regards to stable carbon isotope geochemistry as no global  $\delta^{13}\text{C}_{\text{org}}$  excursions currently exist (Bergstroem et al., 2009). The interpretation of ancient organic carbon stable isotopic excursions in marine basins based on whole rock bulk organic matter rather than biomarker-specific isotopes, is complicated by the potential for variability in organic matter transport, provenance, and degradation (Pancost et al., 1999; Davies et al., 2012). Organic carbon isotopic excursions in chemostratigraphic studies require the understanding of sedimentological heterogeneities derived in nearshore marginal marine mudstones. This study addresses the sedimentological context of the Redmans Formation in relation to organic matter composition and isotopic variability on the global carbon cycle. Understanding variations in TOC and  $\delta^{13}\text{C}_{\text{org}}$  on a facies by facies basis has the potential to inform the use, and reveal the misuse, of stable organic carbon isotopes in chemostratigraphy.

### **3.3 METHODS AND MATERIALS**

#### **3.3.1 Sampling strategy and rock description**

This study builds on our earlier documentation of the sedimentology of the Bell Island Redmans Formation core at a variety of scales, which used both hand samples and a total of 46 polished thin sections (Miller and McIlroy in press). Sedimentary structures, bedding, contacts, lithology, and grain-size were recorded at centimeter scale. Ichnological datasets were collected using the ichnological analysis method outlined in (McIlroy 2004, 2008).

#### **3.3.2 Geochemical measurements**

A total of 53 mudstone and siltstone samples were collected from core for whole-rock TOC and  $\delta^{13}\text{C}_{\text{org}}$  analysis. Approximately 1.5 g was prepared into a powder, decalcified with 5M hydrochloric acid, washed with deionized water, and then left to dry in tin capsules. The dried samples were then ground with a mortar and pestle and using a Mettler Toledo microbalance the powdered samples were weighed out into tin capsules of 1.5-2 milligram portions. Samples were analysed using a Carlo-Erba NA1500 Elemental Analyser (EA), and a Delta V Plus mass spectrometer to determine TOC (wt %) and  $\delta^{13}\text{C}_{\text{org}}$  (‰) values reported to the Vienna Pee Dee Belemnite standard (V-PDB). To assess accuracy, every seventh sample was run as a duplicate. Samples and standards were reproduced within  $\pm 0.1\%$  for TOC values and  $< 0.2\%$  for  $\delta^{13}\text{C}_{\text{org}}$ .

#### **3.3.3 Fourier-Transform-Infrared Spectroscopy (FTIR)**

Fourier transform infrared (FT-IR) spectroscopy, employing attenuated total reflection (ATR) mode, was used to screen decalcified samples and to subsequently

eliminate samples containing insoluble manganiferous or ferroan carbonate that are common in the succession. The FT-IR spectrometer analyzes a small sample of powder by identifying the structure of elemental bonds as a characteristic spectrum. Samples with peaks at  $1400\text{ cm}^{-1}$  on the spectrum can be determined to contain carbonates and must therefore be removed for future analysis since the stable isotopes of carbonate carbon are typically much heavier than those of organic carbon.

### **3.4 RESULTS**

#### **3.4.1 Geochemical characteristics**

High-energy mudstone beds exhibit large organic carbon isotopic excursions (Fig. 3.3 and Table 3.1). Stable organic carbon isotopic values ranging from  $-25.6\text{‰}$  to  $-30.3\text{‰}$  (a difference of  $4.3\text{‰}$ ) and TOC from  $0.06\%$  to  $0.84\%$  (a difference of  $<0.8\text{ wt \%}$ ) were documented through the 76 m of Redmans Formation core (Fig. 3.3). Possible fragmented microbial mats and amorphous organic matter were identified as dark brown to opaque stringers within mudstones (Fig. 3.4). The relationship between  $\delta^{13}\text{C}_{\text{org}}$  and TOC follows an exponential trend and exhibits an  $R^2$  value of 0.38 (Fig. 3.8e). The slope of this curve approximates organic matter recycling with the degradation of organic matter; lower TOC content and isotopically heavier carbon (Tyson, 1995).

Bioturbated facies dominated by deposit feeding burrows are found to have a narrow range of isotopic values ( $-27.1\text{‰}$  to  $-29.6\text{‰}$ ), and low TOC ( $0.17\%$  to  $0.49\%$ ) (Table 3.1, Fig. 3.8c). Biological activity and sediment reworking is predicted to increase the degradation of organic matter (should be reflected in more positive  $\delta^{13}\text{C}_{\text{org}}$  values),

and to lower TOC (Tyson, 1995). This study found that there was a wide range of TOC and isotopic values and that there is no simple systematic relationship between bioturbation intensity, TOC, and  $\delta^{13}\text{C}_{\text{org}}$  in which certain intensities exhibit the same TOC and  $\delta^{13}\text{C}_{\text{org}}$  (Fig. 3.8).

Mudstone-bearing facies can be subdivided into four groups based upon sandstone-mudstone ratio, bioturbation, and sedimentary structures. Each of these four mudstone classes has consistent and distinct ranges of  $\delta^{13}\text{C}_{\text{org}}$  and TOC (Fig. 3.8, Table 3.1). Individual facies are separated into mudstone classes and described below:

1) Facies M1 was characterized by upward fining silty mudstones that become organic-matter rich at the top of the bed due to the inferred presence of microbial mats (cf. Harazim et al 2013; Miller and McIlroy in press). The microbial mat layer is commonly cross-cut by sharp margined sand-filled burrows that are considered to post-date an early phase of sediment dewatering and simultaneous firm-ground formation (Fig. 3.5a, b, c; cf. Harazim 2013). There is a significant range in  $\delta^{13}\text{C}_{\text{org}}$  ranging from -27.6‰ to -30.3‰ (a difference of 2.67‰) and TOC ranging from 0.14% to 0.84% (a difference of 0.70%) values (Figs 3.8a, 3.9).

2) Facies M2 was defined as a thin (<5 cm) unbioturbated, high energy, erosive fluid mudstone deposit with disseminated microbial mats (Fig. 3.5d; Miller and McIlroy in press). Facies M2 has a  $\delta^{13}\text{C}_{\text{org}}$  range of 3.4‰ from the most enriched to the most depleted samples (-26.5‰ to -29.9‰) including outliers (Fig. 3.8b). TOC ranges from 0.27% to 0.77% (a difference of 0.50%). The fluid mud deposits of Facies M2 have the highest TOC values (Fig. 3.9). In regards to organic carbon isotopes, both Facies M1 and M2 were isotopically light in  $\delta^{13}\text{C}_{\text{org}}$  values.

3) Facies SS1 was a sandy siltstone identified by an intense *Planolites* deposit feeding ichnofabric. Abundant sand-filled burrows parallel to bedding rework approx. 80% of the primary sedimentary fabric (Fig. 5.6b; Miller and McIlroy in press). Facies SS1 was characterized by reduced sediment supply and/or low energy with wave and tide reworking that develops approx. 20 cm of slowly deposited beds. Facies H1 was defined as a heterolithic bioturbated silty mudstone and fine-grained sandstone. *Planolites* deposit feeding bioturbation is particularly abundant in the mud-rich inter-beds (approx. 60%) although bioturbation is pervasive and occurs at a slightly lesser extent (approx. 40%) throughout the facies with accessory *Cruziana*, *Trichophycus*, and *Teichichnus* (Fig. 3.6a; Miller and McIlroy in press). Facies SS1 and H1 are both characterized by abundant deposit feeding ichnofauna in low energy conditions with low sedimentation rates. The deposit feeding facies (Facies SS1 and H1) show a narrow  $\delta^{13}\text{C}_{\text{org}}$  range in isotopic values -27.1‰ to -29.6‰ (a difference of 2.56‰) and a more limited spread in TOC 0.17% to 0.49% (a difference of 0.32%; Figs 3.6, 3.8c). Facies with bioturbation that includes deposit feeding trace fossils typically have moderately depleted  $\delta^{13}\text{C}_{\text{org}}$  and moderate TOC values with some outliers when compared to Facies M1 and M2.

4) Facies S5 was a parallel to ripple cross-laminated sandstone forming c. 20 cm thick bedsets that are rarely bioturbated with organic matter-rich clay drapes often found as couplets (Fig. 3.7a; Miller and McIlroy in press). Facies S6 was a parallel laminated silty to very fine-grained sandstone that shows rare bioturbation and contains clay couplets with an approximate thickness of 5 cm (Fig. 3.7b; Miller and McIlroy in press). Facies SS2 was a rarely bioturbated, thinly laminated micaceous clay-rich siltstone with a maximum thickness of 7 cm (Fig. 3.7c; Miller and McIlroy in press). A siltstone with an

erosive base that includes a few discrete but unidentifiable trace fossils characterizes Facies SS3 (Fig. 3.7d; Miller and McIlroy in press). The described facies (Facies S5, S6, SS2, SS3) are composed of silt-rich sandstones and siltstones deposited under energetic conditions with rare bioturbation. These facies perhaps unsurprisingly, exhibit a large  $\delta^{13}\text{C}_{\text{org}}$  range of -25.6‰ to -29.2‰ (a difference of 3.54‰) with low TOC values with a significant range from 0.06% to 0.68% (a difference of 0.62%) (Fig. 3.8d). Silt- and sand- rich facies (Facies S5, S6, SS2, SS3) have slightly more enriched  $\delta^{13}\text{C}_{\text{org}}$  values and generally exhibit the lowest TOC compared to the more mud-rich facies.

### 3.5 DISCUSSION

Macerals from the Redmans Formation have an exclusively marine provenance despite the deltaic paleoenvironment of deposition. Petrographic and palynological studies demonstrate the absence of terrestrial plant debris, consistent with the Early Ordovician age of the Redmans Formation that pre-dates terrestrialization and the evolution of land plants (Dean and Martin, 1978; Kenrick and Crane, 1997; Wellman et al., 2003; Gensel, 2008; Kenrick et al., 2012; Harazim, 2013). As such it is likely that the  $\delta^{13}\text{C}_{\text{org}}$  value of any given bed in the Redmans Formation exclusively reflects aspects of the marine carbon cycle. The particulate organic matter in the Redmans Formation likely includes amorphous organic matter, fecal pellets, and marine plankton (mainly acritarchs; Dean and Martin, 1978; Harazim, 2013). In some cases high benthic primary productivity at the sediment water interface overlying organic poor mudstones is inferred to have resulted in the accumulation of thick microbial mats (cf. Harazim et al. 2013).

This simplified depositional and its associated, exclusively marine, carbon isotopic system allows consideration of some of the fundamental controls on  $\delta^{13}\text{C}_{\text{org}}$  in marine ecosystems.

The stable isotopic composition of deposited organic matter in sediments and sedimentary rocks has the potential to be modified by post-depositional breakdown of particulate organic matter (Strauss et al., 1992; Tyson, 1995; Hayes et al., 1999). Post-depositional fractionation of  $\delta^{13}\text{C}_{\text{org}}$  can result from the ingestion and (mainly aerobic) metabolism of sediment organic matter by both macro-organisms and micro-organisms (Tyson, 1995; Rullkötter, 2006). The net result of this metabolism is the release of remineralized carbon in the form of carbon dioxide, preferentially  $^{12}\text{C}$  rather than  $^{13}\text{C}$ , thereby causing a positive shift in  $\delta^{13}\text{C}_{\text{org}}$ . In high energy mud-belts such as are inferred herein for the Redmans Formation, organic matter is commonly subjected to multiple cycles of deposition and re-suspension. Through each cycle of re-suspension and microbial degradation/metazoan digestion, organic matter has the potential to become progressively more fractionated relative to its primary isotopic composition (Blair and Aller, 2012), as well as potentially being subjected to the hydrolyzing effects of metazoan guts multiple times (McIlroy et al., 2003). With multiple cycles of deposition and re-suspension organic matter follows a trend of decreasing TOC and heavier  $\delta^{13}\text{C}_{\text{org}}$  values. We therefore propose that  $\delta^{13}\text{C}_{\text{org}}$  is predominately a proxy for the efficacy of the local carbon cycle rather than reflecting the oceanic  $\delta^{13}\text{C}_{\text{org}}$ .

Any isotopic fractionation due to burial diagenesis is likely to have had the same impact throughout the Redmans Formation, and can not account for isotopic bed-by-bed variability (cf. Stahl, 1979; Álvaro et al., 2008; Pancost et al., 2013). The stable isotopic



signature of organic carbon is not significantly fractionated during early burial diagenesis (Tyson, 1995), although metamorphism can cause a positive shift in  $\delta^{13}\text{C}_{\text{org}}$  (Stahl, 1979; Strauss et al., 1992; Álvaro et al., 2008; Pancost et al., 2013).

### 3.5.1 The effect of sediment transport on TOC and $\delta^{13}\text{C}_{\text{org}}$

Intense hydrodynamic regimes are not known to directly cause fractionation of  $\delta^{13}\text{C}_{\text{org}}$ . There are however demonstrable exponential relationships between facies and both TOC and  $\delta^{13}\text{C}_{\text{org}}$  in the Redmans Formation (Fig. 3.8, 3.9). A high TOC concentration is typically associated with lighter  $\delta^{13}\text{C}_{\text{org}}$  values (Fig. 3.8e) in primary organic matter before and soon after burial (Álvaro et al., 2008). In most cases there is a correlation between increased grain size and low TOC, which is inferred to be a function of organic matter dilution due to increased sediment deposition rates. The effects of sediment transport on  $\delta^{13}\text{C}_{\text{org}}$  are, however, more complex in mud-rich wave-dominated depositional systems such as the Redmans Formation.

Re-suspension of sediment, and long transport times both contribute to the metabolic “burning” of organic carbon by microbial metabolism as well as the more obvious deposit feeding activity of macro-organisms results in fractionation of  $\delta^{13}\text{C}_{\text{org}}$ ; being enriched in  $^{13}\text{C}$ . Organic matter will become isotopically heavier with multiple cycles of sediment reworking, prior to final burial. Since the transport history of fine grained sediments does not have an obvious lithological expression, nor can it be determined from sedimentary structures within a mudstone (since only the last phase of deposition is recorded not previous cycles of erosion and re-deposition), it is perhaps unsurprising that the relationship between  $\delta^{13}\text{C}_{\text{org}}$  and sedimentary facies is not entirely

clear (Fig. 3.8). It appears that individual facies within the distributary mouth bar have a particular isotopic spread due to both physical and biological processes unique to that facies (Fig. 3.10). The wide isotopic spread of  $\delta^{13}\text{C}_{\text{org}}$  and TOC within some sedimentary facies does, however, attest to the innate variability within the depositional system (Fig. 3.8, 3.9).

### **3.5.2 Organism-sediment interaction**

Bioturbation increases sediment advection and exposure times to oxygen decreasing the preservation potential of sedimentary organic matter. The extent to which biological activity impacts pre-burial isotopic fractionation is unknown (Tesi et al., 2012). Macrobenthic activity does, however, result in the remineralization of organic matter constituents to  $\text{CO}_2$  (Berner, 1980a; Berner, 1980b; Tyson, 1987, 1995; Aller et al., 2001). With ongoing biologically mediated oxidative reduction of detrital organic matter, any organic matter remaining in bioturbated sediment becomes progressively inert and less bio-available (Pratt et al., 1986). Bioturbation in fine-grained sediment increases the proportions of bacterial biomass relative to detrital organic matter (Purdy, 1964; Pearson and Rosenberg, 1978; Yingst and Rhoads, 1980; Aller, 1982; Berner and Westrich, 1985; 1985; Kristensen and Blackburn, 1987; Tyson, 1995; McIlroy and Logan, 1999). The enhanced macrobenthic activity that results from this microbial productivity is inferred to cause a shift towards progressively heavier  $\delta^{13}\text{C}_{\text{org}}$  values (Brasier and McIlroy, 1998; McIlroy and Logan, 1999).

Perhaps the most remarkable sedimentary facies in the Redmans Formation are the unbioturbated mudstones. Study of modern depositional environments tells

neiochnologists that most marine muds are teeming with endobenthic life. Those sedimentary facies from the Redmans Formation that have ichnofabrics resulting from the action of deposit feeding organisms show a range of  $\delta^{13}\text{C}_{\text{org}}$  and TOC values consistent with the presence of detrital organic matter and significant microbial biomass at the time of burial. The anomalous unbioturbated mudstones (Facies M1 and M2) would typically show low TOC preservation and heavy  $\delta^{13}\text{C}_{\text{org}}$  values of recalcitrant organic matter unsuitable for deposit feeding macro-organisms. Organic rich microbial mats on the surface and disseminated through these unbioturbated mudstones result in higher TOC and lighter  $\delta^{13}\text{C}_{\text{org}}$  than the originally deposited organic matter (Fig. 3.9; Harazim et al, 2013). The only evidence for benthic life in these facies are:

- 1) Microbial mats at the upper surfaces of beds of Facies M1 (Fig. 3.4, 3.5) have highly negative values of  $\delta^{13}\text{C}_{\text{org}}$  consistent with abundant primary production by microbial biomass in the form of microbial mats (Noffke, 2010). The underlying mudstones are depleted in organic matter and are isotopically more positive (e.g. Harazim et al. 2013).
- 2) Abundant sharp-margined, largely uncompressed, sand filled burrows that postdate sediment dewatering and compaction, and therefore do not reflect the organic matter composition of the mudstone. The burrows themselves are inferred to be dominantly permanent dwelling burrows rather than transient deposit feeding burrows, excavated into concealed firm-grounds (Bromley, 1996).

### 3.5.3 Implications for global organic carbon cycling

Stable isotopic perturbations in  $\delta^{13}\text{C}_{\text{org}}$  values are commonly linked to changes in the global carbon cycle resulting from changes in ocean productivity, biochemistry, and  $\rho\text{CO}_2$  (Pancost et al., 1999; Weissert et al., 2008; Davies et al., 2012). Such excursions in the global carbon cycle have been widely used to correlate stratigraphic successions based on the premise that  $\delta^{13}\text{C}_{\text{org}}$  in sediments records the isotopic composition of the oceans on a global scale (Weissert et al., 2008).

Attempts to use organic carbon for chemostratigraphy are compromised in post-Ordovician strata by terrestrial organic matter contamination, which commonly has a different isotopic composition to contemporaneous marine organic carbon (Pancost et al., 1999; Davies et al., 2012). The only real way to get a marine isotopic signal from such post-Ordovician successions is to use compound-specific carbon isotopes (Gunter, 1986). In studying the Lower Ordovician Redmans Formation we can address other potential factors that may control  $\delta^{13}\text{C}_{\text{org}}$ . The large isotopic spread (approx. 4.3‰) between and within facies is substantial and, when plotted stratigraphically, includes excursions of a magnitude that in other successions have been interpreted as globally significant excursions (e.g. Zhang et al., 2010).

Comparison of the Redmans Formation  $\delta^{13}\text{C}_{\text{org}}$  curve to that of the Floian Hunghuayuan and Meitan Formations of Guizhou Province, China does not show any significant correlation. The Redmans Formation has a smaller  $\delta^{13}\text{C}_{\text{org}}$  spread, 4‰ vs 8‰, compared to the Chinese successions (Zhang et al., 2010; Fig. 3.11). While the Chinese successions have been considered to reflect the global carbon isotopic curve for the Floian, it is clear that data from the Redmans Formation was significantly different.

Possible explanations for the isotopic differences between these two datasets include: 1) The basin in which the Redmans Formation was deposited may have been isolated from the oceanic carbon isotope pool, and the isolated basin was significantly fractionated; or 2)  $\delta^{13}\text{C}_{\text{org}}$  in one or both successions were significantly fractionated, probably by microbial and metazoan metabolic processes, that overprints any global isotopic signature.

The significant facies control on  $\delta^{13}\text{C}_{\text{org}}$  within the Redmans Formation leads us to suspect that at least our dataset should not be used for chemostratigraphy. Organic carbon isotopic excursions of the Redmans Formation are thereby a factor of facies development. The intensity of sediment reworking in wave-dominated shallow marine mud-belts (Bhattacharya and Walker, 1991; Aller, 1998; Vakarelov et al., 2012) leads us to suggest that the depositional setting of the Redmans Formation is particularly unsuitable for chemostratigraphy. We do note however that cross-shelf transport of such fluid muds is common, and results in hypopycnal flows in submarine canyons and even onto deep basin floors. Similarly, the prominent shift in  $\delta^{13}\text{C}_{\text{org}}$  between the Hunghuayuan Formation (-29.4‰) and the Meitan Formation (-21.1‰) in the Floian reference sections of Guizhou Province, China (Zhang et al., 2010), is likely associated with a lithological change from limestones to inter-bedded mudstones and siltstones (Renbin and Jisuo, 2007), rather than a global isotopic shift (Fig. 3.11). As such, extreme caution needs to be exercised particularly in sediments with low TOC such as are derived from mud-rich coastal systems.

### 3.6 CONCLUSION

The Early Ordovician Redmans Formation was deposited in a wave-dominated shallow marine paleoenvironment with abundant fluid mud deposits. Stable isotopic and TOC characterization of the organic matter in the mudstones demonstrates a range of 0.8 wt % for TOC and 4.3‰ for  $\delta^{13}\text{C}_{\text{org}}$ . The organic matter is exclusively of marine provenance, and is dominated by acritarchs, organic-aggregates, and microbial mats.

The intense hydrodynamic regime is inferred to include multiple phases of erosion, re-suspension, and re-deposition, the effect of which is to expose detrital organic matter to multiple cycles of aerobic metabolism, which decreases TOC and fractionates  $\delta^{13}\text{C}_{\text{org}}$  (becoming enriched in  $^{13}\text{C}$ ). When plotted stratigraphically, the succession would appear to have numerous stable isotopic excursions suitable for chemostratigraphic correlation. The excursions do not correspond to reference  $\delta^{13}\text{C}_{\text{org}}$  curves for the Floian (Zhang et al. 2010) and are instead inferred to reflect facies-related variability in fractionation induced by the metabolic effects of aerobic microbes and macro-organisms.

While the shallow marine mobile fluid mud belts of the Redmans Formation might be an extreme end-member of unsuitability for  $\delta^{13}\text{C}_{\text{org}}$  based chemostratigraphy, it does demonstrate the fact that it is difficult to know the transport history of organic matter and that  $\delta^{13}\text{C}_{\text{org}}$  is significantly prone to fractionation by ingestion by macro-organisms and the metabolic effects of aerobic microbes.

### **3.7 ACKNOWLEDGEMENTS**

It is with great appreciation and gratitude that we thank those involved in this project. Many thanks are extended to the people and facilities involved in sample preparation and processing: Dr. Dario Harazim, Helen Gillespie, Alison Pye, Kris Poduska, and Ben Xu. Many thanks to those involved in the geochemical lab work done by the University of Ottawa and Memorial University of Newfoundland. The members of the Ichnology Research Group are thanked for helpful discussions and continued support.

### 3.8 FIGURES AND TABLES

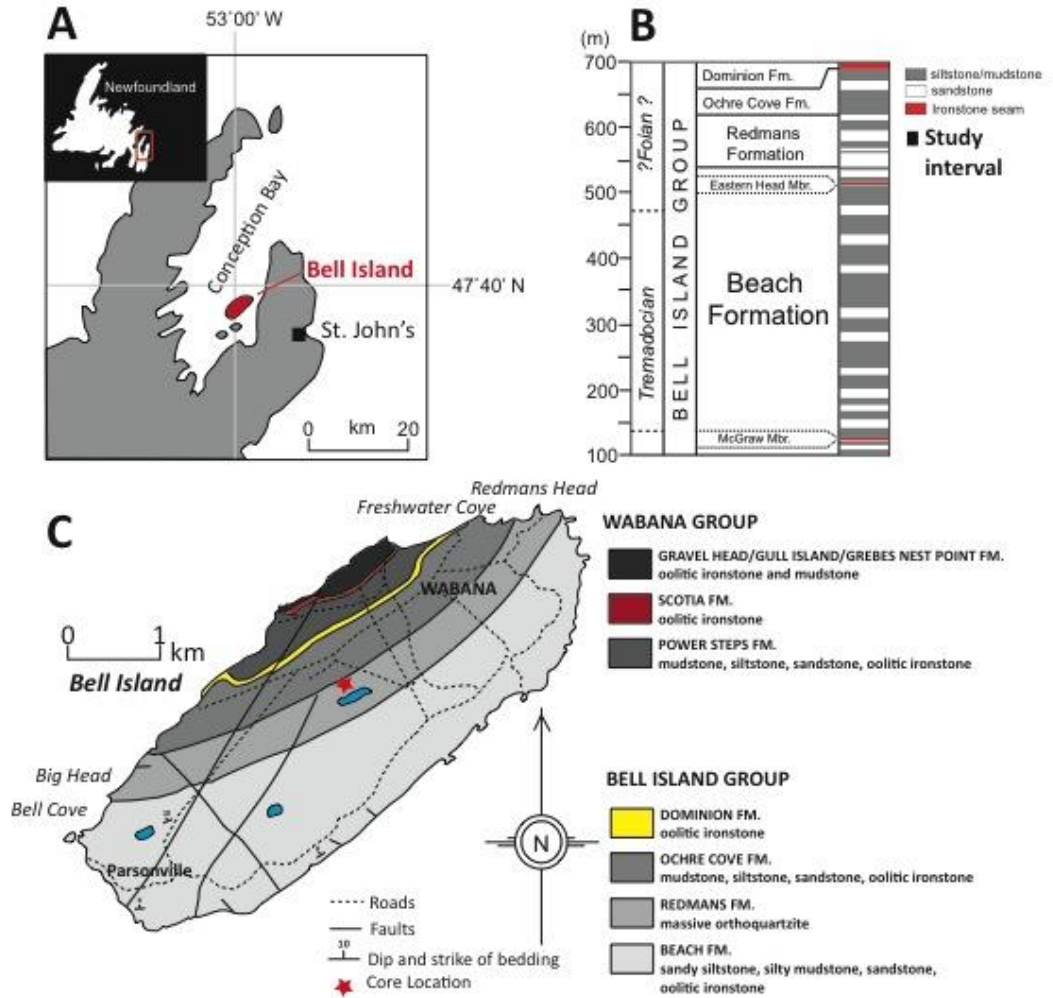
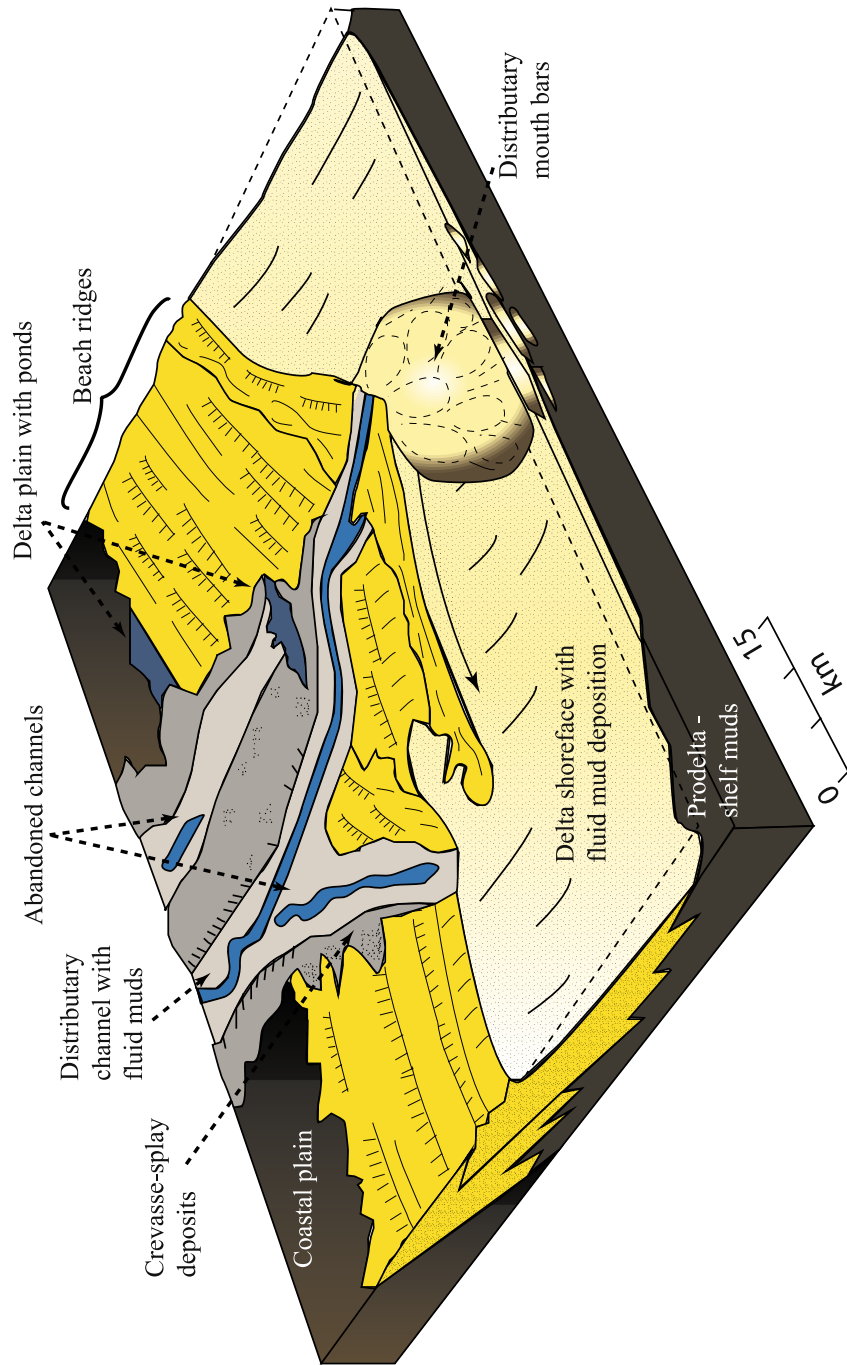


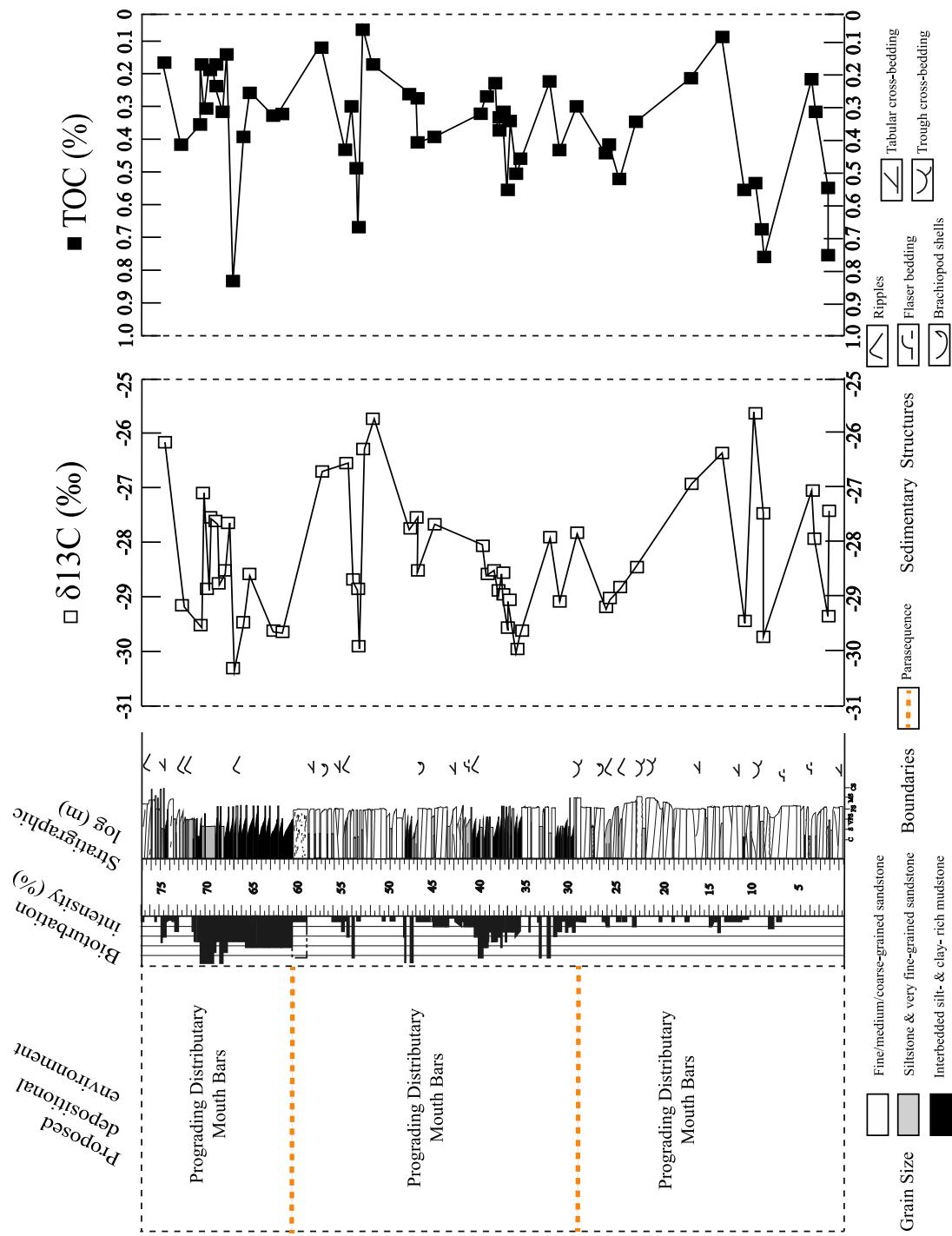
Fig. 3.1. (a) Bell Island, Newfoundland location map. (b) Stratigraphic section of the Bell Island Group, Redmans Formation. Redmans Formation is Floian in age (~477.7 Ma). (c) Bell Island geological map with the studied core location indicated (modified after Ranger et al., 1984; Harazim et al., 2013).

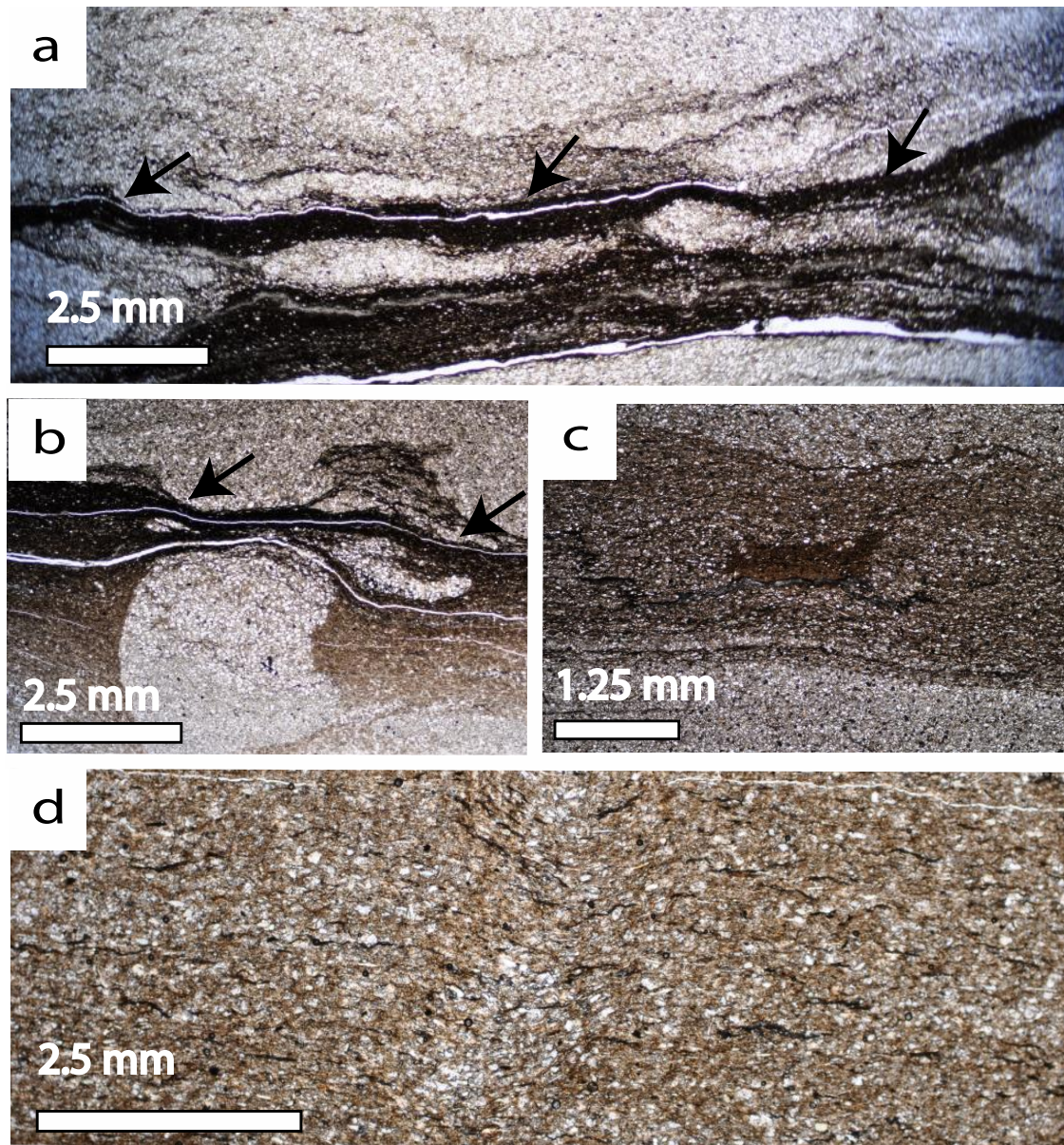


**Fig. 3.2 A wave-dominated delta is the interpreted paleoenvironment in which the distributary mouth bars of the Redmans Formation were deposited. Erosive fluid muds were likely carried in from the distributary channel (modified from Weise, 1980).**



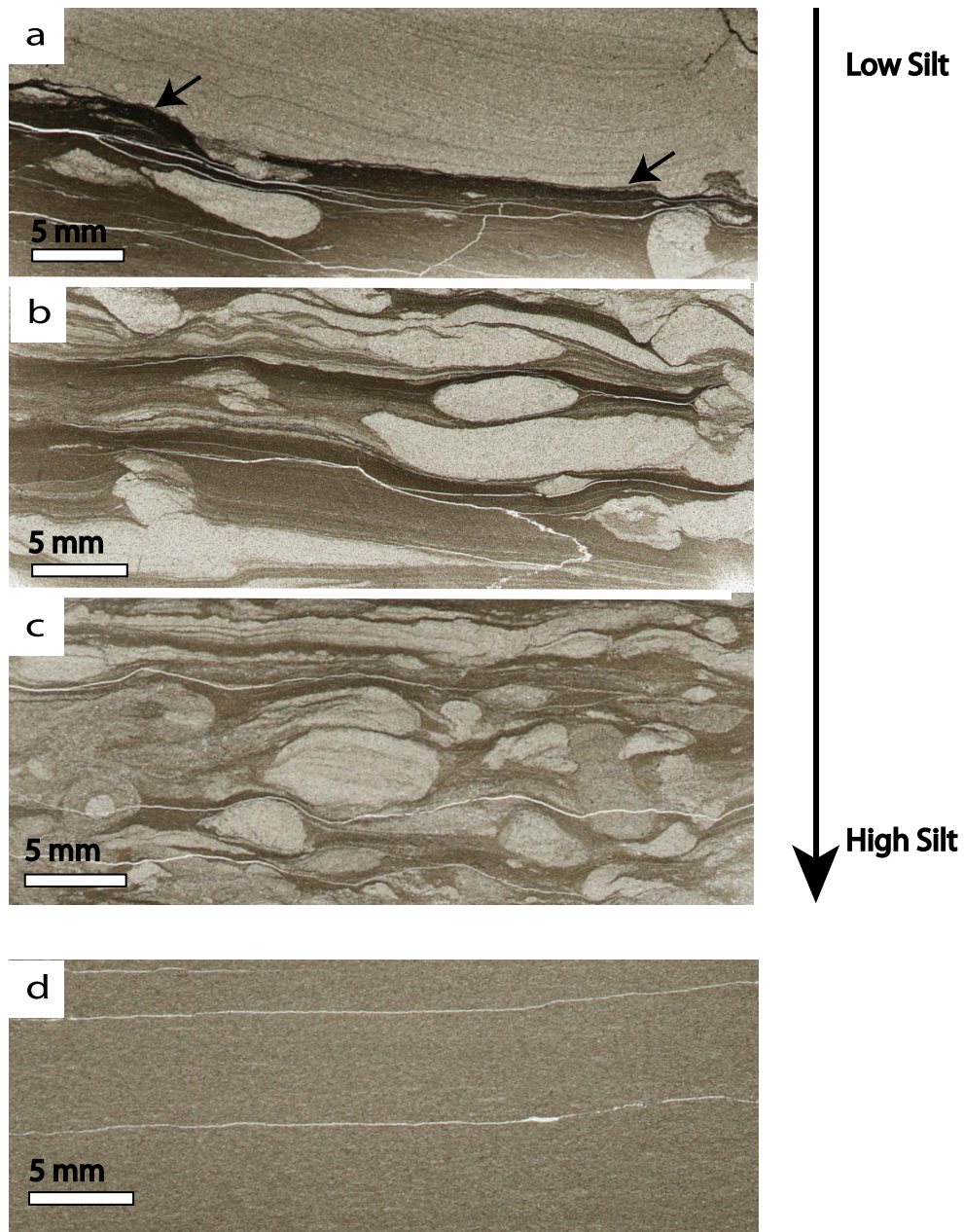
**Fig. 3.3 Summary stratigraphic log of the Redmans Formation's 76.5 m of core from Bell Island, Newfoundland showing bioturbation percentage, grain size, sedimentary structures, depositional environment, and grain size trends. The stratigraphic log in cross-comparison to  $\delta^{13}\text{C}_{\text{org}}$  (‰) and TOC (%). Large spreads in isotopic and TOC data are shown to span 4.3‰ and 0.8% between and within facies.**



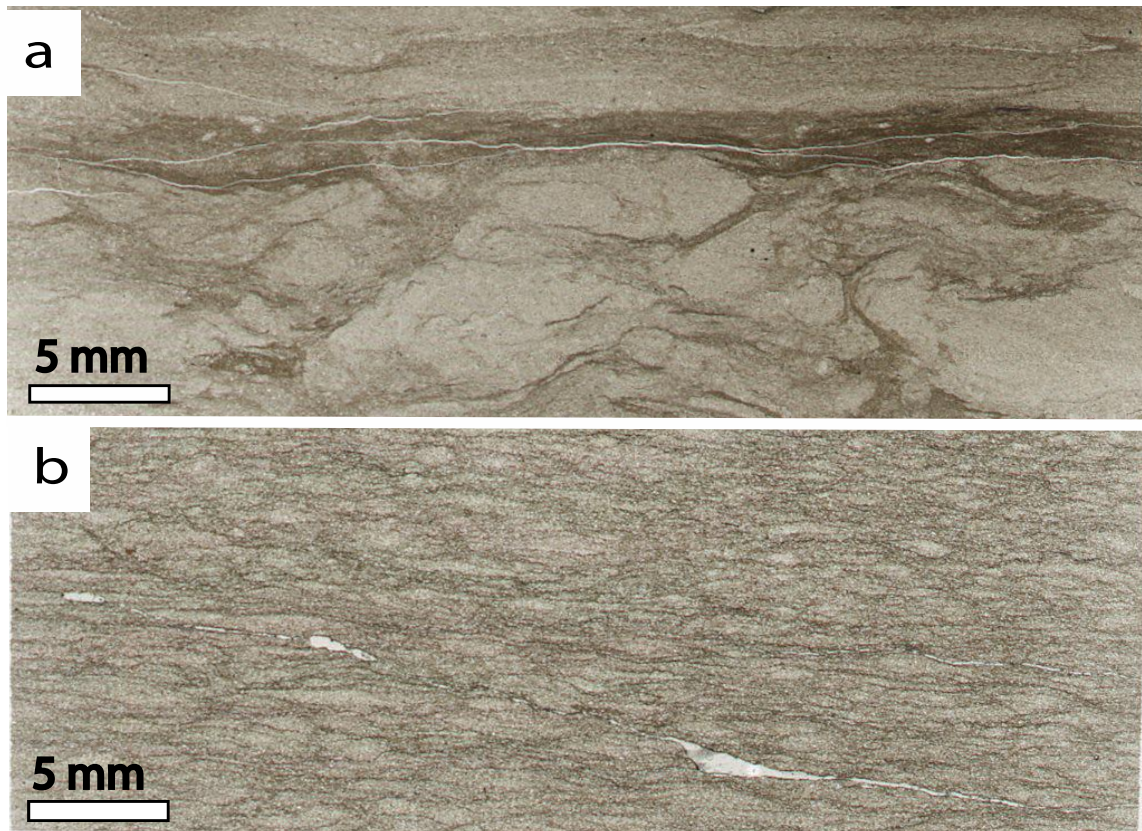


**Fig. 3.4 (a) Dark organic rich laminae indicated by arrows are possible microbial mats with sand filled burrows belonging to Facies M1. (b) Facies M1, showing upward fining into the possible dark organic rich microbial mats. (c) Thin section showing either an organic aggregate or that of a shale clast that has been re-deposited. (d) Apparent organic matter fragments dispersed parallel to bedding.**



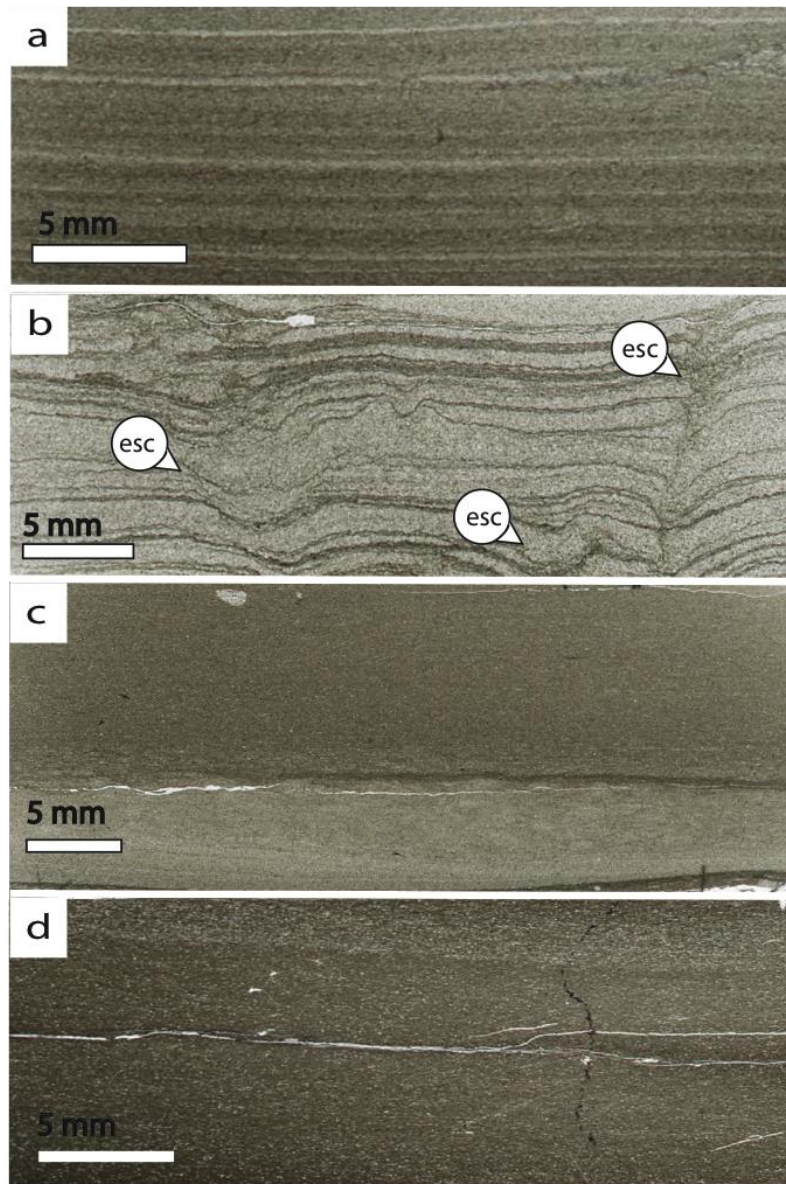


**Fig. 3.5 (a,b,c) Facies M1, showing upward fining, erosively based mudstone with sand-filled burrows such as *Planolites isp*, and other vertical dwelling burrows in a scanned thin section with possible microbial mats indicated by the arrows. Bioturbation intensity varies in Facies M1, increasing silt and sand content is the result of increased bioturbation intensity. (d) Facies M2, showing the erosive dark mudstones in thin section with no sedimentary structures or bioturbation.**



**Fig. 3.6 (a) Facies H1, showing heterolithic silty mudstone with mantle swirl bioturbation due to deposit feeding organisms in soft ground conditions. (b) Facies SS1, showing intensely bioturbated silty sandstone dominated by *Planolites isp* in a scanned thin section.**

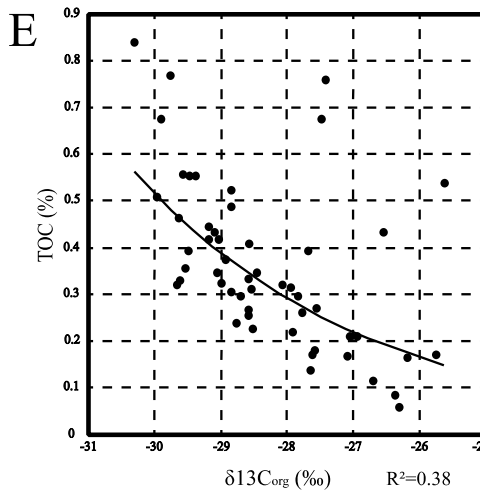
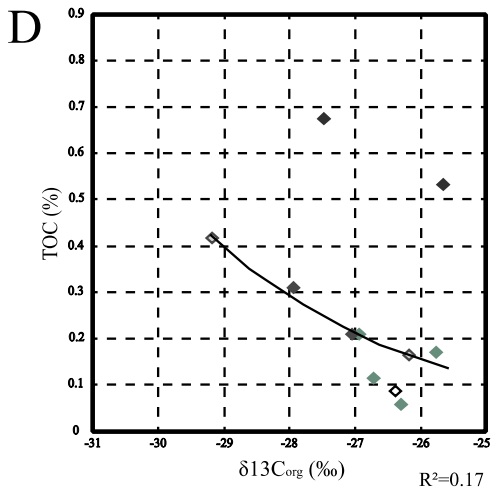
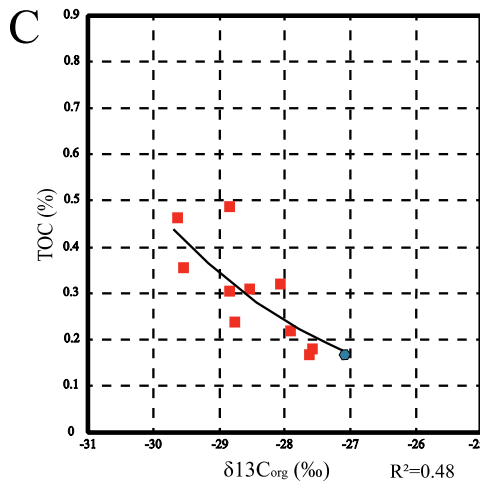
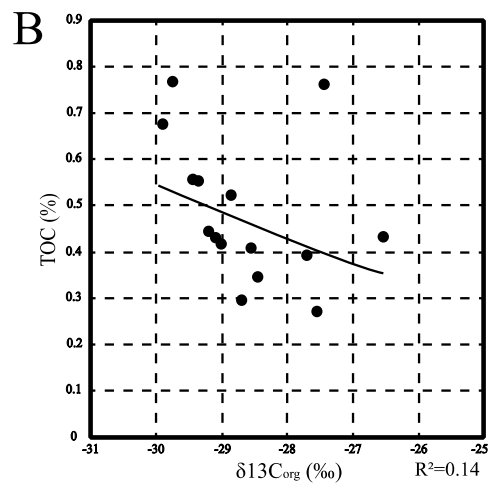
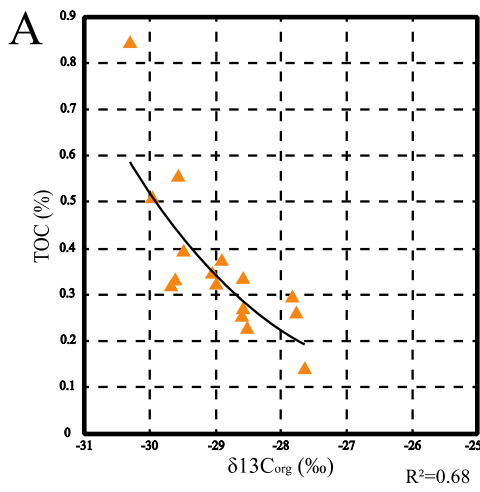




**Fig. 3.7 (a) Facies S5, showing densely parallel-laminated sandstone alternating between clay/silt with sand rich laminae. (b) Facies S6, showing densely mud draped siltstone in a thin section scan (perpendicular to bedding). Mud couplets and escape traces (esc) are present. (c) Facies SS2, showing laminated clay rich siltstone and a few sand filled burrows in a scanned thin section. (d) Facies SS3, showing erosive based siltstone with some variations in grain size and content upwards shown in a scanned thin section.**



**Fig. 3.8 Graphical representation of individual facies cross-plotted with a geochemical classification scheme of  $\delta^{13}\text{C}_{\text{org}}$  (‰) versus TOC (%). (a) Graphical representation of Facies M1 having the lightest isotopic signature. (b) Facies M2 has light isotopic signatures with a few outliers. Facies M1 and M2 show a wide range of both  $\delta^{13}\text{C}_{\text{org}}$  and TOC. (c) A narrower grouping of the deposit feeding traces of Facies SS1 and H1. (d) The siltstones and silty sandstones of Facies SS2, SS3, S5, and S6, show enriched isotopic values and low TOC and are situated with a more narrow range of values. Results include outliers. (e) Graphical representation of 53 samples from mudstone, siltstone, and sandstone facies with an  $R^2=0.38$ .**



Erosive Mudstone, Sand Filled Burrows, Microbial Mat Facies

Erosive Mudstone Facies

▲ M1

● M2

Deposit Feeding Bioturbation Facies

Silt/Sand Rich Facies

■ SS1

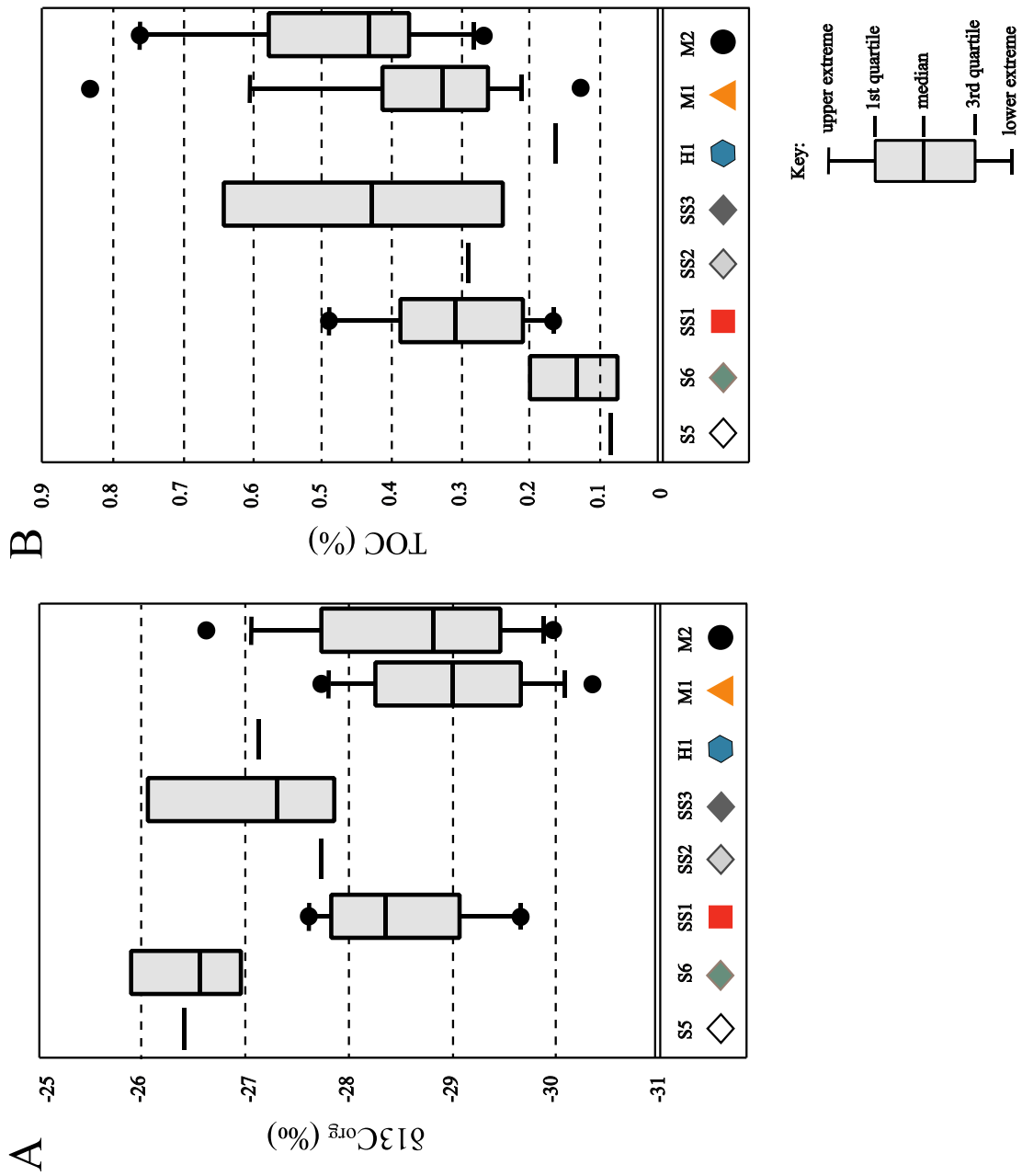
◇ S5

◇ SS2

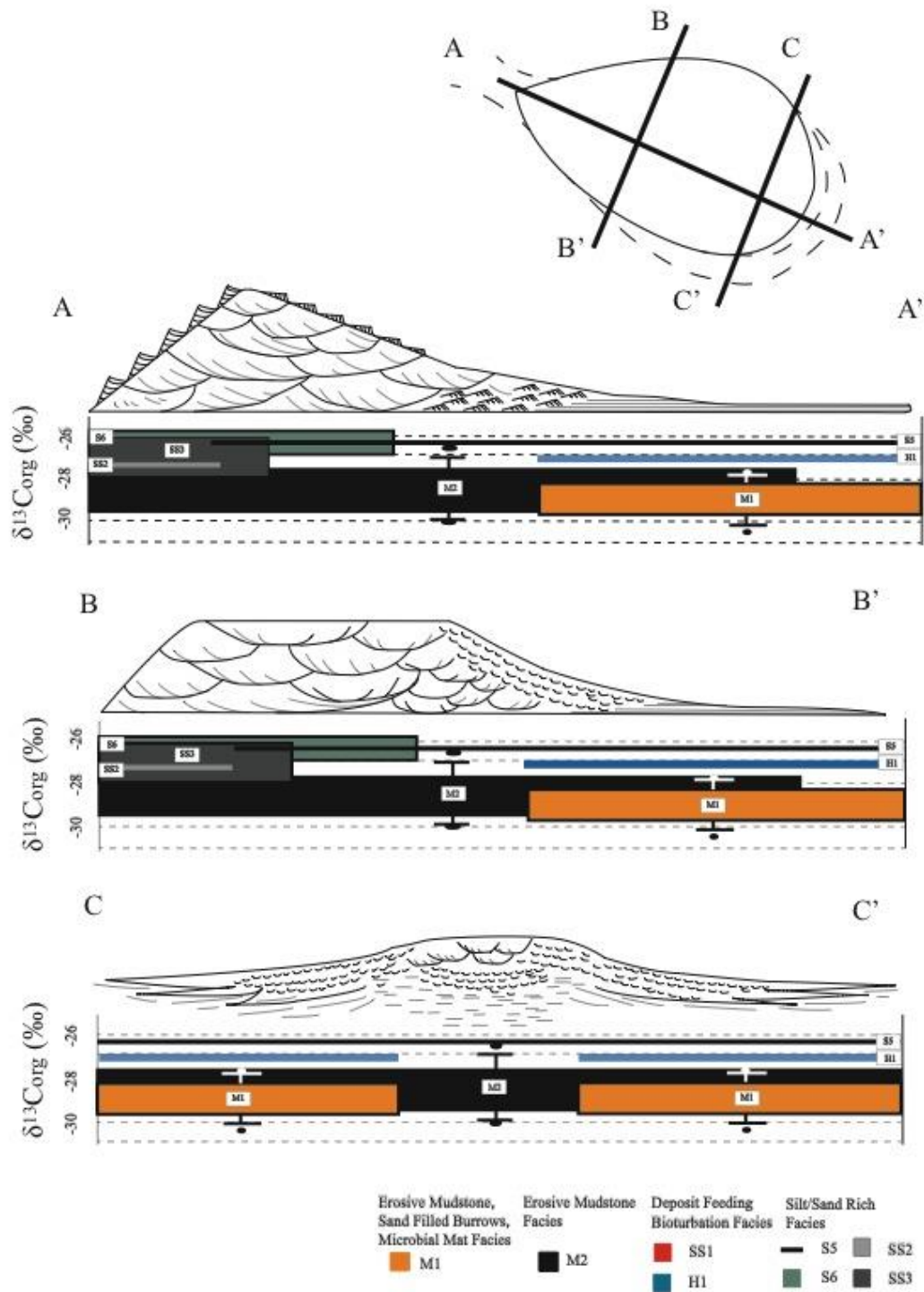
⬡ H1

◇ S6

◇ SS3



**Fig. 3.9** Box and whisker plots (a) of  $\delta^{13}\text{C}_{\text{org}}$  (‰) showing individual facies spread and (b) TOC that are separated into individual facies. See text for detailed descriptions and Fig. 3.8 for symbols and corresponding facies type.



**Fig. 3.10 (a,b,c) Paleoenvironmental and geochemical model of facies distribution in three interpreted cross-sections of the distributary mouth bar with isotopic spread based on facies distribution.**



**Fig. 3.11: A small portion of the Honghuayuan section in the Guizhou Province of southern China have  $\delta^{13}\text{C}_{\text{org}}$  spreads of approximately 8 ‰ (Zhang et al., 2010). The isotopic spread has been interpreted as a global perturbation in the carbon cycle; in contrast the Redmans Formation has an unparalleled isotopic expression derived from physical and biological reworking.**

**Table 3.1. Table summarizing the sedimentology, mineralogy, palaeontology, ichnology, depositional environment, and geochemistry of the mudstones, siltstones, and sandstones of the Redmans Formation.**

Facies code	Facies name	Facies association	Lithology	Sedimentary structures and palaeontology	Composition and mineralogy	Ichthyology	n=?	Difference :13,Org. (%)	Difference TOC (%)	Interpreted depositional environment
S1	Medium grained, trough cross-stratified sandstone	FA1	Clay, silt, and medium sand	Millimeter to centimeter thick steep angled cross-lamination; erosional based with mudstone rip up clasts. Phosphatic ligulid brachiopods	Bimodal; subangular quartz, chert, calcite; equant muscovite and biotite; scattered opaques, chlorite, clay minerals, and plagioclase; pekkilopte calcite cement	BI 0	0	x	x	Proximal distributary mouth bar
S2	Structure-less sandstone	FA1	Fine to medium grained sand	Dark beds; de-watering; no internal sedimentary features	Subangular quartz; equant muscovite; replacement of grains by chlorite; scattered plagioclase, and opaques	Possible burrow modeled or isolated remineralized burrow lining, BI 1 or BI 6	0	x	x	Proximal distributary mouth bar
S3	Planar cross-stratified, mud draped sandstone	FA1	Fine to medium grained sand; clay	Millimeter-sized wavy, even parallel laminae, mud drapes, mud congloms, ripples and pressure solution	Subangular quartz; equant muscovite; replacement of grains by chlorite; scattered plagioclase, biotite, clay minerals, pyrite and opaques	Centimeter-sized <i>Diploporation</i> , <i>Tetrichinus</i> , and vertical traces; BI 2	0	x	x	Proximal distributary mouth bar
S4	Flaser bedded very fine-grained sandstone	FA1	Very fine sand	Millimeter thick even parallel and discontinuous even parallel laminae; flaser bedding, wave ripples	Subangular quartz; equant biotite and muscovite; replacement of grains by chlorite; scattered opaques, and plagioclase	Centimeter-sized low diversity, vertical traces; BI 1	0	x	x	Proximal distributary mouth bar
S5	Parallel to ripple cross-laminated sandstone	FA1	Clay-bearing, silt and very fine sand dominated	Dense millimeter even parallel to nonparallel laminations; flaser bedding, rhythmic mud laminae, wave ripples	Subangular quartz; equant muscovite and biotite; clay minerals; replacement of grains by chlorite; scattered opaques, pyrite, and plagioclase	Centimeter-sized shallow tiered, <i>Planolites</i> , <i>Trichophycus</i> , <i>Rosella</i> , <i>Skolithos</i> , and escape traces; BI 0-2; rare cross-cutting	1	x	x	Distributary mouth bar
S6	Parallel laminated very fine-grained sandstone and silty sandstone	FA1	Silt and clay bearing	Even parallel laminae defined by quartz and clay proportions; mud congloms	Subangular quartz; equant biotite and muscovite; clay minerals; replacement of grains by chlorite; clay minerals; rare plagioclase	Centimeter-sized; <i>Planolites</i> , and escape burrows; BI 0-1	4	1.20	0.15	Subtidal distributary mouth bar
SS1	Intensely bioturbated sandy siltstone	FA1	Silt and clay	No physical sedimentary structures; rare fining up cycles	Subangular quartz; equant muscovite, and biotite; clay mineral dominant; replacement of grains by chlorite; scattered opaques; pyrite, and plagioclase	Millimeter to centimeter-sized low diversity burrows; mottled; silt filled burrows; BI 5	10	2.07	0.32	Abandoned distributary mouth bar
SS2	Thinly laminated micaceous clay rich siltstone	FA1	Silt and clay-rich	Millimeter even parallel laminae alter between quartzose and micaceous; ripple cross-lamination	Subangular quartz; equant biotite and muscovite; clay minerals; replacement of grains by chlorite; scattered opaques, and plagioclase	Millimeter-sized <i>Planolites</i> ; BI 0-2	2	2.99	0.26	Proximal distributary mouth bar
SS3	Siltstone with erosive base	FA1	Silt and clay	Millimeter-sized even parallel quartz rich laminations at contacts; mud stringers; no internal physical sedimentary features; erosive base	Subangular quartz; equant muscovite, and biotite; clay mineral dominant; scattered opaques; pyrite	BI 0	4	2.30	0.46	Proximal distributary mouth bar
H1	Heterolithic bioturbated silty mudstone and fine-grained sandstone	FA1	Clay, silt, and very fine sand; very fine sand infilling burrows.	Centimeter thick heterolithic laminated sandstone and silty mudstone with ripple cross-laminae; erosional and gradational contacts	Subangular quartz grains; and rare plagioclase; equant muscovite and clay minerals dominate mudier portions; scattered opaques, plagioclase, and phosphale	Millimeter to centimeter-sized shallow tiered <i>Planolites</i> , <i>Diploporation</i> , <i>Trichophycus</i> , <i>Crustana</i> and other unidentifiable traces; mantle and swirl structure; BI 3-4; common cross-cutting	1	x	x	Distal distributary mouth bar
M1	Upward-fining mudstone with erosive bases and sand-filled burrows	FA1	Clay and silt bearing; very fine sand infilling burrows	Erosive centimeter beds; fining upwards from silty mudstone to organic rich mudstone; microbial mat upper bed boundary; shrinkage cracks; scours	Subangular quartz; equant muscovite, and biotite; clay mineral dominant; scattered opaques	Millimeter to centimeter-sized shallow tiered <i>Planolites</i> , <i>Diploporation</i> , <i>Trichophycus</i> , and <i>Crustana</i> ; BI 1-2; common cross-cutting	16	2.67	0.70	Distal distributary mouth bar
M2	Thin black mudstone with erosive base	FA1	Clay and silt bearing	Erosive centimeter beds; millimeter-sized mud stringers; no internal physical sedimentary features	Subangular quartz; equant muscovite, and biotite; clay mineral dominant; replacement of grains by chlorite; scattered opaques	BI 0	15	3.37	0.50	Distributary mouth bar



### 3.9 REFERENCES

- Aller, R. C., 1982, The effects of macrobenthos on chemical properties of marine sediment and overlying water, animal-sediment relations, Springer, p. 53-102.
- Aller, R. C., 1998, Mobile deltaic and continental shelf muds as suboxic, fluidized bed reactors: *Marine Chemistry*, v. 61, no. 3, p. 143-155.
- Aller, R. C., Aller, J. Y., and Kemp, P. F., 2001, Effects of Particle and Solute Transport on Rates and Extent of Remineralization in Bioturbated Sediments, Columbia, North Carolina, The Belle W. Baruch Library in Marine Science, Organism-Sediment Interactions.
- Álvaro, J. J., Bauluz, B., Subías, I., Pierre, C., and Vizcaíno, D., 2008, Carbon chemostratigraphy of the Cambrian-Ordovician transition in a midlatitude mixed platform, Montagne Noire, France: *Geological Society of America Bulletin*, v. 120, no. 7-8, p. 962-975
- Bergstroem, S. M., Chen, X., Gutierrez-Marco, J. C., and Dronov, A., 2009, The new chronostratigraphic classification of the Ordovician System and its relations to major regional series and stages and to  $\delta^{13}\text{C}_{\text{org}}$  chemostratigraphy: *Lethaia*, v. 42, no. 1, p. 97-107.
- Berner, R. A., 1980a, Early diagenesis: A theoretical approach, Princeton University Press, v. 1
- Berner, R. A., 1980b, A rate model for organic matter decomposition during bacterial sulfate reduction in marine sediments: *Biogeochemistry of organic matter at the sediment-water interface*, p. 35-44

- Berner, R. A., and Westrich, J. T., 1985, Bioturbation and the early diagenesis of carbon and sulfur: *American Journal of Science*, v. 285, no. 3, p. 193-206.
- Bhattacharya, J., and Walker, R. G., 1991, River-and wave-dominated depositional systems of the Upper Cretaceous Dunvegan Formation, northwestern Alberta: *Bulletin of Canadian Petroleum Geology*, v. 39, no. 2, p. 165-191.
- Blair, N. E., and Aller, R. C., 2012, The Fate of Terrestrial Organic Carbon in the Marine Environment, *in* Carlson, C. A., and Giovannoni, S. J., eds., *Annual Review of Marine Science*, Vol 4, Volume 4, p. 401-423.
- Brasier, M., and McIlroy, D., 1998, *Neonereites uniserialis* from c. 600 Ma year old rocks in western Scotland and the emergence of animals: *Journal of the Geological Society*, v. 155, no. 1, p. 5-12.
- Brenchley, P. J., Pickerill, R. K., and Stromberg, S. G., 1993, The role of wave reworking on the architecture of storm sandstone facies, Bell Island Group (Lower Ordovician), eastern Newfoundland: *Sedimentology*, v. 40, no. 3, p. 359.
- Bromley, R. G., 1996, Trace fossils: biology, taphonomy and applications, Psychology Press.
- Burdige, D. J., 2005, Burial of terrestrial organic matter in marine sediments: A re-assessment: *Global Biogeochemical Cycles*, v. 19, no. 4.
- Davies, S. J., Leng, M. J., Macquaker, J. H. S., and Hawkins, K., 2012, Sedimentary process control on carbon isotope composition of sedimentary organic matter in an ancient shallow-water shelf succession: *Geochemistry, Geophysics, Geosystems*, v. 13, no. 11.

- Dean, W. T., and Martin, F., 1978, Lower Ordovician acritarchs and trilobites from Bell Island, eastern Newfoundland, Geological Survey of Canada.
- Gensel, P. G., 2008, The earliest land plants: *Annual Review of Ecology, Evolution, and Systematics*, v. 39, p. 459-477.
- Gunter, F., 1986, *Principles of Isotope Geology*, John Wiley and Sons.
- Harazim, D., 2013, High-energy seafloor processes and biological reworking as first-order controls on mudstone composition and geochemistry [Phd: Memorial University of Newfoundland].
- Harazim, D., Callow, R. H. T., and McIlroy, D., 2013, Microbial mats implicated in the generation of intrastratal shrinkage ('synaeresis') cracks: *Sedimentology*
- Harazim, D., and McIlroy, D., in press, Mud-rich density-driven flows along an Early Ordovician storm-dominated shoreline: Implications for shallow-marine facies models: *Sedimentology* (in press)
- Hayes, J. M., Strauss, H., and Kaufman, A. J., 1999, The abundance of  $^{13}\text{C}$  in marine organic matter and isotopic fractionation in the global biogeochemical cycle of carbon during the past 800 Ma: *Chemical Geology*, v. 161, no. 1-3, p. 103-125.
- Kenrick, P., and Crane, P. R., 1997, The origin and early evolution of plants on land: *Nature*, v. 389, no. 6646, p. 33-39.
- Kenrick, P., Wellman, C. H., Schneider, H., and Edgecombe, G. D., 2012, A timeline for terrestrialization: consequences for the carbon cycle in the Palaeozoic: *Philosophical Transactions of the Royal Society B: Biological Sciences*, v. 367, no. 1588, p. 519-536.

- Kristensen, E., and Blackburn, T., 1987, The fate of organic carbon and nitrogen in experimental marine sediment systems: influence of bioturbation and anoxia: *Journal of Marine Research*, v. 45, no. 1, p. 231-257.
- McIlroy, D. 2004, Some ichnological concepts, methodologies, applications and frontiers: Geological Society, London, Special Publications, v. 228, p. 3-27
- McIlroy, D., and Logan, G. A., 1999, The impact of bioturbation on infaunal ecology and evolution during the Proterozoic-Cambrian transition: *PALAIOS*, v. 14, no. 1, p. 58-72.
- McIlroy, D., Worden, R., and Needham, S., 2003, Faeces, clay minerals and reservoir potential: *Journal of the Geological Society*, v. 160, no. 3, p. 489-493.
- McIlroy D., 2008, Ichnological analysis: The common ground between ichnofacies workers and ichnofabric analysts: *Palaeogeography, Palaeoclimatology, Palaeoecology*, v. 270, no. 3, p. 332-338.
- Miller, T., and McIlroy, D., in press, Sedimentology and stratigraphy of a wave-dominated delta from the early Ordovician Redmans Formation, Bell Island, Newfoundland: "Ichnology" McIlroy (ed) Special Publication of the Geological Association of Canada
- Noffke, N., 2010, *Geobiology: Microbial mats in sandy deposits from the Archean Era to today*, Springer.
- Pancost, R. D., Freeman, K. H., Herrmann, A. D., Patzkowsky, M. E., Ainsaar, L., and Martma, T., 2013, Reconstructing Late Ordovician carbon cycle variations: *Geochimica et Cosmochimica Acta*, v. 105, no. 0, p. 433-454.

- Pancost, R. D., Freeman, K. H., and Patzkowsky, M. E., 1999, Organic-matter source variation and the expression of a late Middle Ordovician carbon isotope excursion: *Geology*, v. 27, no. 11, p. 1015-1018.
- Pearson, T., and Rosenberg, R., 1978, Macrobenthic succession in relation to organic enrichment and pollution of the marine environment: *Oceanogr. Mar. Biol. Ann. Rev.*, v. 16, p. 229-311.
- Pratt, L. M., Claypool, G. E., and King, J. D., 1986, Geochemical imprint of depositional conditions on organic matter in laminated—bioturbated interbeds from fine-grained marine sequences: *Marine Geology*, v. 70, no. 1–2, p. 67-84.
- Purdy, E. G., 1964, Sediments as substrates: J. Imbrie and N. Newell [eds.], *Approaches to paleoecology*. Wiley, New York, p. 238-271.
- Ranger, M. J., Pickerill, R. K., and Fillion, D., 1984, Lithostratigraphy of the Cambrian? – Lower Ordovician Bell Island and Wabana groups of Bell, Little Bell, and Kellys islands, Conception Bay, eastern Newfoundland: *Canadian Journal of Earth Sciences*, v. 21, no. 11, p. 1245-1261.
- Renbin, Z., and Jisuo, J., 2007, Ordovician-Early Silurian (Llandovery) Stratigraphy and Palaeontology of the Upper Yangtze Platform, South China, Science Press.
- Rullkötter, J., 2006, Organic Matter: The Driving Force for Early Diagenesis. In *Marine Geochemistry*, p. 125-168, Springer Berlin Heidelberg.
- Stahl, W. J., 1979, Lectures in Isotope Geology, Germany, Springer-Verlag Berlin Heidelberg New York, Carbon Isotopes in Petroleum Geochemistry.

- Strauss, H., Bengtson, S., Myrow, P. M., and Vidal, G., 1992, Stable isotope geochemistry and palynology of the late Precambrian to Early Cambrian sequence in Newfoundland: *Canadian Journal of Earth Sciences*, v. 29, no. 8, p. 1662-1673.
- Tesi, T., Langone, L., Goñi, M. A., Wheatcroft, R. A., Miserocchi, S., and Bertotti, L., 2012, Early diagenesis of recently deposited organic matter: A 9-yr time-series study of a flood deposit: *Geochimica et Cosmochimica Acta*, v. 83, no. 0, p. 19-36.
- Tyson, R. V., 1995, *Sedimentary organic matter*, London, UK, Chapman & Hall.
- Vakarelov, B. K., Ainsworth, R. B., and MacEachern, J. A., 2012, Recognition of wave-dominated, tide-influenced shoreline systems in the rock record: Variations from a microtidal shoreline model: *Sedimentary Geology*, v. 279, p. 23-41.
- Weise, B.R., 1980, *Wave-dominated delta systems of the Upper Cretaceous San Miguel Formation, Maverick Basin, South Texas*: Bureau of Economic Geology, University of Texas at Austin
- Weissert, H., Joachimski, M., and Sarnthein, M., 2008, *Chemostratigraphy: Newsletters on Stratigraphy*, v. 42, no. 3, p. 145-179.
- Wellman, C. H., Osterloff, P. L., and Mohiuddin, U., 2003, Fragments of the earliest land plants: *Nature*, v. 425, no. 6955, p. 282-285.
- Yingst, J. Y., and Rhoads, D. C., 1980, *The role of bioturbation in the enhancement of bacterial growth rates in marine sediments: Marine benthic dynamics*. University of South Carolina Press, Columbia, p. 407-421.
- Zhang, T., Shen, Y., and Algeo, T. J., 2010, High-resolution carbon isotopic records from the Ordovician of South China: Links to climatic cooling and the Great

Ordovician Biodiversification Event (GOBE): Palaeogeography,  
Palaeoclimatology, Palaeoecology, v. 289, no. 1, p. 102-112.

## Chapter 4

### Summary

---

To better understand the processes that control sedimentological and geochemical properties of shallow marginal marine environments, an inter-bedded sandstone, siltstone, and mudstone succession from the Redmans Formation, Bell Island, Newfoundland was investigated. This project is important in achieving a clear understanding of nearshore facies processes and their impact on the TOC and  $\delta^{13}\text{C}_{\text{org}}$ . Currently, the processes that control textural and geochemical rock attributes are not well understood in the ancient rock record. The Redmans Formation provides an ideal location to clarify these issues and to test the null hypothesis:

*“Near-shore marine environments have organic carbon isotopic trends that represent the oceanic values of  $\delta^{13}\text{C}_{\text{org}}$ , and are independent of seafloor processes and the effects of detritivory”.*

#### 4.1 REVIEW OF OBJECTIVES

- 1) A paleoenvironmental interpretation of the Redmans Formation was based on detailed facies and facies association descriptions at a range of spatial scales.
- 2) In combination with the sedimentological interpretation of the Redmans Formation, the quality ( $\delta^{13}\text{C}_{\text{org}}$ , ‰) and quantity (TOC, wt %) of organic matter



were analyzed to understand the effects physical and biological seafloor reworking have on organic carbon geochemical signature variability. Organic carbon isotopic heterogeneities have been hypothesized to vary between and within facies and are the result of physical and biological seafloor reworking processes.

- 3) Bulk organic matter isotopic trends were investigated to determine whether global organic carbon signatures can be correlated between different geological successions. It was hypothesized that organic carbon isotopic trends were artefacts of isotopic modification due to physical, biological, and multiple cycles of reworking rather than global isotopic shifts in the dynamic marine environment of the Redmans Formation.

## **4.2 SUMMARY OF CONCLUSIONS**

### **4.2.1 Paleoenvironmental interpretation of the Redmans Formation**

Marginal marine mudstone-dominated systems of Paleozoic age are poorly understood. To more accurately assess the interplay of Paleozoic marginal marine environmental processes at the facies scale, it is important to further our knowledge of these systems. This study aims to integrate the hydrodynamic conditions that mudstones and sandstones were deposited under into a unified paleoenvironmental model. The sedimentology and ichnology of the Redmans Formation's thick quartz arenites interbedded with siltstones and mudstones were reviewed (Table, 2.1). Sandstone facies include *Cruziana*, *Trichophycus*, *Diplocraterion* and *Planolites* traces (~10%), whereas mudstone and siltstone facies are composed of a more diverse and intense assemblage of

*Cruziana*, *Planolites*, *Trichophycus*, *Diplocraterion*, and other identifiable traces (~20-80%). Hyperpycnal fluid mudstones are typically unbioturbated, although post-depositional, deep tiering ichnofabrics were frequent. Twelve sedimentological facies have been classified into a single facies association, composed of proximal to distal distributary mouth bars (Fig. 2.2). A wave-dominated delta with both wave and tidal indicators was the interpreted paleoenvironment (Fig. 2.9). Distributary mouth bar deposits form stacked shallow marine parasequences built from a more distal expression to one of a more proximal sandstone body with storm influence (Fig. 2.8). Detailed sedimentological descriptions allow for more thorough consideration of the interplay between inter-bedded sandstones, mudstones, and siltstones with respect to the paleoenvironment interpretation in the Early Ordovician Redmans Formation.

#### **4.2.2 Facies-scale depositional mechanisms and biological-sediment interactions with respect to organic carbon cycling**

Processes controlling the physical and biological reworking of mud-laden marginal marine sediment are poorly constrained in the Paleozoic rock record (Harazim, 2013). Environmental studies on the physical and biological controls of organic matter quality ( $\delta^{13}\text{C}_{\text{org}}$ , ‰) and quantity (TOC, wt %) in muddy marine coastlines have rarely been undertaken (Burdige, 2005; Aplin and Macquaker, 2011; Blair and Aller, 2012). An integrated sedimentological and geochemical approach was used in the Redmans Formation to provide a clearer understanding of the significance that biogenic activity and physical reworking have on the relationships between total organic carbon content (TOC, wt %) and quality ( $\delta^{13}\text{C}_{\text{org}}$ , ‰) at the facies-scale.

The Redmans Formation is primarily sourced from marine organic matter such as marine algae, aggregates, and microbial mats (Blair and Aller, 2012; Davies et al., 2012). Source mixing of terrestrial organic matter in the Redmans Formation did not occur, confirmed by non-vegetated hinterland during the Early Ordovician and the lack of woody and terrestrial material in petrographic and palynological studies (Dean and Martin, 1978; Kenrick and Crane, 1997; Wellman et al., 2003; Gensel, 2008; Kenrick et al., 2012; Harazim, 2013).

Biological activity and physical reworking modify the original organic material, generating a significant range of 0.8 wt % for TOC and approx. 4.3‰ for  $\delta^{13}\text{C}_{\text{org}}$  values. Biological-sediment interactions directly metabolize organic matter and indirectly degrade organic matter by increasing oxygen exposure time and encouraging microbial activity; resulting in an enriched organic carbon isotopic signature (Tyson, 1995; Hartnett et al., 1998; Aller et al., 2001; Fermann, 2002). Multiple reworking cycles increase the potential for organic matter alteration/remineralization. Organic carbon isotopic values will be more enriched when organic matter has undergone multiple cycles of remineralization and biogenic fractionation, prior to final burial. Stable organic carbon enrichment is represented by large isotopic ranges (approx. 4‰), which vary within and between facies of the distributary mouth bars of the Redmans Formation (Fig. 3.8). The depositional environment dictates facies distribution and as a result isotopic variability is a factor of facies distributed (Fig. 3.10).

### **4.2.3 Implications for global organic carbon cycling using bulk organic matter isotopic trends correlations**

Chemostratigraphy studies geochemical perturbations in the global carbon cycle, identified by excursions or shifts in isotopic signatures (Pancost et al., 1999; Blair and Aller, 2012; Davies et al., 2012). Global excursions are used to correlate multiple sections from different paleocontinents when biostratigraphic means are unavailable (Weissert et al., 2008). Facies in the Redmans Formation show substantial  $\delta^{13}\text{C}_{\text{org}}$  variability between and within facies. Localized physical reworking and biological processes controlled facies development and in turn modified the original  $\delta^{13}\text{C}_{\text{org}}$  values. Isotopic excursions in the Redmans Formation reflect changes in transport, source, and biological processes rather than global carbon perturbations. Stable isotopic curves used in global chemostratigraphic studies must take into consideration  $\delta^{13}\text{C}_{\text{org}}$  variations by basinal processes. Stable organic carbon isotopic shifts in the Redmans Formation are a factor of facies development including physical, biological, and microbial reworking rather than a shift in the global carbon cycle.

### 4.3 REFERENCES

- Aller, R. C., Aller, J. Y., and Kemp, P. F., 2001, Effects of Particle and Solute Transport on Rates and Extent of Remineralization in Bioturbated Sediments, Columbia, North Carolina, The Belle W. Baruch Library in Marine Science, Organism-Sediment Interactions.
- Aplin, A. C., and Macquaker, J. H. S., 2011, Mudstone diversity: Origin and implications for source, seal, and reservoir properties in petroleum systems: AAPG Bulletin, v. 95, no. 12, p. 2031-2059.
- Blair, N. E., and Aller, R. C., 2012, The Fate of Terrestrial Organic Carbon in the Marine Environment, *in* Carlson, C. A., and Giovannoni, S. J., eds., Annual Review of Marine Science, Vol 4, Volume 4, p. 401-423.
- Burdige, D. J., 2005, Burial of terrestrial organic matter in marine sediments: A re-assessment: Global Biogeochemical Cycles, v. 19, no. 4.
- Davies, S. J., Leng, M. J., Macquaker, J. H. S., and Hawkins, K., 2012, Sedimentary process control on carbon isotope composition of sedimentary organic matter in an ancient shallow-water shelf succession: Geochemistry, Geophysics, Geosystems, v. 13, no. 11.
- Dean, W. T., and Martin, F., 1978, Lower Ordovician acritarchs and trilobites from Bell Island, eastern Newfoundland, Geological Survey of Canada.

- Fermann, E. J., 2002, Early and Middle Cambrian carbon and strontium isotopic chemostratigraphy and the influence of bioturbation on the carbon cycle [PhD: Cornell University].
- Gensel, P. G., 2008, The earliest land plants: *Annual Review of Ecology, Evolution, and Systematics*, v. 39, p. 459-477.
- Harazim, D., 2013, High-energy seafloor processes and biological reworking as first-order controls on mudstone composition and geochemistry [PhD: Memorial University of Newfoundland].
- Hartnett, H. E., Keil, R. G., Hedges, J. I., and Devol, A. H., 1998, Influence of oxygen exposure time on organic carbon preservation in continental margin sediments: *Nature*, v. 391, no. 6667, p. 572-575.
- Kenrick, P., and Crane, P. R., 1997, The origin and early evolution of plants on land: *Nature*, v. 389, no. 6646, p. 33-39.
- Kenrick, P., Wellman, C. H., Schneider, H., and Edgecombe, G. D., 2012, A timeline for terrestrialization: consequences for the carbon cycle in the Palaeozoic: *Philosophical Transactions of the Royal Society B: Biological Sciences*, v. 367, no. 1588, p. 519-536.
- Pancost, R. D., Freeman, K. H., and Patzkowsky, M. E., 1999, Organic-matter source variation and the expression of a late Middle Ordovician carbon isotope excursion: *Geology*, v. 27, no. 11, p. 1015-1018.
- Tyson, R. V., 1995, *Sedimentary organic matter*, London, UK, Chapman & Hall.
- Weissert, H., Joachimski, M., and Sarnthein, M., 2008, Chemostratigraphy: *Newsletters on Stratigraphy*, v. 42, no. 3, p. 145-179.

Wellman, C. H., Osterloff, P. L., and Mohiuddin, U., 2003, Fragments of the earliest land plants: *Nature*, v. 425, no. 6955, p. 282-285.

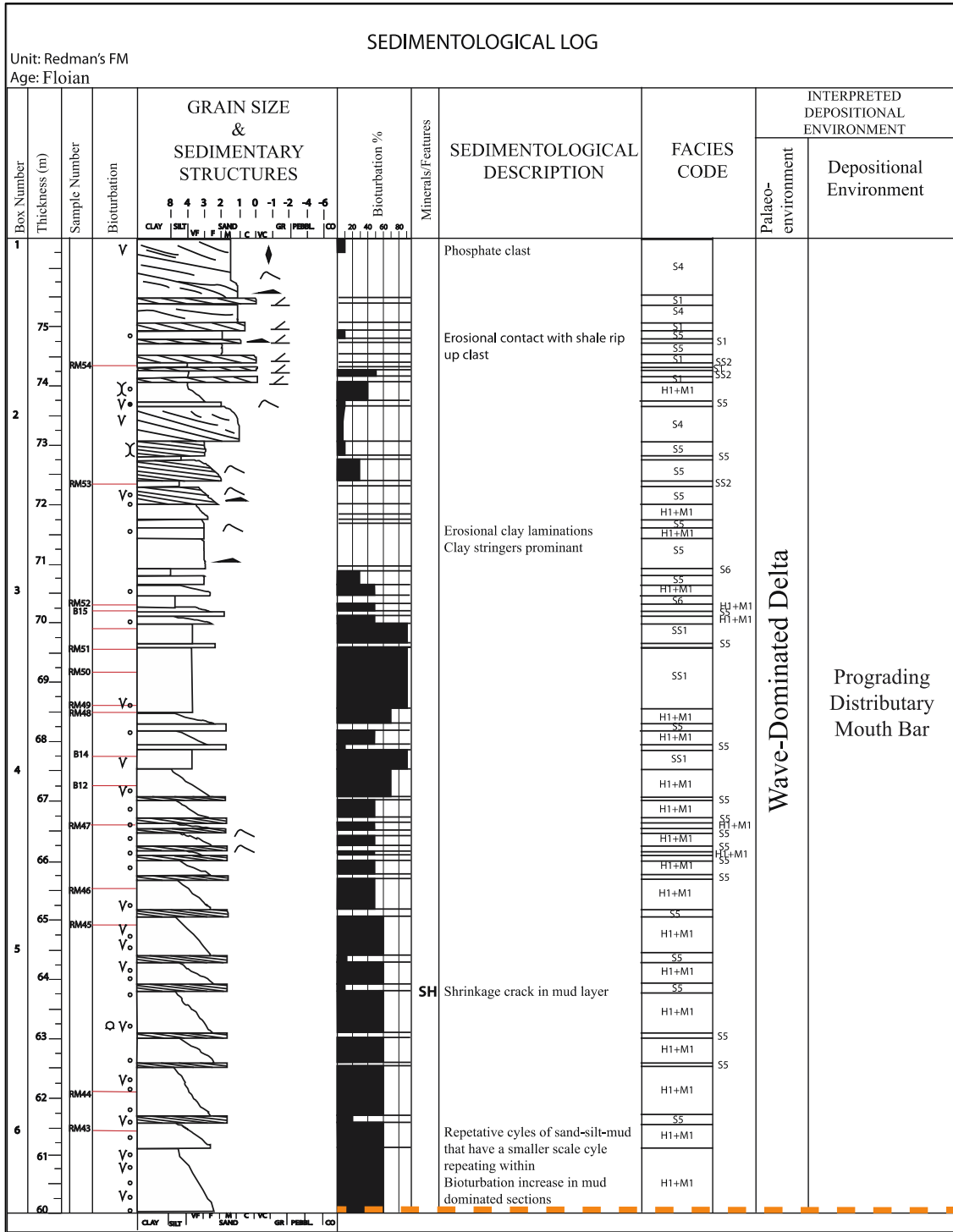
## **Appendices**

### **Appendix A**

#### **Sedimentology and Stratigraphy**

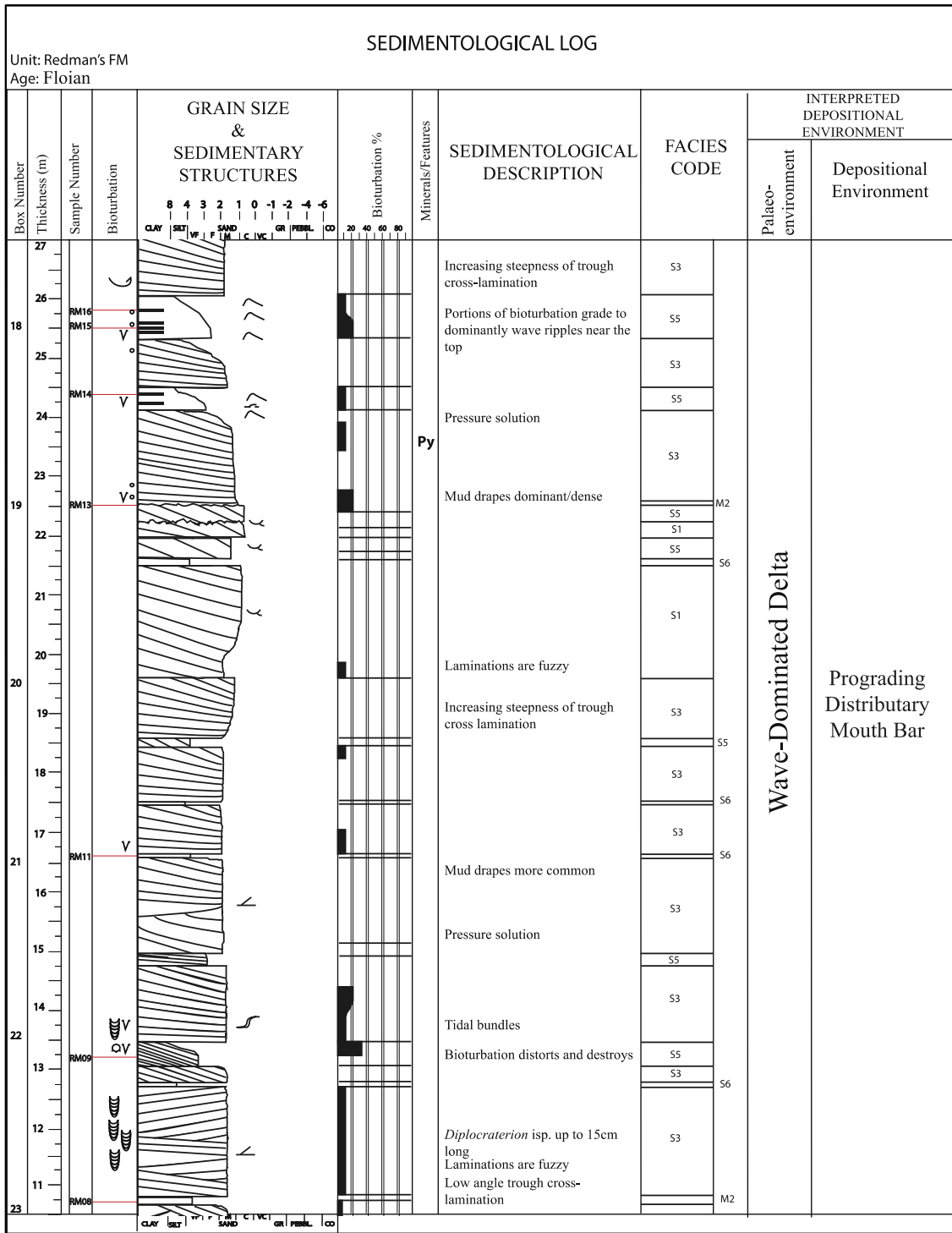
Appendix A contains the sedimentological and ichnological data from 76.5m of core from the Redmans Formation, Bell Island. Data from Appendix A is presented in Chapters 2 and 3. Graphic logs describe the sedimentary features, grain size, type and intensity of bioturbation, facies code, and the interpreted depositional environment. The graphic logs also identify the depth at which samples were taken for geochemical analyses.

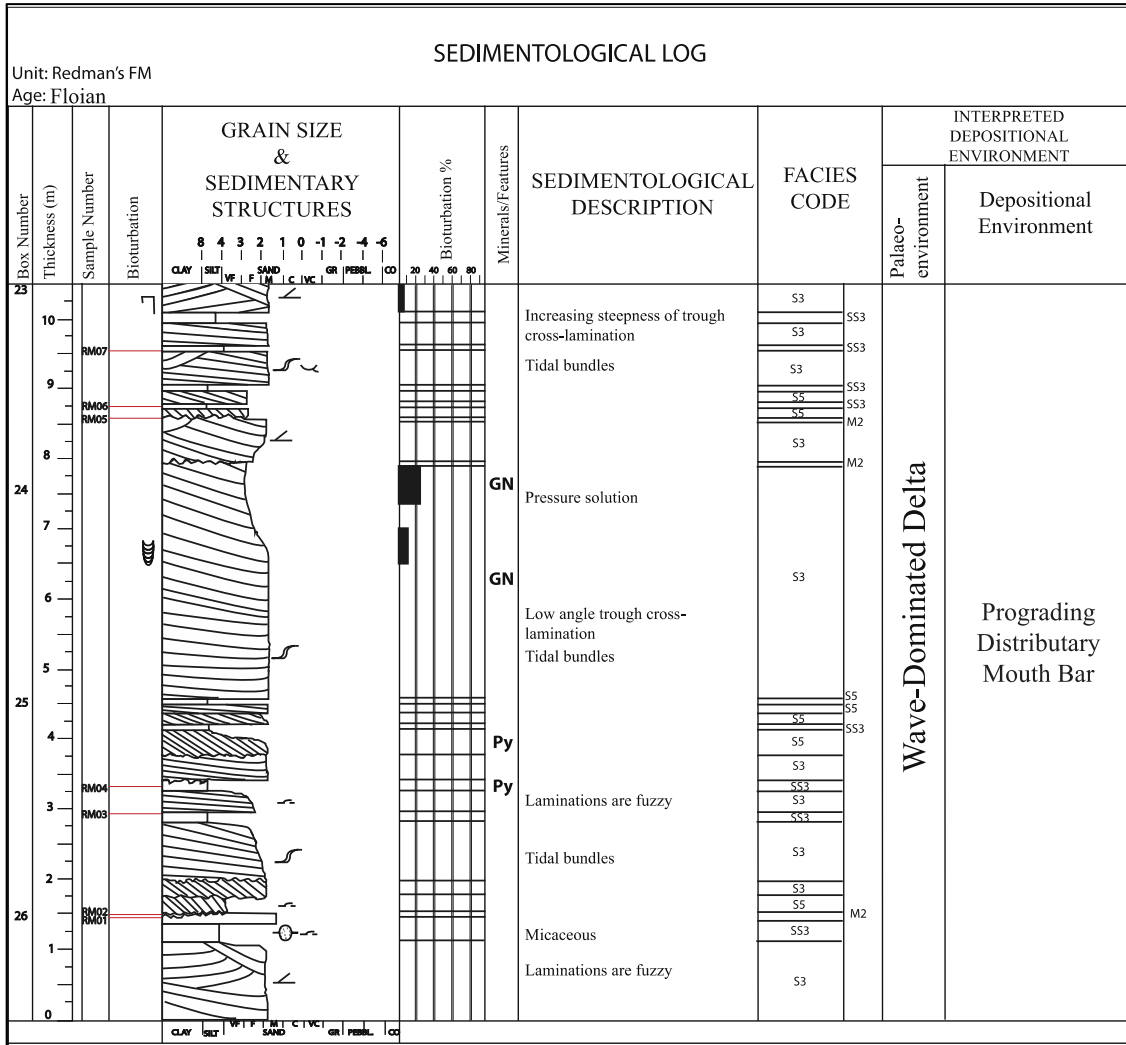








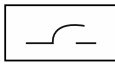
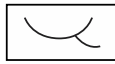
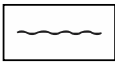


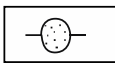
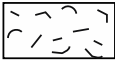
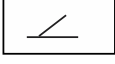





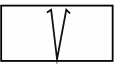


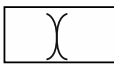



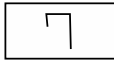


# Legend


## Sedimentary Features

	Wave Ripple
	Mud Couplet
	Flaser Lamination
	Trough Cross-Stratification
	Erosional Contact
	Mudstone Clast
	Phosphate Clast
	Sandstone Clast
	Dark Flecks
	Cross-Stratification

## Biogenic Features

	Brachiopod Shell
	Vertical Burrow
	<i>Diplocraterion</i> isp.
	<i>Rosselia</i> isp.
	Escape Trace
	<i>Trichophycus</i> isp.
	<i>Planolites</i> isp.
	<i>Palaeophycus</i> isp.
	<i>Trichichnus</i> isp.

## Boundaries

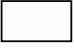


	Parasequence Boundary
---	-----------------------

**GN:** Galena

**SH:** Shrinkage Cracks

**Py:** Pyrite

## Grain Size

	Fine/medium/coarse-grained sandstone
	Siltstone & very fine-grained sandstone
	Interbedded silt- & clay- rich mudstone

## **Appendix B**

### **Whole rock stable organic carbon isotopic and total organic carbon (TOC) data, Bell Island**

Appendix B consists of whole rock geochemical data from 76.5 m of core obtained from the Redmans Formation, Bell Island. Tables in Appendix B list sample number, stratigraphic height (m), facies code, total organic carbon (TOC, wt%), and stable organic carbon ( $\delta^{13}\text{C}_{\text{org}}$ , ‰) data. Chapter 3 presents the data described in the tables. TOC (wt %) and  $\delta^{13}\text{C}_{\text{org}}$  (‰) values reported to the Vienna Pee Dee Belemnite standard (V-PDB), were analysed using a Carlo-Erba NA1500 Elemental Analyser (EA), and a Delta V Plus mass spectrometer.

Sample number	Stratigraphic height (m)	Facies code	$\delta^{13}\text{C}_{\text{org}}$ (‰)	TOC (wt%)
B01	36.52	M1	-29.06	0.345
B02	36.66	M1	-29.57	0.556
B03	37.05	M1	-28.98	0.322
B04	37.3	M1	-28.57	0.335
B05	37.55	M1	-28.91	0.374
B06	37.95	M1	-28.52	0.227
B07	38.9	M1	-28.58	0.268
B08	53.12	SS1	-28.85	0.489
B12	67.24	M1	-27.64	0.137
B14	67.75	SS1	-28.53	0.313
B15	70.12	H1	-27.08	0.168
RM01	1.45	M2	-27.42	0.759
RM02	1.6	M2	-29.38	0.552
RM03	2.95	SS3	-27.93	0.314
RM04	3.3	SS3	-27.05	0.211
RM05	8.55	M2	-29.75	0.768
RM06	8.75	SS3	-27.47	0.675
RM07	9.55	SS3	-25.63	0.538
RM08	10.65	M2	-29.45	0.554
RM09	13.17	S5	-26.36	0.086
RM11	16.55	S6	-26.94	0.211
RM13	22.5	M2	-28.45	0.346
RM14	24.35	M2	-28.83	0.522
RM15	25.5	M2	-29.03	0.418
RM16	25.8	M2	-29.2	0.444
RM17	29.1	M1	-27.83	0.297



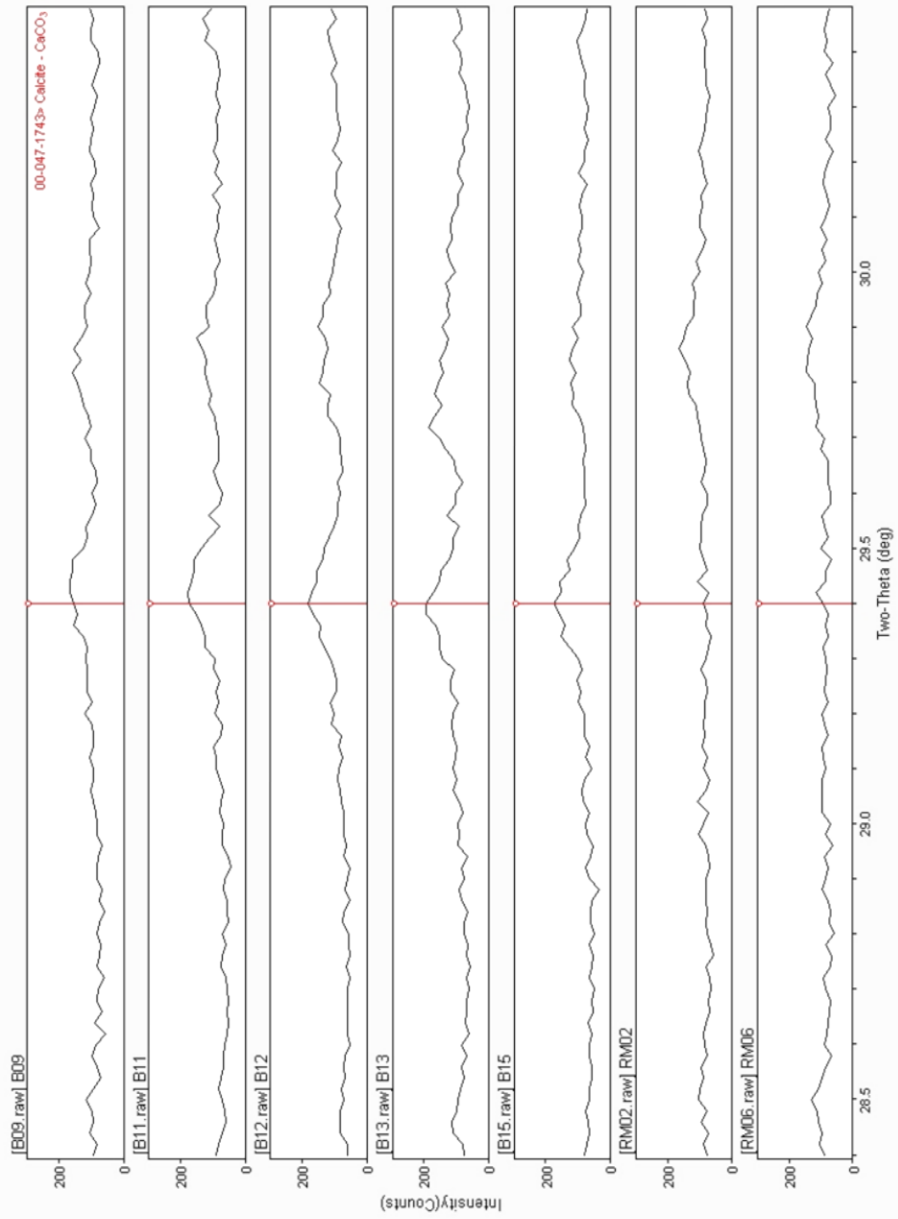
Sample number	Stratigraphic height (m)	Facies code	$\delta^{13}\text{C}_{\text{org}}$ (‰)	TOC (wt%)
RM18	30.95	M2	-29.09	0.433
RM19	32	SS1	-27.91	0.22
RM20	35.15	SS1	-29.64	0.464
RM21	35.6	M1	-29.96	0.507
RM23	39.55	SS1	-28.06	0.32
RM26	44.6	M2	-27.68	0.392
RM27	46.48	M2	-28.56	0.409
RM28	46.7	M2	-27.55	0.272
RM29	47.38	M1	-27.76	0.26
RM34	51.35	S6	-25.74	0.171
RM35	52.45	S6	-26.30	0.06
RM36	52.95	M2	-29.91	0.67
RM37	53.7	M2	-28.69	0.30
RM39	54.35	M2	-26.54	0.43
RM42	57	S6	-26.7	0.115
RM43	61.5	M1	-29.66	0.321
RM44	62.2	M1	-29.62	0.329
RM45	64.9	M1	-28.59	0.256
RM46	65.58	M1	-29.49	0.394
RM47	66.7	M1	-30.31	0.839
RM48	68.5	SS1	-28.77	0.238
RM49	68.7	SS1	-27.61	0.171
RM50	69.17	SS1	-27.57	0.179
RM51	69.55	SS1	-28.84	0.305
RM52	70.25	SS1	-29.53	0.357
RM53	72.3	SS2	-29.17	0.42
RM54	74.2	SS2	-26.18	0.165

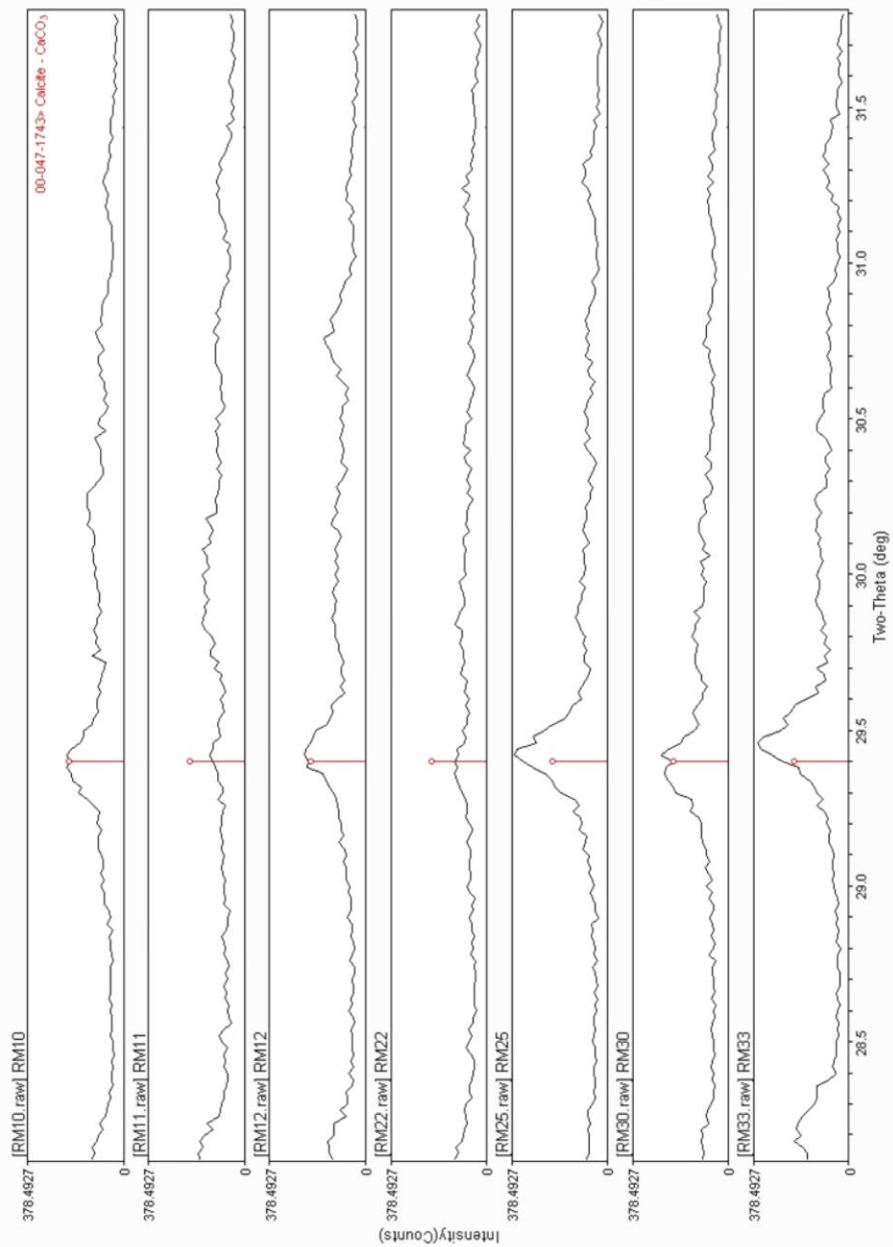
## Appendix C

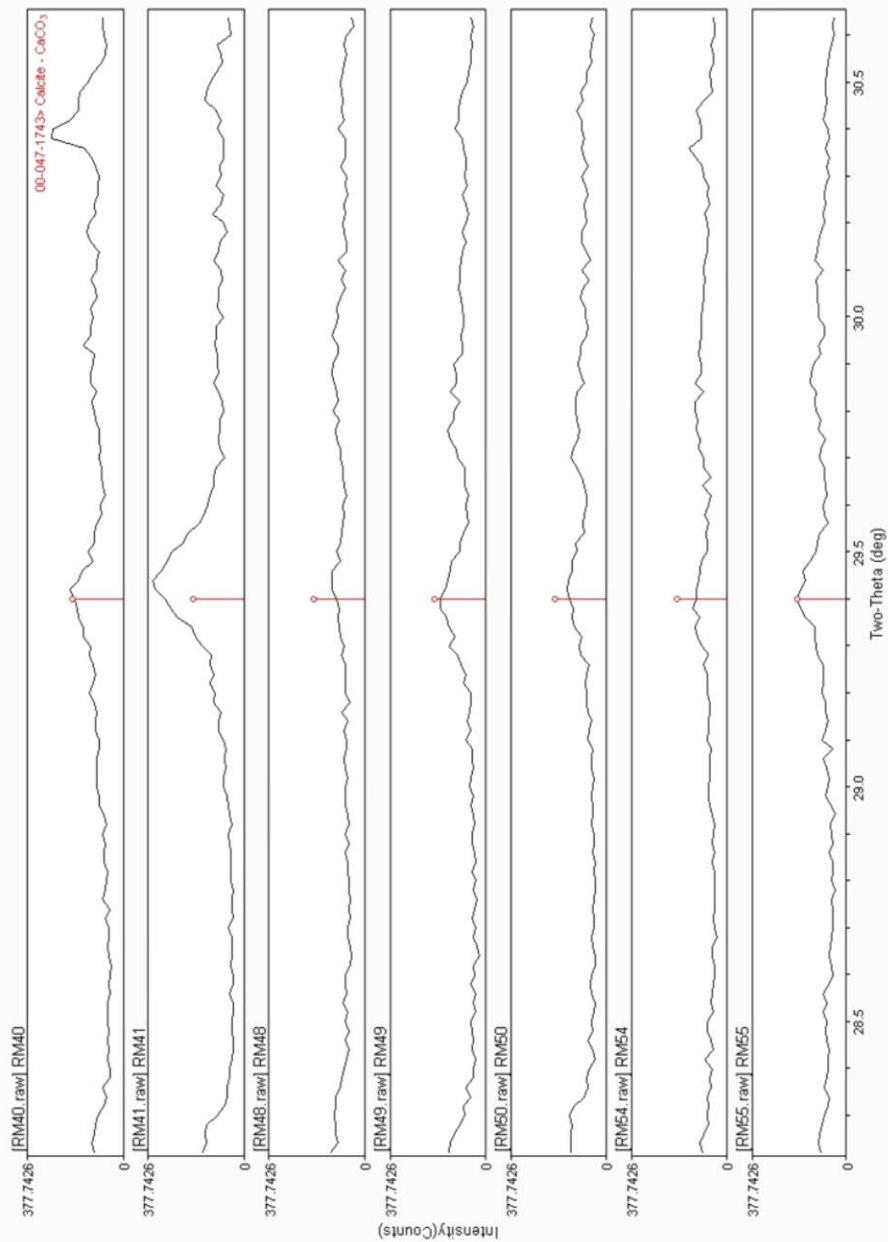
### X-ray Diffractometry (XRD)

To confirm the viability of the results in Chapter 3, X-ray diffraction (XRD) was used on 21 samples from all facies, to detect the presence and type of carbonate present in the sample based on peak orientation. Calcite was the only carbonate to have occurred in XRD sample analyses, having a peak at 29.4 two-theta. Samples were analysed in an air-dried state. Samples RM02 and RM06 had no calcite cement indicated by the flat wavelength. Appendix C includes the operating conditions used in the analyses and the following results.

XRD Operating Conditions	Explanation
<i>X-Ray</i> Cu            40kV            44mA <i>Scan Speed</i> 2.000 deg./min <i>Sampling width</i> 0.0200 deg. <i>Scan range</i> 20.0000->80.0000 deg	Faster because it was cheaper and still capable of identifying calcite cement. Typically ran at 1.000 deg./min  Step size that the machine moves
<i>Slit Settings</i> <i>Before sample:</i> DivSlit        2/3 deg. DivH.L.Slit    10mm <i>After sample:</i> SctSlit        2/3 deg. RecSlit        0.3mm	







## **Appendix D**

### **Fourier Transform Infrared (FT-IR) Spectroscopy**

Appendix D contains FT-IR spectra from whole rock samples that were ground into a powder using an agate mortar and pestle. Attenuated total reflection (ATR) mode was employed to screen decalcified samples to eliminate samples with insoluble carbonate. Elemental bond have a characteristic spectrum with calcium carbonate having a peak of  $1400\text{ cm}^{-1}$ . Samples with this signature are removed from the sample base in Chapter 3.

